

043  
DAS  
12296

PLASMA PROCESSES  
IN  
MULTISPECIES DISPERSIVE MEDIA

BY  
SHEFALI SUSHIL DASH

A THESIS  
SUBMITTED FOR THE DEGREE OF  
DOCTOR OF PHILOSOPHY

OF THE  
GUJARAT UNIVERSITY

DECEMBER 1983

043



B12296

PHYSICAL RESEARCH LABORATORY

AHMEDABAD 380009

TO  
MUM AND PAPA



## CONTENTS

Page

CERTIFICATE

ACKNOWLEDGEMENTS

ABSTRACT OF THE THESIS

CHAPTER 1	INTRODUCTION	1-18
CHAPTER 2	EFFECT OF HOT IONS ON ION ACOUSTIC SOLITONS AND HOLES	19-33
2.1	Introduction	19
2.2	Energy Integral	22
2.3	Solitary Waves	25
2.4	Small Amplitude Limit	29
2.5	Numerical Results	31
2.6	Conclusions	33
CHAPTER 3	COMPRESSIVE AND RAREFACTORY ELECTRO-STATIC ION CYCLOTRON SOLITARY WAVES IN MULTISPECIES MAGNETO PLASMAS	34-58
3.1	Introduction	34
3.2	Basic Equations	37
3.3	Electrostatic Ion Cyclotron Solitary Waves	42
3.4	Small Amplitude Sonic Ion Cyclotron Solitary Waves	46
3.5	Numerical Results	50

3.6	Discussion	53
3.7	Conclusions	58
CHAPTER 4	EVOLUTION OF NONLINEAR ION ACOUSTIC WAVES IN AN INHOMOGENEOUS TWO ELECTRON TEMPERATURE PLASMA	59-82
4.1	Introduction	59
4.2	Modified Nonlinear Schrodinger Equation	62
4.3	Linear Stability	78
4.4	Nonlinear Analysis	79
4.5	Conclusions	85
CHAPTER 5	ELECTRON ACOUSTIC AND ION-ION-HYBRID RESONANCE WAVES IN MULTI-ION-SPECIES MAGNETOPLASMAS	86-99
5.1	Introduction	86
5.2	Dispersion Relation	90
5.3	Discussion	95
5.4	Summary	99
CHAPTER 6	ELECTRON ACOUSTIC AND ION-ION-HYBRID RESONANCE-DRIFT INSTABILITY IN INHOMOGENEOUS MULTI-ION-SPECIES MAGNETOPLASMAS	100-114
6.1	Introduction	100
6.2	Dispersion Relation	104

Page

6.3 EA and IIHR Drift Instabilities 110

6.4 Discussion and Conclusions 113

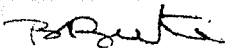
REFERENCES 115-120

CERTIFICATE

I hereby declare that the work presented in this Thesis is original and has not formed the basis for the award of any degree or diploma by any University or Institution.

Shefali Sushil Dash  
SHEFALI SUSHIL DASH  
(AUTHOR)

Certified by:



B. BUTI  
(Professor-in-charge)

December 26, 1983.

## ACKNOWLEDGEMENTS

The work presented in this Thesis has been carried out under the valuable and competent guidance of Professor B. Buti. I wish to express here my deep sense of gratitude to her for her keen interest in my progress and her encouragement in my endeavours. Her critical reading of the manuscript and constructive comments have helped me substantially in finalising the Thesis. It is a great pleasure to thank her.

My sincere thanks are due to Professors R.V. Pratap, R.K. Varma, A.C. Das, K.H. Bhatt, J.C. Parikh, S.B. Khadkikar, A. Sen, A.K. Sundaram, Y.C. Saxena, R.N. Keshavamurty, A.R. Prasanna and V.B. Sheorey for many valuable discussions I had with them.

It is a pleasure to thank Drs. M. Mohan, N. Nagesha Rao and A.S. Sharma with whom I had a number of helpful and illuminating discussions.

Thanks are also due to my colleagues Meenakshi, Aparna, Kailash, Patro, Subbaraman, Usha, Chitra, Avinash, Subhashish and Baskaran, who have helped me in a number of ways.

I acknowledge here the help offered by Mr.P.S. Shah and his colleagues, Mrs. R.R. Bharucha, Mrs. Urmila Ghiya, Miss Swadha Majumdar and their colleagues. I wish to thank them.

I am grateful to Mr.P.P. Narayanan and Mr.V. Sahadevan for their excellent typing of this Thesis and to Mr. Babulal Brahmbhatt for the neat cyclostyling.

Lastly, I must take this opportunity to thank Sushil whose patient understanding and warm companionship have encouraged me throughout this research.

## ABSTRACT

Plasmas, more often than not, have more than one species of electrons and ions. Some examples of such multi-species plasmas are the beam plasma systems, turbulent plasmas of thermonuclear interest, solar wind near 1 AU, fusion plasmas with impurities, magnetospheric plasmas, etc. But most of the theoretical work dealing with these systems consider the plasma to have one species of electrons and one species of ions only. However, some recent theoretical investigations have shown that the presence of more than two species of particles can



change the dispersive properties of the medium rather drastically. For example, only compressive ion acoustic solitary waves (solitons or density humps) exist in a single electron component plasma, whereas, rarefactory ion acoustic solitary waves (holes or density dips) also can exist when the presence of a second electron species is taken into account. Similarly, electron acoustic (EA) holes also can occur, in addition to the EA solitons, if the plasma consists of more than one species of ions. So, in order to obtain correct information about the processes occurring in such multi-species-plasmas, it is only proper that all the particle species be taken into account.

In this thesis we have considered the multispecies plasmas and have investigated the existence and propagation of solitary ion acoustic waves, solitary ion cyclotron waves, EA waves, ion-ion-hybrid-resonance (IIHR) waves, the drift instability of EA and IIHR waves and the possibility of mode conversion between the EA and IIHR waves. As regards the ion acoustic waves, in a two electron component plasma both solitons and holes can occur even when the ions are cold. However when the finite temperature of the ions is appropriately accounted for, we find that the maximum amplitude of solitons as well as holes is reduced significantly. Finite ion temperature also reduces the allowed regions (regions in parameter



space where solitons and holes occur); in some cases the holes are even forbidden. When two species of electrons are present in a magnetoplasma, in addition to the rarefactive electrostatic ion cyclotron solitary waves, which exist in a single electron component plasma, a new type of solitary wave, namely, the compressive solitary wave can also occur. The allowed regions for the existence of these solitary waves are greatly affected by any change in the ion temperature and the ratio of density and temperature of the hot and warm electron components. The formation of the paired perpendicular electrostatic shocks observed in the auroral plasmas at an altitude of  $\sim 1 R_E$  can be nicely explained in terms of these **EIC** solitary waves only if the presence of the second electron species is taken into account. An ion acoustic envelope soliton propagating in a two-electron-species inhomogeneous plasma, with the density gradient scalelength of the order of the width of the envelope soliton, is found to split into two solitary waves. However, the splitting time is longer compared to the one in a single electron species plasma. Furthermore, the splitting of the envelope holes in a two-electron-component plasma is found to be delayed so much that splitting does not occur within a practical length of time.

In a magnetised plasma with ions more energetic than the electrons, electron acoustic waves can propagate in a direction almost perpendicular to the magnetic field. If more than one species of ions are present in the plasma, the ion-ion-hybrid resonance mode also is excited. The effect of any change in the relative concentration, mass and temperature of the two ion species on the characteristic frequencies of the electron acoustic and the ion-ion-hybrid resonance modes in the magnetospheric plasmas and the 2XIIB mirror machine is studied. The presence of weak density gradients perpendicular to the magnetic field and the direction of wave propagation, gives rise to drift waves. Coupling of these drift waves with the electron acoustic ion-ion-hybrid resonance waves can give rise to the corresponding drift instabilities. The range, over which these drift instabilities occur is larger when the medium has stronger inhomogeneities. The presence of density gradients, in principle, can lead to mode conversion between the EA and IIHR waves. But within the approximation of fluid theory and in the limit of weak inhomogeneities, it is found that mode conversion between the EA and IIHR waves does not occur in the magnetospheric plasmas or in the 2XIIB mirror machine.

## CHAPTER 1

### INTRODUCTION

Recent measurements have shown the presence of more than one species of ions and electrons in the laboratory as well as in the space plasmas. Electrons having two distinct velocity distributions are common in hot cathode discharge plasmas (Oleson and Found, 1949), turbulent plasmas of thermonuclear interest (Krall and Trivelpiece, 1973). IMP-8 satellite data have shown a double Maxwellian distribution for electrons in the solar

wind near 1 AU (Feldman et al., 1975). Auroral plasmas also contain two types of electrons (Garret, 1979). Several theoretical investigations have shown that the second electron component can change the nature of the waves significantly. For example, the ion acoustic solitary wave is compressive in a single electron species plasma (Sagdeev, 1966), whereas, when a second electron species is present, rarefactory ion acoustic solitary wave (hole) can also exist (Buti, 1980). Lisak (1980) had shown that the range of wavenumbers corresponding to modulational instability of electrostatic ion cyclotron waves is significantly changed by the presence of the second electron species. It has also been found that the second electron species affects the nature of the Langmuir solitons (Buti and Yu, 1981). In addition to the solitary Langmuir waves where the density scales as the square of the electric field amplitude, similar to those in a single electron species plasma, new type of solitons can also exist where the density and the field amplitude have the same scaling.

Data from the polar orbiting satellite ISIS2 show that at an altitude of 1400 Km,  $H^+$  is the dominant ion species, followed by  $O^+$ ,  $He^+$ ,  $N^+$  and  $O^{++}$  in concentration level (Hoffman, 1974). Johnson et al. (1977) had

reported the presence of heavy ions like  $\text{He}^+$ ,  $\text{He}^{++}$  and  $\text{O}^+$  in the ring current at a distance of 3 to 10 earth radii ( $R_E$ ). ISEE1,2 measurements indicate that besides protons,  $\text{He}^+$ ,  $\text{He}^{++}$  and  $\text{O}^+$  ions are also present in the magnetotail region around 19  $R_E$  (Williams et al., 1979; Peterson et al., 1981; Horwitz, 1982). From these observations one can see that more than one species of ions are present in the plasmasphere, ring current and magnetotail of the terrestrial magnetosphere. Moreover, these ions are more energetic than the local electrons. For example, in the ring current around 7  $R_E$ , ions have energies of the order of 40 KeV, whereas, electrons have energies of the order of 1-4 KeV only (Russel and Thorne, 1970; Frank, 1971). It is known that magnetised plasmas with ions hotter than the electrons can support electron acoustic (EA) waves (Lashmore-Davies and Martin, 1973). The existence of supersonic compressive EA waves had been established by Buti et al. (1980). Furthermore, it has been shown by Buti (1980a) that if more than one species of ions are present in the plasma, electron acoustic holes can also occur.

Presence of impurity ions is not uncommon in the tokamaks and mirror machines (Takahashi et al., 1977, Hosea et al., 1979). These minority ions can have a profound

effect on the dispersion properties of the plasmas.

Buchsbaum (1960) had shown that if two species of ions are present in the system, there exists a plasma resonance involving the two ion cyclotron frequencies. This mode is known as the ion-ion-hybrid resonance (IIHR).

Considering these observational facts and noting that an additional electron or ion species can affect the nature of the waves significantly, in order to have a realistic model, it is only proper that all the particle species be taken into account. In this thesis, we have investigated some problems relating to the existence and propagation of nonlinear ion acoustic waves, nonlinear ion cyclotron waves, electron acoustic waves, ion-ion hybrid resonance waves and the drift instability of the EA and IIHR waves in a multispecies dispersive medium with and without inhomogeneities. A brief summary of each of the investigations is given below.

In chapter 2, we have investigated the ion acoustic solitary waves in a strongly nonlinear two electron species plasma with hot ions ( $T_i \neq 0$ , but  $T_i < T_1, T_2$ , where  $T_i, T_1$  and  $T_2$  are the ion and electron temperatures respectively). Since we are considering a strongly nonlinear plasma, the perturbation techniques are no longer

valid and we have to treat the governing equations exactly by retaining all the nonlinear terms. Handling such situations can be difficult but sometimes a great deal of information can be obtained about the solution without actually solving the nonlinear equations. Usually this procedure is used to find out the existence of localised stationary solitary wave solutions for a set of nonlinear differential equations. This method can be briefly outlined as follows:

Let us consider a system which is governed by the set of equations of the form

$$L_i(\phi_1, \phi_2, \dots, \phi_N) = 0, \quad i = 1, 2, \dots, N \quad (1.1)$$

where  $L_i$  are functions of differential operators with respect to  $x$  and  $t$ . To obtain stationary solutions, the equations (1.1) are transformed to the frame of reference  $\xi = x - Mt$ . On eliminating all the variables except one, say the potential  $\phi$ , one finds that the governing equation is of the form,

$$\frac{1}{2} \left( \frac{d\phi}{d\xi} \right)^2 + \psi(\phi) = 0. \quad (1.2)$$

Eq. (1.2) resembles the energy integral of a classical particle of unit mass moving in an effective potential

$\psi(\phi)$ ;  $\xi$  playing the role of the time. Integrating (1.2)

over  $\xi$  once, we obtain

$$\xi = \int [-2\psi(\phi)]^{-1/2} d\phi + \xi_0. \quad (1.3)$$

For real values of  $\xi$ ,  $\psi(\phi)$  must be negative.

Expanding  $\psi(\phi)$  around  $\phi = 0$ , we get

$$\psi(\phi) = \psi(0) + \phi \left. \frac{\partial \psi}{\partial \phi} \right|_{\phi=0} + \frac{1}{2} \phi^2 \left. \frac{\partial^2 \psi}{\partial \phi^2} \right|_{\phi=0} + \dots \quad (1.4)$$

If  $\psi(0) = 0$  and  $\partial\psi/\partial\phi = 0$  but  $\partial^2\psi/\partial\phi^2 \neq 0$  at  $\phi = 0$ , then from Eqs. (1.3) and (1.4), we observe that the points  $(0,0)$  in the  $\phi - \psi$  plane can be mapped to the points  $(\pm\infty, 0)$  in the  $\xi - \phi$  plane. For a single-valued potential with an extremum at  $\phi = \phi_M$ , we can expand  $\psi(\phi)$  in the neighbourhood of  $\phi = \phi_M$  as

$$\psi(\phi) = \psi(\phi_M) + (\phi - \phi_M) \left. \frac{\partial \psi}{\partial \phi} \right|_{\phi=\phi_M} + \frac{1}{2} (\phi - \phi_M)^2 \left. \frac{\partial^2 \psi}{\partial \phi^2} \right|_{\phi=\phi_M} + \dots \quad (1.16)$$

For  $\psi(\phi_M) = 0$  but  $\partial\psi/\partial\phi$  and  $\partial^2\psi/\partial\phi^2$  finite at  $\phi = \phi_M$ , from Eq. (1.3) one can see that the point  $(\phi_M, 0)$  in the  $\phi - \psi$  plane is mapped to  $(\xi_0, \phi_M)$  in the  $\xi - \phi$  plane. Thus the quasiparticle, in the



potential  $\psi$ , moves from  $\phi = 0$  to  $\phi = \phi_M$  and back in a single transit and  $\phi(\xi)$  corresponds to a stationary wave solution. Hence the conditions for the existence of solitary wave solutions are as follows:

$$\psi(\phi=0) = 0 = \psi(\phi = \phi_M), \quad (1.7)$$

$$\frac{\partial \psi}{\partial \phi} = 0 \text{ at } \phi = 0, \quad (1.8)$$

$$\frac{\partial \psi}{\partial \phi} \neq 0 \text{ at } \phi = \phi_M, \quad (1.9)$$

and

$$\frac{\partial^2 \psi}{\partial \phi^2} \neq 0 \text{ at } \phi = 0 \text{ and } \phi_M, \quad (1.10)$$

with  $\psi(\phi) < 0$  in the range  $0 < \phi < \phi_M$ . In other words  $\phi = 0$  being a double root ensures the existence of solitary waves.

Following the above mentioned method, we have found that in the system considered in chapter 2, ion acoustic solitons (density humps) as well as holes (density depressions) can exist and even an extremely small but finite  $T_i$  can modify these solitons and holes significantly

(Dash and Buti, 1981). When  $T_i$  is finite the maximum amplitude of solitons and holes gets drastically reduced. The permissible regions (regions where solitons and holes can occur) are smaller for  $T_i \neq 0$  compared to the ones for  $T_i = 0$ . The hotter the ions, more drastic are these effects, so much so that in some cases the holes are even forbidden.

Having investigated the solitary ion acoustic waves (IAW) in a two electron component plasma in the absence of a magnetic field in chapter 2, we have extended our study of nonlinear waves to magnetoplasmas in chapter 3. In addition to the IAW propagating parallel to the magnetic field, another mode, namely, the electrostatic ion cyclotron (EIC) mode arises. EIC wave propagates almost perpendicular to the magnetic field. Accounting for the full nonlinearities in the plasma with hot and relatively cold electrons components, the wave equation for EIC wave is derived. Unlike in a single electron species plasma, which allows only rarefactive EIC solitary waves (Yu, 1977), our numerical computations show that in a two electron component plasma, there is a possibility of the existence of compressive EIC solitary waves (Dash and Buti, 1983a). The allowed regions for the existence of rarefactive (compressive) solitary waves decrease (increase) with increase in the

ratio of density and temperature of the hot and cold components. However, an increase in the ratio of ion to hot electron temperature increases the allowed regions for both the rarefactory as well as the compressive solitary waves. An analytic solution for the solitary waves is obtained in the small amplitude limit and it is shown that even in this limit, under certain conditions compressive solitary waves are more favourable than the rarefactory solitary waves. The observed paired electrostatic shock structures in the auroral plasma (Mozer et al., 1977) can be very nicely explained in terms of these EIC solitary waves. Implications of our model to auroral kilometric radiation (Benson and Calvert, 1979) are discussed.

When the plasma is strongly dispersive, the wave broadens quickly and one has to study the behaviour of the wave envelope. In such systems, by using reductive perturbation technique, Tanjuti (1974) had shown that the non-linear Schrödinger equation (NSE) governs the IAW envelope. In this method, the scaling of the space and time variables are decided apriori. An alternative perturbation scheme (Bogoliubov and Mitropolsky, 1961) which uses the multiple space-time scales and requires no apriori scaling of the space-time variables can also be used to derive the NSE

governing the wave envelope (Kakutani and Sutimoto, 1974). The KBM method which we have used in chapter 4, is briefly outlined below.

The wave motion in general can be described by a set of nonlinear partial differential equations given by

$$\frac{\partial \phi}{\partial t} + A \frac{\partial \phi}{\partial x} + \left[ \sum_{\beta=1}^S \sum_{\alpha=1}^N (H_{\alpha}^{\beta} \frac{\partial}{\partial t} + K_{\alpha}^{\beta} \frac{\partial}{\partial x}) \right] \phi = 0, \quad (1.11)$$

where  $\phi$  is a column vector with components  $\phi_1, \phi_2, \dots, \phi_N$  representing various physical quantities of the system and  $A, H_{\alpha}^{\beta}, K_{\alpha}^{\beta}$  are  $n \times n$  matrices, whose elements are functions of  $\phi$  (Taniuti and Wei, 1968). In the limit of weak nonlinearity,  $\phi_i^{(1)}$  can be expanded as

$$\phi_i = \phi_i^{(0)} + \epsilon \phi_i^{(1)} + \epsilon^2 \phi_i^{(2)} + \dots, \quad (1.12)$$

where  $\epsilon$  is the smallness parameter. Let us consider a monochromatic plane wave solution for one of the variables

$$\phi_i^{(1)} \quad \text{i.e.}$$

$$\phi_i^{(1)} = a \exp(i\psi) + \bar{a} \exp(-i\psi), \quad (1.13)$$

where  $\psi = kx - \omega t$  is the phase and 'a' is the complex amplitude which varies slowly with time and space as

$$\begin{aligned}\frac{\partial a}{\partial t} &= \epsilon A_1(a, \bar{a}) + \epsilon^2 A_2(a, \bar{a}) + \dots \\ \frac{\partial a}{\partial x} &= \epsilon B_1(a, \bar{a}) + \epsilon^2 B_2(a, \bar{a}) + \dots\end{aligned}\quad (1.14)$$

with  $\bar{a}$  as the complex conjugate of 'a'. The unknown functions  $A_1, B_1, A_2, B_2, \dots$  etc. are determined from the requirements that the solutions of (1.12) to all orders be free of any secularities. To order  $\epsilon$ , the Eqs. (1.11) to (1.14) give the linear dispersion relation

$$D(\omega, k) = 0. \quad (1.15)$$

From Eqs. (1.11) to (1.14), to order  $\epsilon^2$ , the secularity removal condition is

$$A_1 + V_g B_1 = 0, \quad (1.16)$$

where  $V_g$  is the group velocity of the plane waves. Similarly the condition for the removal of the secularity, to order  $\epsilon^3$ , can be shown to be

$$\begin{aligned}& i(A_2 + V_g B_2) + P(B_1, \frac{\partial B_1}{\partial a} + \bar{B}_1, \frac{\partial B_1}{\partial \bar{a}}) + \\ & Q|a|^2 + R a = 0,\end{aligned}\quad (1.17)$$

where  $P, Q$  and  $R$  are functions of  $\omega$  and  $k$ . The Eqs. (1.16) and (1.17) describe the variation of 'a' with respect to space and time. These conditions can be converted into partial differential equations governing the evolution of 'a' by introducing multiple space and time scales. Let us define the new space and time variables as  $t_2 = \epsilon t$ ,  $t_1 = \epsilon t$ ,  $x_2 = \epsilon x$ ,  $x_1 = \epsilon x$ , then Eq. (1.16) can be written as,

$$\frac{\partial a}{\partial t_1} + v_g \frac{\partial a}{\partial x_1} = 0. \quad (1.18)$$

This equation indicates that in the slower scale  $x_1, t_1$ , the amplitude 'a' propagates with the group velocity  $v_g$  without any change of form. Similarly Eq. (1.17) can be written as

$$i \frac{\partial a}{\partial \tau} + P \frac{\partial^2 a}{\partial \xi^2} + Q |a|^2 a + R a = 0, \quad (1.19)$$

where  $\tau = \epsilon^2 t$  and  $\xi = \epsilon(x - v_g t)$ .

This is the nonlinear Schrödinger equation.

In chapter 4, with the help of KMB scheme, we have investigated the time evolution of nonlinear IAW in a highly dispersive and weakly inhomogeneous two electron species plasma with nonuniform temperatures. The electron temperature inhomogeneities are taken to be much weaker than

the density inhomogeneities because the heat conductivity ( $\sim T_{1,2}^{5/2}$ , where  $T_{1,2}$  are the electron temperatures) is very large at high temperatures and in that case it is difficult to maintain large temperature gradients. IAW are found to be governed by the modified NSE. Since it is difficult to solve the modified nonlinear Schrödinger equation (MNSE) analytically, we have computed the time evolution of the envelope solitons and holes numerically. Our computations show that the width and maximum amplitude of the envelope soliton decrease because of the second electron component. An envelope soliton propagating towards higher density and temperature, splits into two solitary waves, however, the splitting time is longer compared to the one in a single electron component plasma. The effect of the second electron species on the envelope holes is more drastic in the sense that splitting either does not take place or if it does, it happens after a very long time which may not be practical.

In all our previous investigations, we have considered plasmas where electrons are hotter than the ions. But the satellite measurements in the earth's magnetosphere have indicated that in the ring current around  $7 R_E$  (Russel and Thorne, 1970), at geocentric radial distances of  $23-46 R_E$  in the magnetotail (Frank et al., 1976), ions

are hotter than the electrons. Magnetised plasmas with hot ions and relatively colder electrons also occur in some fusion plasma devices like the 2 X II B mirror machine (Coensgen et al., 1976), neutral beam injected tokamak (Eubank et al., 1979), etc. In plasmas where ions are hotter than the electrons, for oscillations across the magnetic field, the electrons are more tightly bound to the magnetic field than the ions and the effective mass of the electrons can be greater than ion mass. Under these conditions, electron acoustic waves (EAW) are generated. EAW are similar to the IAW, with the role of ions and electrons interchanged.

The plasma which contains two species of magnetised ions, can sustain a new resonance branch which depends on the motion of the ions only. This branch is known as ion-ion-hybrid resonance (IIHR) mode. Thus in a multi-ion-species magnetoplasma with ions hotter than the electrons, both EA and IIHR modes can exist. Since EAW arises due to the balance between the ion thermal pressure and electron inertia, the wave characteristics will strongly depend on the temperature of both species of ions and their relative concentration. The motion of two species of magnetised ions result in IIHR mode and hence their properties will



be modified by any change in the mass, temperature and relative concentration of the two ion components. In chapter 5, we have investigated the effect of the relative concentration, mass and temperature of the second ion species on the EA and IIHR waves (Dash, Sharma and Buti, 1983).

One of the most challenging problems in the field of plasma physics is to find a method to heat the plasma to a thermonuclear temperature. The process of mode conversion provides an excellent tool for achieving this goal. Since the pioneering work of Stix (1965), this process has received increased attention. The process of mode conversion can be described as follows. Plasmas in presence of a magnetic field can support a number of modes at nearly equal frequencies. In general, these modes can have different wave numbers but for certain value of the parameters of the system the wavenumbers may coalesce. For example, when inhomogeneity in different physical quantities (like density, temperature, magnetic field etc.) is present, there may exist certain localised regions where the wave numbers corresponding to two modes at same frequency are equal. If one of these modes, while propagating in the medium approaches the region

where its wavenumber will coalesce with that of the other mode at the same frequency, the incident wave may be reflected or refracted in the same mode, or absorbed or converted into the other, or even may undergo some combination of all these. When the wave accessible from plasma periphery is thus converted to another mode which in turn can be damped by cyclotron damping, Landau damping etc., the electrons and the ions can be heated. Recent experimental results suggest that mode conversion plays an important role in heating of the plasmas near the ion cyclotron frequency (Hosea, 1979). Near the ion cyclotron frequency, mode conversion may take place between the fast magnetosonic wave and the ion Bernstein wave at the second and higher ion cyclotron harmonics (Weynants, 1974; Swanson and Ngan, 1975). Stix (1965) had shown that if a fast electromagnetic wave is excited in the plasma by shining electromagnetic radiation on it, the wave will travel inward and at the lower hybrid critical layer it is reflected and converted into the slow ion plasma mode. While travelling out, this mode slows down further and its velocity and wavelength become comparable to the ion thermal velocity and electron Larmor radius. If the frequency of this slow wave is close to the harmonics of ion cyclotron frequency, the wave energy will be

absorbed via collisionless ion cyclotron damping and the ions can be heated. When a few percent of impurity ions like hydrogen or  $^3\text{He}$  in deuteron plasma are present, mode conversion can occur near ion-ion hybrid resonance. Swanson (1976) had investigated the mode conversion of fast Alfvén waves to ion Bernstein waves near the IIHR layer and found that fast Alfvén waves incident from the high magnetic field side will experience mode conversion whereas, those Alfvén waves incident from the low field side will be reflected back in the same mode.

When inhomogeneity is present in a plasma in a direction perpendicular to the magnetic field, drift waves may be excited with a phase velocity, across the magnetic field, of the order of drift velocity of the particles. These drift waves can couple with the electron acoustic waves giving rise to electron acoustic drift instability (Sharma et al., 1982).

Since a magnetoplasma in presence of inhomogeneity, can sustain more than one type of wave, there is a possibility of mode conversion between them; coupling with the drift wave, they can also become drift unstable. In chapter 6, we have studied the propagation characteristics of EA and IIHR waves in a multi ion species plasmas with

ions hotter than electrons and with density gradients perpendicular to the magnetic field and the direction of wave propagation. We have also examined the drift instabilities of EA and IIHR waves and the possibility of mode conversion between them. Numerical analysis of the dispersion relation shows that the coupling between the drift wave and EA and IIHR waves can give rise to instabilities when the strength of inhomogeneity  $L^{-1} (= n_{e0}^{-1} dn_e/dx)$ , where  $n_{e0}$  is the equilibrium electron density) exceeds a certain threshold value (Dash, Sharma and Buti, 1983). The threshold value of  $L^{-1}$  for EA-drift instability is found to be lower than the threshold value of  $L^{-1}$  for IIHR drift instability. It is noted that the region of instability for both the modes increase with an increase in inhomogeneity. We have also found that for weakly inhomogeneous plasmas with density gradients perpendicular to the magnetic field as well as the direction of wave propagation, within the framework of fluid theory, there is no possibility of mode conversion between the EA and the IIHR waves in the systems we have studied, i.e. the 2XIIB mirror machines and the earth's magnetosphere.

## CHAPTER 2

### EFFECT OF HOT IONS ON ION ACOUSTIC SOLITONS AND HOLES

#### 2.1 Introduction

The coexistence of relatively cold electrons in the bulk of hot electrons is not uncommon in the laboratory as well as in space. Examples of such plasmas can be found in hot cathode discharge plasmas (Oleson and Found, 1949), in the ELMO confinement device (Krall and Trivelpiece, 1973) etc. Turbulent plasmas of thermonuclear interest have high energy tails in the electron distribution; these super-

thermal electrons are produced due to the interaction of localised high frequency fields with the charged particles (Morales and Lee, 1974). IMP 7 and 8 Satellite data have also shown the existence of double Maxwellian electron distribution in the solar wind near 1 AU (Feldman et al., 1975).

When the plasma contains two species of electrons with different temperatures, the system is governed by the effective temperature which depends on the temperature and fractional densities of the two electron components (Jones et al., 1975). They had shown that as the difference of temperature, between the two components, increases, the effective temperature and hence the propagation characteristics of the ion acoustic wave (IAW) is dominantly governed by the colder temperature. In a weakly nonlinear system with two electron components, Goswami and Buti (1976) had shown that the ion acoustic solitary wave has a larger amplitude for a given width compared to the one in a plasma with single electron species. Investigating the exact localised nonlinear IAW in a two electron component plasma with cold ions, Buti (1980) has shown the possible existence of ion acoustic solitons (density humps) as well as holes (density dips).

In a weakly nonlinear plasma the IAW is governed by KdV equation (Washimi and Taniuti, 1966) which predicts the relationship between velocity and amplitude of the KdV soliton. But the experimental value of velocity was found to be larger than the value predicted theoretically (Ikezi et al., 1970). This discrepancy in theoretical and experimental results suggests that finite ion temperature effects should be incorporated into the theory. Tappert (1972) had modified the KdV equation by taking the finite ion temperature into account but the velocity increased only slightly. Instead of restricting the analysis to weakly nonlinear systems, Sakanaka had worked with strongly nonlinear plasmas and had shown that the inclusion of finite ion temperature could predict a more realistic value for velocity. By retaining the full nonlinearities, in this chapter, we have investigated the effect of hot ions ( $T_i \neq 0$ , but  $T_i \ll T_1, T_2$ : the subscripts 1 and 2 refer to the hot and warm electron components respectively) on the ion acoustic solitary waves. From the original set of equations a single equation is obtained. This equation is similar to the energy integral of a classical particle of unit mass moving in an effective potential. Our analysis shows that even an extremely small ion temperature can drastically reduce the maximum amplitude for solitons

as well as holes (Dash and Buti, 1981).

## 2.2 Energy Integral

Let us consider a plasma with ions and two species of electrons with densities  $n_{i0}$ ,  $n_{10}$  and  $n_{20}$  respectively. The basic equations governing such a system are the ion continuity equation, the momentum transfer equation for ions and both types of electrons and the Poisson equation, namely,

$$\frac{\partial n_i}{\partial t} + \frac{\partial}{\partial x} (n_i v_i) = 0, \quad (2.1)$$

$$m_i \left( \frac{\partial v_i}{\partial t} + v_i \frac{\partial v_i}{\partial x} \right) = -e \frac{\partial \phi}{\partial x} - \frac{T_i}{n_i} \frac{\partial n_i}{\partial x}, \quad (2.2)$$

$$e \frac{\partial \phi}{\partial x} - \frac{T_1}{n_1} \frac{\partial n_1}{\partial x} = 0, \quad (2.3)$$

$$e \frac{\partial \phi}{\partial x} - \frac{T_2}{n_2} \frac{\partial n_2}{\partial x} = 0, \quad (2.4)$$

and

$$\frac{\partial^2 \phi}{\partial x^2} = -4\pi e (n_i - n_1 - n_2). \quad (2.5)$$



In writing Eqs.(2.3) and (2.4), electron inertia is neglected and we have assumed that both the electron components are separately in equilibrium with the potential  $\phi$ . This assumption is justified provided the phase velocity of the wave is much smaller than the thermal velocity of both the electron components separately, i.e.  $T_{\text{eff}}/m_i \ll T_{1,2}/m_e$ , where  $T_{\text{eff}} (= n_0 T_1 T_2 (n_1 T_2 + n_2 T_1)^{-1})$  is the effective temperature of the electrons. Since  $T_i \ll T_{1,2}$ , we have neglected the effect of Landau damping. Furthermore, the plasma is treated as collisionless; this assumption is valid for the solar wind plasma at 1 AU.

Normalising the densities to  $n_0 = n_{10} + n_{20}$ ,  $t$  to  $\omega_{p_i}^{-1}$ ,  $x$  to  $v_{\text{eff}}/\omega_{p_i}$ ,  $v$  to  $v_{\text{eff}}$  and  $\phi$  to  $T_{\text{eff}}/e$ , where  $v_{\text{eff}} = (T_{\text{eff}}/m_i)^{1/2}$ , the equations (2.1) to (2.5) can be written as,

$$\frac{\partial n}{\partial t} + \frac{\partial}{\partial x}(nv) = 0, \quad (2.6)$$

$$\frac{\partial v}{\partial t} + v \frac{\partial v}{\partial x} = -\frac{\partial \phi}{\partial x} - \frac{T_i}{T_{\text{eff}}} \frac{\partial}{\partial x} \ln x, \quad (2.7)$$

$$n_i = \alpha_i \exp\left(\frac{T_{\text{eff}}}{T_i} \phi\right), \quad (2.8)$$

$$n_2 = \alpha_2 \exp\left(\frac{T_{\text{eff}}}{T_2} \phi\right), \quad (2.9)$$

and

$$\frac{\partial^2 \phi}{\partial x^2} = -n + \alpha_1 \exp\left(\frac{T_{\text{eff}}}{T_1} \phi\right) + \alpha_2 \exp\left(\frac{T_{\text{eff}}}{T_2} \phi\right), \quad (2.10)$$

where  $n$ ,  $\alpha_1$ , and  $\alpha_2$  denote the normalised ion and electron densities respectively. Transforming to a frame of reference  $\xi = x - Mt$ , which moves with a constant velocity  $M$  with respect to the  $x$ - $t$  coordinate frame, and eliminating  $v$  from equations (2.6) and (2.7), we can write

$$n = M \left[ M^2 - 2\phi - 2(T_i/T_{\text{eff}}) \ln n \right]^{-1/2}. \quad (2.11)$$

Eliminating  $\phi$  between (2.10) and (2.11), we obtain

$$\frac{1}{2} \left( \frac{dn}{d\xi} \right)^2 + \psi(n, M) = 0, \quad (2.12)$$

where

$$\begin{aligned} \psi(n, M) = & \left( M^2 n^{-3} - n^{-1} T_i / T_{\text{eff}} \right)^{-2} \left[ M^2 (1 - n^{-1}) + \right. \\ & (1 - n) T_i / T_{\text{eff}} + \alpha_1 (T_i / T_{\text{eff}}) \left[ 1 - \exp \left\{ (T_{\text{eff}} / T_1) \times \right. \right. \\ & \left. \left. \left[ - (T_i / T_{\text{eff}}) \ln n + \frac{1}{2} M^2 (1 - n^{-2}) \right] \right\} \right] + \alpha_2 (T_2 / T_{\text{eff}}) \left[ \right. \\ & \left. \left. - \exp \left\{ (T_{\text{eff}} / T_2) \left[ - (T_i / T_{\text{eff}}) \ln n + \frac{1}{2} M^2 (1 - n^{-2}) \right] \right\} \right] \right] \quad (2.13) \end{aligned}$$

Eq.(2.12) is the energy integral of a classical particle of unit mass moving in the effective potential  $\psi(n, M)$  (more commonly known as the Sagdeev potential) with the kinetic energy  $1/2(dn/d\xi)^2$ . In deriving the energy integral, the boundary conditions  $n = 1$  and  $dn/d\xi = 0$  at  $\xi = \pm \infty$  have been used.

### 2.3 Solitary Waves

To ascertain the existence of solitary waves, we have analysed the Sagdeev potential. Expanding  $\psi$  around  $n = 1$ , we obtain

$$\psi(n \approx 1, M) = -\frac{1}{2}(n-1)^2(M^2 - T_i/T_{eff})^{-1} \{M^2 - (1 + T_i/T_{eff})\}. \quad (2.14)$$

From Eq.(2.12) it is evident that  $\psi(n, M) < 0$  for real solutions. So  $\psi(n \approx 1, M)$  has to be negative and hence Eq.(2.14) demands that either  $M^2 > (1 + T_i/T_{eff})$  or  $M^2 < T_i/T_{eff}$ . But if  $M^2 < T_i/T_{eff}$ , the IAW will travel with a velocity smaller than the ion thermal speed which is not physical. So such small values of  $M^2$  are not allowed. Hence only the supersonic ion acoustic solitary waves are allowed in the system. Further analysis of  $\psi$  shows that  $n = N$  is an extremum provided the Mach number  $M$

satisfies the relation.

$$\begin{aligned}
 & M^2 \left(1 - \frac{1}{N}\right) + \gamma \frac{\mu+2}{\mu+1} (1-N) + \frac{\mu+2}{(\mu+1)^2} \left(\mu + \frac{1}{2}\right) - \\
 & \frac{\mu(\mu+1)}{(\mu+2)^2} \exp \left\{ \frac{\mu+1}{\mu+2} \left[ -\frac{\mu+2}{\mu+1} \gamma \ln N + \right. \right. \\
 & \left. \left. \frac{1}{2} M^2 \left(1 - \frac{1}{N^2}\right) \right] \right\} - \frac{\mu+2}{2(\mu+1)^2} \exp \left\{ \frac{2(\mu+1)}{\mu+2} \left[ -\frac{\mu+2}{\mu+1} \gamma \ln N + \right. \right. \\
 & \left. \left. \frac{1}{2} M^2 \left(1 - \frac{1}{N^2}\right) \right] \right\} = 0. \quad (2.15)
 \end{aligned}$$

This equation gives the relationship between  $M$  and the maximum amplitude  $N$  of the nonlinear wave. In Eq. (2.15),  $\mu = \alpha_1/\alpha_2$ ,  $\nu = T_1/T_2$  and  $\gamma = T_i/T_1$ . For  $T_i = 0$ , Eq. (2.15) reduces to that obtained by Buti (1980). The critical Mach number  $M_c$  (corresponding to the maximum potential) can be calculated easily from Eq. (2.15). The results are shown in table 1. Unlike the cold ion case,  $N$  has an upper limit given by

$$N_u = M_c \gamma^{-1/2} \left[ (\mu+1)/(\mu+2) \right]^{1/2}. \quad (2.16)$$

$N_u$  for different values of  $\mu$ ,  $\nu$  and  $\gamma$  are tabulated in table 2.

Expanding  $\psi$  around  $n = N$ , from Eq. (2.13) we obtain

$$\psi(n \approx N, M) \approx (n - N) \frac{M^2}{N^3} \left( \frac{M^2}{N^3} - \frac{1}{N} \frac{T_c}{T_{eff}} \right)^{-2} F(N, M), \quad (2.17)$$

where

$$\begin{aligned} F(N, M) = & N - \frac{N^3}{M^2} \gamma \frac{\mu+2}{\mu+1} + \left[ \frac{N^2}{M^2} \gamma \times \right. \\ & \left. \frac{\mu(\mu+2)}{(\mu+1)^2} - \frac{\mu}{\mu+1} \right] \exp \left\{ \frac{\mu+1}{\mu+2} \left[ -\frac{\mu+2}{\mu+1} \gamma \ln N \right. \right. \\ & \left. \left. + \frac{1}{2} M^2 \left( 1 - \frac{1}{N^2} \right) \right] \right\} + \left[ \frac{N^2}{M^2} \gamma \frac{\mu+2}{(\mu+1)^2} - \frac{1}{\mu+1} \right] \times \\ & \exp \left\{ \frac{2(\mu+1)}{\mu+2} \left[ -\frac{\mu+2}{\mu+1} \gamma \ln N + \frac{1}{2} M^2 \left( 1 - \frac{1}{N^2} \right) \right] \right\}. \quad (2.18) \end{aligned}$$

From Eq. (2.14) one can see that  $n = 1$  is a double root of the equation  $\psi(n, M) = 0$  which implies that both  $\psi$  and  $d\psi/dn$  vanish but  $d^2\psi/dn^2$  is finite at  $n = 1$ . Again from Eqs. (2.15) and (2.17) it can be seen that  $\psi(n, M)$  vanishes but  $d\psi/dn$  is finite at  $n = N$ . Hence the necessary conditions for the existence of solitary waves (as discussed in chapter 1) are satisfied. Since  $\psi$  has

to be negative, Eq.(2.16) requires that  $F(N,M) < 0$  for holes ( $N < 1$ ) and  $F(N,M) > 0$  for solitons ( $N > 1$ ). Hence in the system under consideration, ion acoustic holes are assured if and only if  $F(N,M) < 0$  and  $M_1^2 > (1 + T_i/T_{eff})$ , where  $M = M_1$  satisfies Eq. (2.15).

In an one electron component plasma, i.e. for  $\nu = 1$ , Eq.(2.17) can be written as

$$\bar{F}(N, M, \nu=1) = \left(1 - \frac{N^2 T_i}{M^2 T_e}\right) \left[ N - \exp\left\{-\frac{T_i}{T_e} \ln N + \frac{M^2}{2} \left(1 - \frac{1}{N^2}\right)\right\} \right] \quad (2.19)$$

Therefore, for  $N < 1$ ,  $F(N,M) > 0$  and the condition for the existence of holes is not satisfied. So hole solutions are not possible in a plasma having one electron species. The presence of the second electron species is essential for the existence of holes.

By solving equations (2.15) and (2.18), the allowed regions for the existence of solitons and holes can in principle be obtained. But since these equations are complicated transcendental equations, it is not possible to solve them analytically. So we have solved them numerically. Before discussing the numerical results,

let us first consider the small amplitude case where analytical solutions can be obtained.

#### 2.4 Small Amplitude Limit

In the small amplitude limit the Sagdeev potential is simplified and it is possible to have an analytic solution. On taking  $n = 1 + \delta n$ , where  $\delta n \ll 1$ , and retaining terms upto  $\delta n^3$ , Eq. (2.11) can be written as

$$\frac{1}{2} \left( \frac{d \delta n}{d \xi} \right)^2 + \chi_1 \delta n^2 + \chi_2 \delta n^3, \quad (2.20)$$

where

$$\chi_1 = -\frac{1}{2} (M^2 - T_i / T_{eff})^{-1} [M^2 - (1 + T_i / T_{eff})], \quad (2.21)$$

$$\chi_2 = \frac{1}{2} (M^2 - T_i / T_{eff})^{-1} \left[ 4 (M^2 - \frac{1}{3} T_i / T_{eff}) (M^2 - T_i / T_{eff})^{-1} - 3 (M^2 - \frac{1}{3} T_i / T_{eff}) - \frac{1}{3} \Delta (M^2 - T_i / T_{eff})^2 \right]. \quad (2.22)$$

and

$$\Delta = (\alpha_1 / T_1^2 + \alpha_2 / T_2^2) T_{\text{eff}}^2. \quad (2.23)$$

Eq.(2.20) has the solution

$$\delta n = -(\chi_1 / \chi_2) \text{sech}^2 [(-\chi_1 / 2)^{1/2} \xi]. \quad (2.24)$$

Since  $\chi_1$  is always negative, depending on whether  $\chi_2 > 0$  or  $\chi_2 < 0$ , soliton or hole solutions are obtained. For  $M^2 - T_i / T_{\text{eff}} \approx 1$ , we find that  $\chi_2 < 0$  if

$$\Delta > (3 + 2 T_i / T_{\text{eff}}). \quad (2.25)$$

Here  $T_i$  appears as a correction factor only, but it is not so in the finite amplitude case as can be seen from the numerical computations. In a single electron component plasma,  $\Delta = 1$  and so the condition (2.25) can never be satisfied. Hence holes do not occur in a single electron component plasma. From Eq.(2.25), it is apparent that the condition for the existence of holes becomes more stringent for finite  $T_i$ .



## 2.5 Numerical Results

IMP 7 satellite data had shown that in the solar wind around the orbit of the earth, two species of electrons, a relatively dense component ( $N_1 \sim 20 \text{ cm}^{-3}$ ) at temperature  $T_1 \sim 2 \times 10^5 \text{ K}$  and a relatively cold component ( $N \sim 5 \text{ cm}^{-3}$ ) at  $T_2 \sim 10^4 \text{ K}$  are present. In the experiment of Jones et al. (1975), two species of electrons are present at temperatures  $3 \times 10^4 \text{ K}$  and  $1 \times 10^4 \text{ K}$  with densities between  $10^8$  and  $10^9 \text{ cm}^{-3}$ . For typical values of  $\gamma = 0.02$  and  $0.05$ , we have computed the allowed regions for the existence of solitons and holes. Let  $M = M^*$  be the root of the equation  $F(N, M) = 0$ . From numerical computations, we find that for  $M < M^*$ ,  $F(N, M) < 0$  for  $N < 1$  and  $F(N, M) > 0$  for  $N > 1$ . So the allowed regions for the existence of holes as well as solitons would be between the lines  $M^2 = M^{*2}$  and  $M^2 = M_L^2$  where  $M_L^2 = (1 + T_i/T_{\text{eff}})$  with the condition that  $M_1^2 < M^{*2}$ .

The critical Mach number  $M_c^2$  is calculated for different values of  $\mu$ ,  $\alpha$  and  $\gamma$  and is tabulated in table 1 which shows that  $M_c^2$  decreases as  $\gamma$  increases. Another interesting result due to the finite temperature of ions is that there exists an upper limit on the maximum value of  $N$ , whereas,  $N \rightarrow \infty$  in the case of cold

ions. In table 2, we have listed the values of  $N_u$  for different values of  $\mu$ ,  $\nu$  and  $\gamma$ . From this table, it is apparent that  $N_u$  decreases as  $\gamma$  increases. So increase in  $\gamma$  causes  $M_c^2$  and  $N_u$  to decrease. Hence the allowed regions for solitons are decreased by the limits set by  $M_c^2$  and  $N_u$ . In fig.1 we have plotted  $M^2$  versus  $N$  for  $\mu = 3$ ,  $\nu = 5$  and  $\gamma = 0.0, 0.02$  and  $0.05$ . It is clearly seen that the allowed regions for solitons decrease as  $\gamma$  increases from  $0.0$  to  $0.05$ . From fig.2 it is apparent that the allowed regions for solitons decrease as  $\nu$  increases. However, fig.3 shows that the allowed regions for solitons increase as  $\mu$  increases. This last result is in contradiction with the results obtained in a plasma having cold ions. In such a plasma, with two electron species, the allowed region for solitons decrease as  $\mu$  increases (Buti, 1980). This discrepancy can be explained as follows. Due to the finite ion temperature, there exists an upper limit for  $N$  which is larger for larger  $\mu$ . So, even though  $M_c^2$  is smaller for larger  $\mu$ ,  $M_c^2$  is also smaller and together with larger  $N_u$ , the allowed region for solitons increases as  $\mu$  increases.

Let us now discuss about the holes. In fig.4  $M^2$  is plotted against  $N$  for  $\mu = 3$ ,  $\nu = 20$  and  $\gamma = 0.02$  which shows that as  $\gamma$  increases from  $0.0$  to  $0.02$ , the

allowed region for holes is drastically reduced. Moreover, as  $\gamma$  increases to 0.05, holes are destroyed. From fig.5, it can be seen that for  $\mu = 3$  and  $\gamma = 0.02$ , holes exist when  $\mathcal{V} = 20$ . But when  $\mathcal{V}$  is reduced to 18.0, holes are forbidden. As a matter of fact, there exist a critical value of  $\mathcal{V}$  ( $= \mathcal{V}_c$ ), below which holes do not occur. For  $\mu = 3$  and  $\gamma = 0.02$ ,  $\mathcal{V}_c$  is found to be 19. Fig.6 illustrates allowed regions for holes for different values of  $\mu$ . As is seen, for  $\mathcal{V} = 20.0$  and  $\gamma = 0.02$ , holes are forbidden for  $\mu = 1$  but when  $\mu$  increases to 3, there exists an allowed region for the occurrence of holes.

## 2.6 Conclusions

From the numerical results, we find that for the finite amplitude ion acoustic solitary waves, the allowed regions for the existence of solitons and holes decrease as the ion temperature increases. The hotter the ions, more drastic are these effects, so much so that in some cases holes are even forbidden. Finite ion temperature also reduces the critical Mach number. Furthermore, finite ion temperature imposes an upper limit on  $N$  which is inversely proportional to the square root of  $\gamma$ .

TABLE 1

$M_C^2$  for various values of  $\mu$ ,  $\nu$  and  $\gamma$ .

$\gamma = 0.02$				$\gamma = 0.05$			
$\mu \backslash \nu$	1	5	10	$\mu \backslash \nu$	1	5	
0.1	2.121	1.900	1.364	0.1	1.9997	1.879	
1.0	2.121	1.760	1.664	1.0	1.9997	1.732	
3.0	2.121	1.633	1.432	3.0	1.9997	1.609	
5.0	2.121	1.595	1.322	5.0	1.9997	1.571	
10.0	2.121	1.588	1.207	10.0	1.9997	1.561	

TABLE 2

$N_u$  for various values of  $\mu$ ,  $\nu$  and  $\gamma$ .

$\gamma = 0.02$				$\gamma = 0.05$		
$\mu \backslash \nu$	1	5	10	$\mu \backslash \nu$	1	5
0.1	10.29	4.52	3.185	0.1	6.32	2.84
1.0	10.29	5.4	3.88	1.0	6.32	3.39
3.0	10.29	6.38	4.69	3.0	6.32	4.01
5.0	10.29	6.92	5.14	5.0	6.32	4.34
10.0	10.29	7.63	5.76	10.0	6.32	4.78

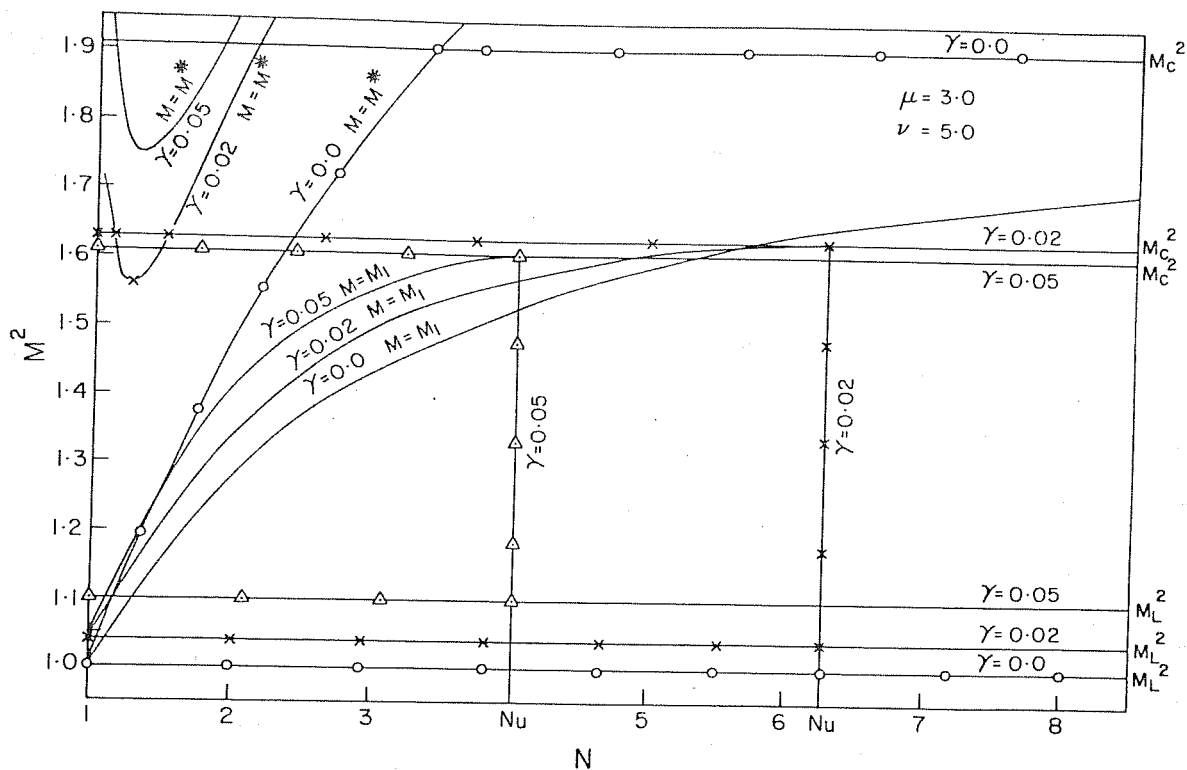


Fig.1 :  $M^2$  versus  $N(N > 1)$  for  $\mu = 3$ ,  $\nu = 5$  and  $\gamma = 0.00$ ,  $0.02$  and  $0.05$ . The upper allowed value of  $M$  is given by either  $M_c^2$  or  $M^*$ , whichever is the smaller. The region bounded by the lines  $-\circ-\circ-$  ( $\gamma = 0$ ),  $-x-x-$  ( $\gamma = 0.02$ ) and  $-\triangle-\triangle-$  ( $\gamma = 0.05$ ) are the allowed regions for solitons.

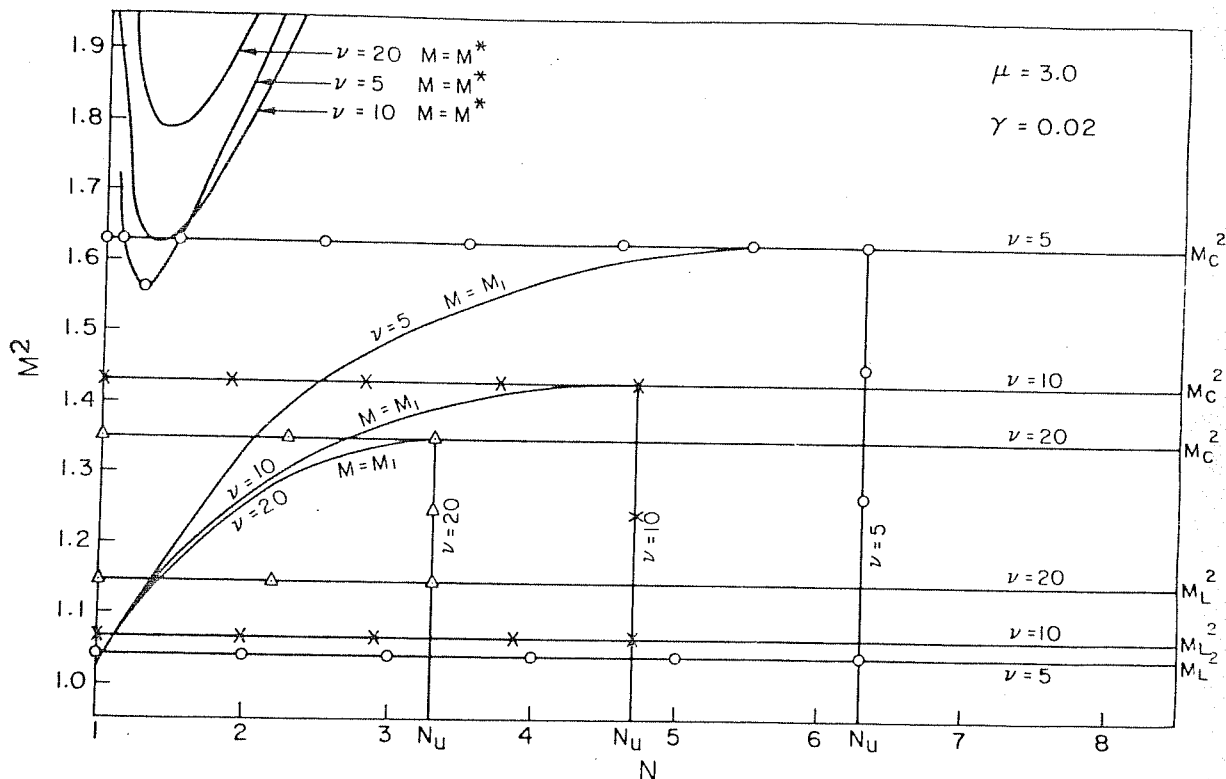


Fig. 2 :  $M^2$  versus  $N$  for  $\mu = 3$ ,  $\gamma = 0.02$  and  $\nu = 5, 10$  and 20. The upper allowed value of  $M$  is given by either  $M_C$  or  $M^*$ , whichever is the smaller. The region bounded by the lines  $-o-o-$  ( $\nu = 5$ ),  $-x-x-$  ( $\nu = 10$ ) and  $-\triangle-\triangle-$  ( $\nu = 20$ ) are the allowed regions for solitons.

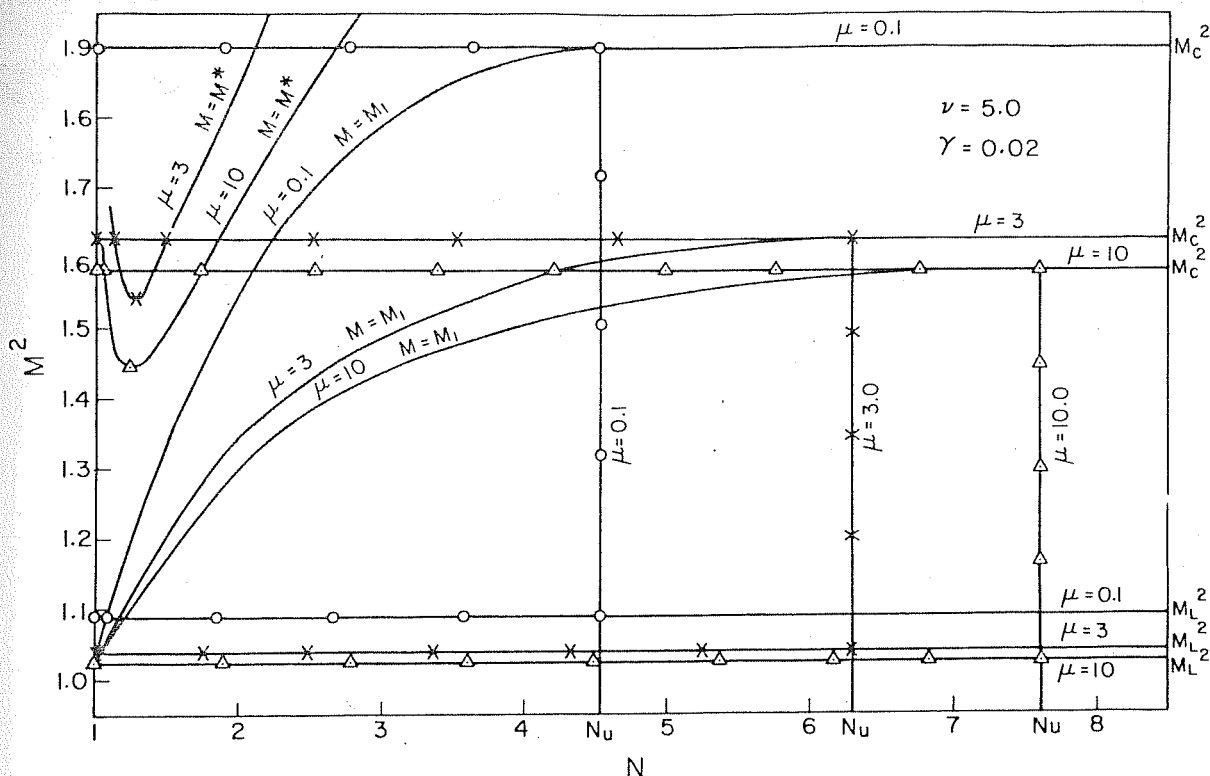


Fig.3 :  $M^2$  versus  $N$  for  $\nu = 5$ ,  $\gamma = 0.02$  and  $\mu = 0.1, 3$  and 10. The upper allowed value of  $M$  is given by either  $M_c$  or  $M^*$ , whichever is the smaller. The region bounded by the lines  $-o-o-$  ( $\mu = 0.1$ ),  $-x-x-$  ( $\mu = 3$ ) and  $-\triangle\triangle-$  ( $\mu = 10$ ) are the allowed regions for solitons.



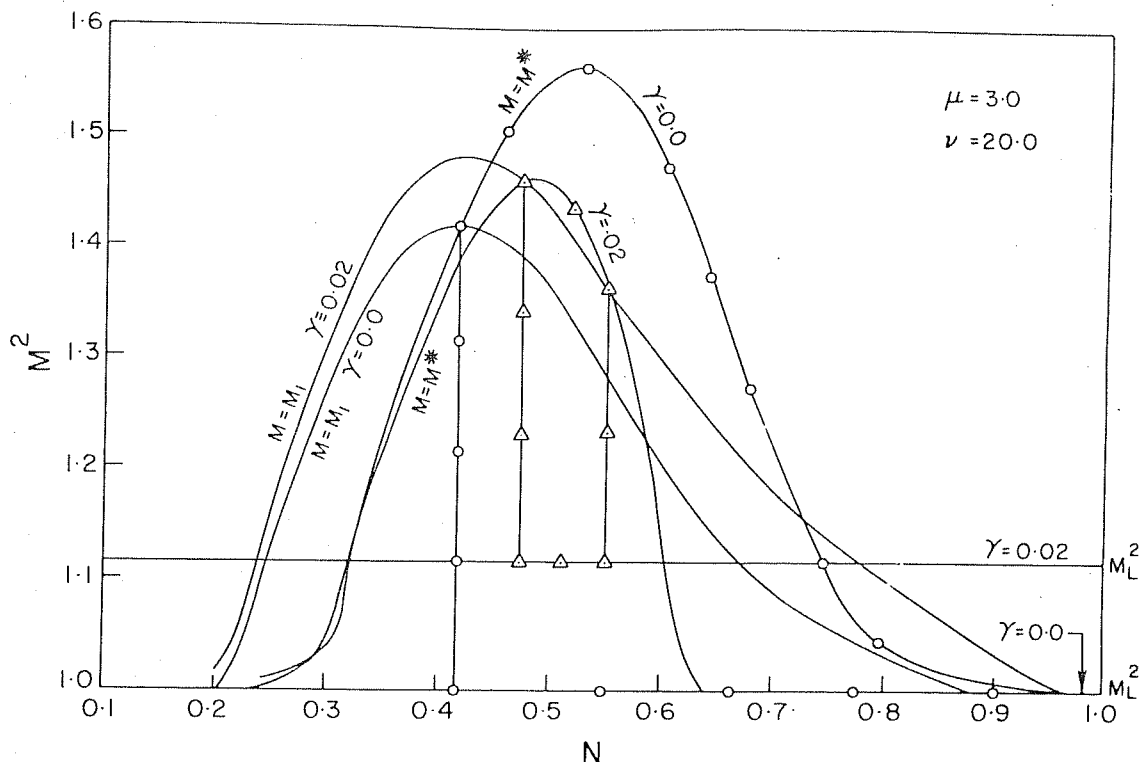


Fig.4 :  $M^2$  versus  $N$  ( $N < 1$ ) for  $\mu = 3$ ,  $\nu = 20$ ,  $\gamma = 0.0$  and  $0.02$ . The region between the curves  $M = M_1$  and  $M = M^*$  bounded by the lines  $oo$  ( $\gamma = 0$ ) and  $zz$  ( $\gamma = 0.02$ ) are the allowed regions for holes.

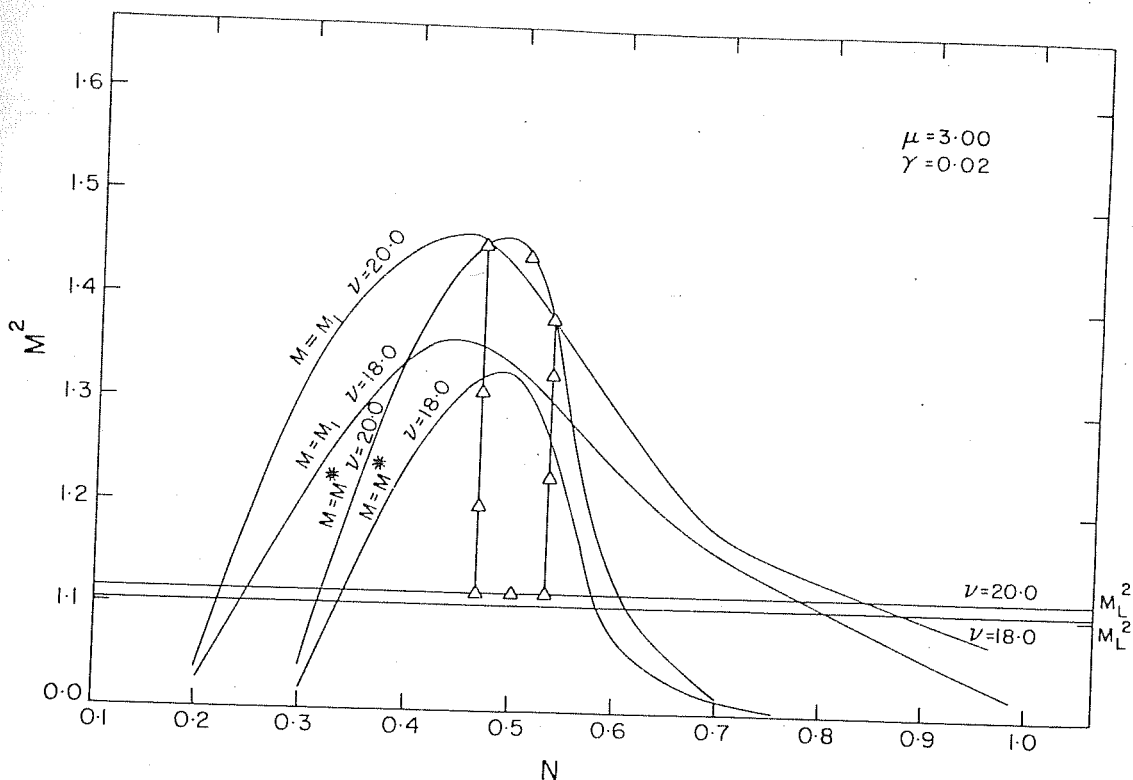


Fig.5 :  $M^2$  versus  $N$  for  $\mu = 3$ ,  $\gamma = 0.02$  and  $\nu = 18$  and  $20$ .  
 The region between the curves  $M = M_1$  and  $M = M^*$  bounded by  
 the lines  $\Delta\Delta(\nu = 20)$  is the allowed region for holes.  
 Holes are forbidden for  $\nu = 18$ .



## CHAPTER 3

### COMPRESSIVE AND RAREFACTORY ELECTROSTATIC ION CYCLOTRON SOLITARY WAVES IN MULTISPECIES MAGNETOPLASMAS

#### 3.1 Introduction

The existence of electrostatic ion cyclotron (EIC) waves in magnetised plasmas is well known. These EIC waves were first observed by Motley and D'Angelo (1963). Recently the interest in EIC waves have been revived due to their importance in heating of the plasmas (Edgley et al., 1975; Bohmer et al., 1976; Colestock and Kashuba, 1982). Kelley et al. (1975) had observed electric field oscillations near the local ion gyrofrequency and the presence of an

intense beam of plasma ions at the edge of an auroral arc. They had also detected large amplitude EIC waves at the equatorial edge of an auroral arc. The satellite S3-3 measurements have confirmed the presence of EIC waves in the auroral plasma between the altitudes of 5000 and 8000 km (Hudson et al., 1978; Temerin et al., 1979). Yu (1977) had investigated the nonlinear EIC waves in a single electron species plasma and had shown that solitary EIC waves do exist in the plasma. These solitary waves were found to be rarefactive waves.

As we have mentioned in the earlier chapters, there exist situations, both in the laboratory as well as in space, where the plasma contains two species of electrons at different temperatures. The presence of EIC waves have been detected in many such plasmas. As an example, the auroral plasmas have two components of electrons (Garret, 1979) and EIC waves are observed in this region (Hudson et al., 1978; etc.). Previous studies had shown that the nature of wave propagation is significantly modified in a multi-component plasma (Jones et al., 1975; Goswami and Buti, 1976; Lisak, 1980; Buti, 1980; Buti and Yu, 1981). Lisak (1980) had investigated the modulational instability of plane EIC waves in a plasma consisting of cold ions and

two species of electrons at different temperatures and had shown that the range of wavenumbers corresponding to the instability is substantially affected by the presence of the second electron component. Investigations on nonlinear IAW in a multi-component plasma by Buti (1980) indicate that because of the second electron species it is possible to have rarefactive solitons besides compressive solitons. It would be interesting to see if the presence of the second electron component can introduce compressive EIC solitary waves.

Recently Witt and Lotko (1983) have studied the obliquely propagating ion acoustic solitary waves in a two-electron-component magnetoplasma. Using quasineutrality, they have obtained an exact, time-stationary nonlinear equation relating the ion density to the electrostatic potential. This equation describes ion acoustic solitary waves in the limit  $M \gtrsim \cos \theta$  and EIC solitary waves in the limit  $M \lesssim 1$ , where  $M$  is the Mach number and  $\theta$  is the angle between the magnetic field and the direction of wave propagation. However, Witt and Lotko (1983) have confined their studies to the ion acoustic solitary waves.

In this chapter, we present our investigations relating to the existence and nature of EIC solitary waves

in a two electron component magnetoplasma. Taking into account the complete ion nonlinearities, we obtain an equation governing the waves in such a plasma. In the limit of zero magnetic field, this equation governs the ion acoustic solitary waves, whereas, it governs EIC solitary waves when the condition of charge neutrality is imposed. Our analysis have revealed that besides the rarefactive EIC solitary waves, which exists in a single electron species plasma, a new type of solitary wave, namely, the compressive solitary wave can also arise because of the second electron species. Under certain restricted conditions both rarefactive and compressive solitary waves can even coexist. We also show that the presence of the second electron component in the auroral plasma can explain the formation of perpendicular shocks observed by Mozer et al. (1977).

### 3.2 Basic Equations

Let us consider a two-electron-component plasma with hot ions in an external magnetic field  $B_0$ . Further, let the densities and the temperatures of electrons and ions be  $n_{10}$ ,  $n_{20}$ ,  $n_{i0}$  and  $T_1$ ,  $T_2$ ,  $T_i$  respectively with

$T_i \ll T_1, T_2$ . For  $B_0$  along the  $z$ -direction and  $k_z/k \gg (m_e/m_i)^{1/2}$ , the electrons can move along the field lines and have Boltzmann distribution. However, the ions move essentially in a plane perpendicular to the magnetic field and their motion along the magnetic field can be neglected i.e.,  $k_z \ll k_x$ . Thus the relevant set of fluid equations for the system under consideration are,

$$\frac{\partial n_i}{\partial t} + \frac{\partial}{\partial x} (n_i v_x) = 0, \quad (3.1)$$

$$\begin{aligned} \frac{\partial v_x}{\partial t} + v_x \frac{\partial v_x}{\partial x} = & -\frac{e}{m_i} \frac{\partial \phi}{\partial x} - \frac{T_i}{m_i n_i} \frac{\partial n_i}{\partial x} \\ & + \Omega_i v_y, \end{aligned} \quad (3.2)$$

$$\frac{\partial v_y}{\partial t} + v_x \frac{\partial v_y}{\partial x} = -\Omega_i v_x, \quad (3.3)$$

$$n_1 = n_{10} \exp(e\phi/T_1), \quad (3.4)$$

$$n_2 = n_{20} \exp(e\phi/T_2), \quad (3.5)$$

and

$$\frac{\partial^2 \phi}{\partial x^2} = 4\pi e (n_1 + n_2 - n_i), \quad (3.6)$$



where  $v$  is the ion fluid velocity,  $\phi$  is the potential, and  $\Omega_i = eB_0/m_i c$  is the ion cyclotron frequency. To obtain the localized stationary solutions, let us go to the frame of reference  $\xi = x - Vt$ ; Eqs. (3.1) to (3.3) can then be written as

$$U_x \left\{ \frac{1}{2} \frac{d^2}{d\xi^2} U_x^2 + \frac{e}{m_i} \frac{d^2 \phi}{d\xi^2} - \frac{T_i}{m_i} \frac{d^2}{d\xi^2} \ln U_x + \Omega^2 \right\} = -\Omega^2 V, \quad (3.7)$$

where  $U_x = v_x - V$ . With the help of Eqs. (3.4) and (3.5), we can write Eq. (3.6) as

$$U_x \frac{d^2 \phi}{d\xi^2} = 4\pi n_0 e \left\{ U_x \alpha_1 \exp(e\phi/T_1) + U_x \alpha_2 \exp(e\phi/T_2) + V \right\}, \quad (3.8)$$

where  $\alpha_{1,2} = n_{1,2}/n_0$ . In deriving Eq. (3.8), we have used the boundary conditions,  $v_x = 0$ , at  $\xi = \pm \infty$ . Eliminating  $U_x$  between Eqs. (3.7) and (3.8), we obtain

$$\begin{aligned}
& (\lambda_{\text{eff}}^2 + R_s^2) \frac{d^2 \phi}{d\xi^2} + \frac{M^2 R_s^2}{2} \frac{d^2}{d\xi^2} \left\{ \lambda_{\text{eff}}^2 \frac{d^2 \phi}{d\xi^2} - \right. \\
& \left. A(\phi) \right\}^{-2} + \frac{T_i}{T_{\text{eff}}} R_s^2 \frac{d^2}{d\xi^2} \ln \left\{ \lambda_{\text{eff}}^2 \frac{d^2 \phi}{d\xi^2} - A(\phi) \right\}^{-2} \\
& = A(\phi) - 1.
\end{aligned}
\tag{3.9}$$

In Eq.(3.9),  $\phi = e\varphi/T_{\text{eff}}$ ,  $C_s = (T_{\text{eff}}/m_i)^{1/2}$ ,  $M = V/c_s$ ,  $R_s = c_s/\Omega_i$ , with  $T_{\text{eff}} = T_1 T_2 (\alpha_1 T_2 + \alpha_2 T_1)^{-1}$ ,  $\lambda_{\text{eff}} = (T_{\text{eff}}/4\pi n_0 e^2)^{1/2}$  and  $A(\phi) = \alpha_1 \exp \left\{ (T_{\text{eff}}/T_1) \phi \right\} + \alpha_2 \exp \left\{ \phi (T_{\text{eff}}/T_2) \right\}$ . In an one electron component plasma, with cold ions, Eq.(3.9) reduces to that obtained by Yu (1977). In the limit  $B_0 = 0$ , Eq.(3.9) can be written as

$$\begin{aligned}
& \frac{d^2}{d\xi^2} \left[ \phi + \frac{M^2}{2} \left\{ \lambda_{\text{eff}}^2 \frac{d^2 \phi}{d\xi^2} - A(\phi) \right\}^{-2} \right. \\
& \left. + \frac{T_i}{T_{\text{eff}}} \ln \left\{ \lambda_{\text{eff}}^2 \frac{d^2 \phi}{d\xi^2} - A(\phi) \right\} \right] = 0.
\end{aligned}
\tag{3.10}$$

Integrating Eq.(3.10) thrice and using the boundary conditions namely,  $\phi = 0$  and  $d\phi/d\xi = 0$  at  $\xi = \pm \infty$ , we obtain the

relation,

$$\frac{1}{2} \left( \frac{d\phi}{d\xi} \right)^2 + \psi(\phi, M) = 0, \quad (3.11)$$

where

$$\begin{aligned} \psi(\phi, M) = & \frac{1}{\lambda_{\text{eff}}^2} \left[ \frac{\alpha_1 T_1}{T_{\text{eff}}} \{1 - \exp(\frac{T_{\text{eff}}}{T_1} \phi)\} \right. \\ & + \frac{\alpha_2 T_2}{T_{\text{eff}}} \{1 - \exp(\frac{T_{\text{eff}}}{T_2} \phi)\} + M^2 \{1 - A(\phi) - \\ & \left. \lambda_{\text{eff}}^2 \frac{d^2 \phi}{d\xi^2} \} \right] + \frac{T_1}{T_{\text{eff}}} \left\{ 1 - A(\phi) + \lambda_{\text{eff}}^2 \frac{d^2 \phi}{d\xi^2} \right\} \quad (3.12) \end{aligned}$$

Eq.(3.11) is the energy integral of a classical particle of unit mass moving in the effective potential  $\psi(\phi, M)$ , which when written in terms of ion density  $n$ , with the help of the relation (2.11), is identical to  $\psi(n, M)$  given by Eq.(2.13). So in the limit  $B_0 = 0$ , Eq. (3.9) governs the solitary IAW.

### 3.3 Electrostatic Ion Cyclotron Solitary Waves

To investigate the existence of EIC solitary waves, let us impose the condition of quasi charge neutrality, i.e.  $n_1 + n_2 = n_i$ . In this limit, Eq.(3.9) reduces to ,

$$\frac{d^2}{d\eta^2} \left[ \phi + \frac{M^2}{2} A(\phi)^{-2} + \frac{T_i}{T_{eff}} \ln A(\phi) \right] = A(\phi) - 1 , \quad (3.13)$$

where  $\eta = \xi / R_s$ . Integrating Eq.(3.13) over  $\eta$  and using the boundary conditions,  $\phi = 0$  and  $d\phi/d\eta = 0$  at  $\eta = \pm \infty$ , we obtain the energy integral as

$$\frac{1}{2} \left( \frac{d\phi}{d\eta} \right)^2 + \Psi(\phi, M) = 0 , \quad (3.14)$$

where

$$\begin{aligned}
\Psi(\phi, M) = & \left[ 1 - T_{\text{eff}} \left\{ \frac{\alpha_1}{T_1} \exp\left(\frac{T_{\text{eff}}}{T_1} \phi\right) + \frac{\alpha_2}{T_2} \exp\left(\frac{T_{\text{eff}}}{T_2} \phi\right) \right\} A(\phi)^{-1} \left\{ \frac{M^2}{A(\phi)^2} - \frac{T_c}{T_{\text{eff}}} \right\}^{-2} \right. \\
& \left. \left[ \frac{\alpha_1 T_1}{T_{\text{eff}}} \left\{ 1 - \exp\left(\frac{T_{\text{eff}}}{T_1} \phi\right) \right\} + \frac{\alpha_2 T_2}{T_{\text{eff}}} \left\{ 1 - \exp\left(\frac{T_{\text{eff}}}{T_2} \phi\right) \right\} + \frac{M^2}{2} \left\{ 1 - \frac{1}{A(\phi)} \right\}^2 \right. \right. \\
& \left. \left. + \frac{T_c}{T_{\text{eff}}} \left\{ 1 - A(\phi) + \ln A(\phi) \right\} + \phi \right] \right]. \quad (3.15)
\end{aligned}$$

To obtain informations about the EIC solitary waves, we analyse the effective potential  $\Psi(\phi, M)$ . From Eq.(3.15), it can be seen that  $\Psi(\phi, M)$  becomes infinite at  $\phi = \phi_b$ , where  $\phi_b$  is the root of the equation

$$\begin{aligned}
1 - T_{\text{eff}} \left\{ \frac{\alpha_1}{T_1} \exp\left(\frac{T_{\text{eff}}}{T_1} \phi\right) + \frac{\alpha_2}{T_2} \exp\left(\frac{T_{\text{eff}}}{T_2} \phi\right) \right\} \times \\
A(\phi)^{-1} \left\{ \frac{M^2}{A(\phi)^2} - \frac{T_c}{T_{\text{eff}}} \right\} = 0. \quad (3.16)
\end{aligned}$$

Let  $\phi = 0$  and  $\phi_M$  be the extremum points where  $\Psi(\phi, M)$  vanishes. Expanding  $\Psi$  around  $\phi = 0$ , we obtain

$$\Psi(\phi \approx 0, M) \approx \frac{1}{2} \phi^2 \left\{ M^2 - (1 + T_c/T_{\text{eff}}) \right\}^{-1}. \quad (3.17)$$

Equation (3.14) demands  $\Psi(\phi, M) < 0$  for real solutions; according to Eq.(3.17) this inequality can be satisfied only if  $M^2 < (1 + T_i/T_{\text{eff}})$ . Further analysis of  $\Psi(\phi, M)$  reveals that  $\phi = \phi_M$  is an extremum provided the Mach number  $M$  satisfies the relation

$$\begin{aligned} & \frac{\mu(\mu+2)}{(\mu+1)^2} \left[ 1 - \exp\left(\frac{\mu+1}{\mu+2} \phi_M\right) \right] + \frac{\mu+2}{2(\mu+1)^2} \times \\ & \left[ 1 - \exp\left\{ 2 \left( \frac{\mu+1}{\mu+2} \right) \phi_M \right\} \right] + \frac{M^2}{2} \left[ 1 - \frac{\mu+1}{A_1(\phi_M)} \right]^2 \\ & + \gamma \frac{\mu+2}{\mu+1} \left[ 1 - \frac{A_1(\phi_M)}{\mu+1} + \ln \left\{ \frac{A_1(\phi_M)}{\mu+1} \right\} \right] \\ & + \phi_M = 0, \end{aligned} \tag{3.18}$$

where

$$A_1(\phi_M) = \mu \exp \left\{ \left( \frac{\mu+1}{\mu+2} \right) \phi_M \right\} + \exp \left\{ 2 \left( \frac{\mu+1}{\mu+2} \right) \phi_M \right\},$$

with  $\mu = \alpha_1 / \alpha_2$ ,  $2 = T_1 / T_2$  and  $\gamma = T_c / T_i$ .

Once again, from Eq.(3.15) we find that

$$\Psi(\phi \approx \phi_M, M) \approx (\phi - \phi_M) D(\phi_M, M)^{-2} F(\phi_M, M), \quad (3.19)$$

where

$$D(\phi_M, M) = 1 - \frac{\mu+1}{\mu+2} \frac{A_2(\phi_M)}{A_1(\phi_M)} \left[ \frac{M^2 (\mu+1)^2}{A_1^2(\phi_M)} - \gamma \left( \frac{\mu+2}{\mu+1} \right) \right], \quad (3.20)$$

and

$$F(\phi_M, M) = \frac{M^2}{\mu+2} \left\{ 1 - \frac{\mu+1}{A_1(\phi_M)} \right\} \frac{A_2(\phi_M)}{A_1(\phi_M)^2} - \frac{1}{\mu+1} \left[ A_1(\phi_M) + \gamma A_2(\phi_M) \left\{ 1 - \frac{\mu+1}{A_1(\phi_M)} \right\} \right] + 1, \quad (3.21)$$

with

$$A_2(\phi_M) = \mu \exp\left(\frac{\mu+1}{\mu+2} \phi_M\right) + 2 \exp\left(2 \frac{\mu+1}{\mu+2} \phi_M\right).$$

From Eqs. (3.17) to (3.19), it can be seen that both  $\Psi$  and  $d\Psi/d\phi$  vanish at  $\phi = 0$ , however, at  $\phi = \phi_M$ ,  $\Psi$  vanishes but  $d\Psi/d\phi$  is finite. Hence the conditions

for the existence of EIC solitary waves are satisfied.

Since  $\Psi$  has to be negative, Eq.(3.19) guarantees the existence of rarefactive solitary waves if

$$F(\phi_M, M) < 0, \quad (3.22)$$

and compressive solitary waves if

$$F(\phi_M, M) > 0. \quad (3.23)$$

In a single electron component plasma, i.e. for  $\nu = 1$ , Eq. (3.21) gives

$$F(\phi_M, M) = (1 - e^{-\phi_M}) e^{-\phi_M} \{ M^2 - (1 + \gamma) e^{2\phi_M} \}, \quad \text{which}$$

Since the last factor is negative, it shows that  $F(\phi_M, M) < 0$  for  $\phi_M > 0$ , and hence the condition (3.23) is not satisfied. So compressive solitary waves can not exist in a single electron species plasma.

### 3.4 Small Amplitude Sonic Ion Cyclotron Solitary Waves

The effective potential  $\Psi(\phi, M)$  is a complicated



function of  $\phi$  and it is not possible to obtain an exact solution of Eq.(3.14) analytically. However, in the small amplitude limit i.e.  $\phi \ll 1$ , an analytical solution is possible. On taking both  $\phi$  and  $(1 + T_i/T_{\text{eff}} - M^2)$  of order  $\epsilon$  ( $\epsilon \ll 1$ ), and retaining terms of order  $\phi^3$ , Eq.(3.15) gives

$$\Psi(\phi) = -\frac{1}{2}\phi^2 \frac{\chi_1 + \frac{2}{3}\chi_2\phi}{(\chi_1 + \chi_2\phi)^2}, \quad (3.24)$$

where

$$\chi_1 = 1 + \frac{T_i}{T_{\text{eff}}} - M^2, \quad (3.25)$$

$$\chi_2 = 3 + 2 \frac{T_i}{T_{\text{eff}}} - D_1, \quad (3.26)$$

and

$$D_1 = \left( \frac{\alpha_1}{T_1^2} + \frac{\alpha_2}{T_2^2} \right) T_{\text{eff}}^2. \quad (3.27)$$

So Eq.(3.14) can be written as

$$\left( \frac{d\phi}{d\eta} \right)^2 - \frac{\phi^2}{(\chi_1 + \chi_2\phi)^2} (\chi_1 + \frac{2}{3}\chi_2\phi) = 0. \quad (3.28)$$

Using the boundary conditions, namely  $\phi = 0$  at  $\eta = \pm\infty$ , Eq.(3.2a) can easily be integrated once to give the relation

$$|\eta| = 2\chi_1^{1/2} \operatorname{sech}^{-1} \left( -\frac{2}{3} \frac{\chi_2}{\chi_1} \phi \right)^{1/2} - 3 \left( \chi_1 + \frac{2}{3} \chi_2 \phi \right)^{1/2} \quad (3.29)$$

From this equation, it can be seen that  $\phi_{\max} = -3\chi_1/2\chi_2$ . Since  $M^2 < (1+T_i/T_{\text{eff}})$ ,  $\chi_1$  is positive. So the solitary wave will be rarefactive if  $\chi_2 > 0$  and compressive if  $\chi_2 < 0$ . Hence compressive solitary waves can exist if

$$D_1 > 3 + 2T_i/T_{\text{eff}} \quad (3.30)$$

We may point out that Eq.(3.30) is identical to Eq.(2.25), the requirement for the occurrence of rarefactive ion acoustic solitary waves. In an one electron component plasma,  $D_1 = 1$  and hence the inequality (3.30) can never be satisfied. So compressive small amplitude EIC solitary waves do not exist in a single electron species plasma.

If the temperature and relative concentration of the two electron components are such that  $D_1 \sim 3 + 2T_i/T_{\text{eff}}$

or in other words,  $\chi_2 \ll 1$ , the next higher order term in  $\phi$  becomes important in the expansion for  $\Psi(\phi)$  in Eq.(3.24) and it can not be neglected. So in the limit

$\chi_2 \rightarrow 0$ , Eq.(3.14) can be written as

$$\left(\frac{d\phi}{d\eta}\right)^2 - \frac{\phi^2}{\chi_1^2} (\chi_1 + \chi_3 \phi^2) = 0, \quad (3.31)$$

where

$$\chi_3 = \frac{1}{4} \left\{ 3D_2 - D_1^2 - 24D_1 + 36 - \frac{T_i}{T_{\text{eff}}} (16D_1 - 30) \right\}, \quad (3.32)$$

with

$$D_2 = \left( \frac{\alpha_1}{T_1^3} + \frac{\alpha_2}{T_2^3} \right) T_{\text{eff}}^3. \quad (3.33)$$

The solution of Eq.(3.31) is of the form

$$\phi = \pm \left( -\frac{\chi_1}{\chi_3} \right)^{1/2} \text{sech} \left( \frac{1}{\chi_1^{1/2}} \eta \right). \quad (3.34)$$

This is a new type of solution, the form of this is similar to the ion acoustic soliton obtained in the limit  $|D_1 - 3| \ll 1$  (Krokhin and Eibenko, 1981). We note here that this solution does not occur in a single electron component plasma because in that case  $D_1 = 1$  and so the condition  $D_1 \sim 3 + 2 T_i/T_{\text{eff}}$

can not be satisfied. From Eq.(3.34) we see that under certain conditions, the two electron component plasma can sustain both rarefactory and compressive solitary waves simultaneously.

### 3.5 Numerical Results

As mentioned in chapter 2, the density and temperature ratio of the two electron components in the experiment of Jones et al. (1975) vary between 1/6 to 3 and 2 to 5 respectively. In the auroral plasma, hot and cold electrons have energies  $\sim 1-10$  KeV and 10-500 ev and ions have energies  $\sim 1-10$  ev (Garret, 1979). The density of the colder electron component is about  $10^2$  to  $10^4$  times larger than the density of the hotter component (Banks and Kockarts, 1973) at an altitude of  $\sim 3000$  km. S3-3 satellite data shows that the plasma density in this region is  $10-100 \text{ cm}^{-3}$  (Hudson et al., 1978).

In fig.1, the plot of  $\Psi(\phi)$  against  $\phi$ , for the laboratory plasma, shows that the magnitude of the maximum amplitude  $\phi_M$  in a two electron component plasma is larger than that in an one electron species plasma. It is also seen that in both types of plasmas,  $\Psi$  goes to infinity

at  $\phi = \phi_b$ . Magnitude of  $\phi_b$  in an one electron species plasma is found to be  $-0.2$ , whereas, in a two electron species plasma with  $\mu = 3$ ,  $\nu = 5$ ,  $\phi_b = -0.9$ .

The profile of the EIC solitary wave (in the small amplitude limit) is plotted in figs. 2 and 3. From fig. 2, it can be seen that the amplitude of the rarefactory solitary wave is larger in a two electron species plasma than in a single electron species plasma. This can be explained by analysing Eq.(3.29); from this equation, we observe that the amplitude of the solitary wave is  $|3/2 (\chi_1/\chi_2)|$ . When the second electron species is introduced,  $\nu$  increases from 1 (in this particular case  $\nu = 5$ ). This in turn increases  $D_1$  and so  $\chi_2$  (as given by Eq.(3.26)) decreases. This results in an increase in the magnitude of amplitude of the solitary wave profile in a two electron species plasma. As shown earlier, compressive solitary waves do not exist in a single electron component plasma (Dash and Buti, 1983a).

Eqs. (3.18) and (3.21) are transcendental in nature and it is not possible to solve them analytically. So we have obtained the roots of these two equations numerically for different values of  $\mu$ ,  $\nu$  and  $\gamma$ . Let  $M_1$  and  $M^*$  be the roots of Eq.(3.18) and (3.21) respectively. From our

numerical computations, we find that  $F(\phi_M, M) \gtrless 0$  for  $\phi \lesseqgtr 0$  provided  $M^2 > M^{*2}$ . So the allowed regions for the existence of both types of solitary waves would lie between the lines  $M^2 = M^{*2}$  and  $M^2 = M_U^2$  ( $= 1 + T_i/T_{\text{eff}}$ ) with the condition that  $M_1^2 > M^{*2}$ . In figs. 4 to 6, we have plotted  $M^2$  versus  $\phi_M$  for the rarefactive solitary waves for different values of  $\mu$ ,  $\nu$  and  $\gamma$ . From these figures, we see that the allowed regions for solitary waves decrease when  $\mu$  or  $\nu$  increases. However, the allowed regions increase when  $\gamma$  increases. We have plotted  $M^2$  versus  $\phi_M$  for the compressive solitary waves in figs. 7 to 9. In fig. 7, we see that for  $\mu = 1$ , both  $M_1^2$  and  $M^{*2}$  are larger than  $M_U^2$  and so compressive solitary waves do not exist. But when  $\mu$  increases to 5, there exists a region where compressive solitary waves can occur. When  $\mu$  is increased further (beyond 5), we see that the allowed region for compressive waves increases. Moreover, fig. 8 shows that the allowed regions for the compressive solitary waves increase as  $\nu$  increases. We also note that for  $\mu = 5$  and  $\gamma = 0$ , compressive solitary waves do not exist for  $\nu = 10$ , but they appear when  $\nu$  goes up to 20. So there must exist a critical value of  $\nu$  ( $= \nu_c$ ), above which compressive solitary waves can exist. From our numerical results, we

have found that for  $\mu = 5$ , and  $\gamma = 0$ ,  $\nu_c = 12$ . Fig. 9 shows that an increase in  $\gamma$  increases the allowed regions for the solitary waves.

### 3.6 Discussion

In the auroral plasma, at altitudes between 2000 km and 8000 km, paired electrostatic shock structures with opposite polarities, in directions perpendicular to the magnetic field had been observed (Mozer et al., 1977). Simultaneous observation of these shocks and EIC waves have been reported by several authors indicating a possible correlation between these two phenomena (Mozer et al., 1977; Kintner et al., 1978; Hudson et al., 1978; Temerin et al., 1979; etc.). These EIC waves travel with a phase velocity of the order of 50 km/sec (Kintner et al., 1978).

In the auroral plasma,  $\mu$  varies from  $10^{-2}$  to  $10^{-4}$  (Banks and Kockarts, 1973) and  $\nu$  varies from 10 to 100 (Garret, 1979). For these parameters,  $D_1$  ranges between 1.00008 and 1.001. Hence the condition  $D_1 > 3 + 2 T_1/T_{\text{eff}}$  can not be satisfied. So the solitary waves in this region are rarefactive. Isotropic flow of electrons with energies around 170 eV in the auroral plasma had earlier been

detected by Mizera and Fennel (1977) and Mozer et al. (1977). Such electrons, flowing from the magnetosphere towards the ionosphere, in a direction perpendicular to the magnetic field, can get reflected from the rarefactory EIC solitary waves, thereby giving rise to the observed shock structures. However, the formation of shocks is possible only if the energy of the incident electrons is less than the potential energy of the solitary waves. For the electrons and the ions at energies  $\sim 5$  keV, 250 ev and 10 ev respectively, and the density of the colder electron component  $10^3$  times larger than the density of the hot electron component, maximum amplitude  $|\phi_M|$  of the rarefactory solitary wave is 0.8, whereas,  $|\phi_M| \sim 0.6$  if the hotter electron component is absent. These values of  $|\phi_M|$  correspond to the potential well with energy 200 ev and 150 ev respectively. So the streaming electrons with energies of the order of 170 ev will be reflected from the potential well only if the plasma contains two electron species. Hence the presence of the second electron component in the auroral plasma is pertinent to explain the observed perpendicular shocks. The thickness of the shocks thus formed should be of the order of the width of the rarefactory EIC solitary waves. Corresponding to the observed values of  $\mathcal{V}$  i.e. between 10 and 100, width of the solitary waves turns out to be



$\sim 148$  m -  $469$  m; this is in agreement with the observed shock thickness which is about  $200$  m -  $10$  km (Tobert and Mozer, 1978). Witt and Lotko (1983) have tried to explain these shocks in terms of obliquely propagating IAW. But these obliquely propagating IAW in the auroral region should have phase velocity of the order of  $5$  km/sec, whereas, the observed values of phase velocity of the waves travelling almost perpendicular to the magnetic field is of the order of  $50$  km/sec (Kintner et al., 1978) which is nearly equal to the EIC phase velocity. So it is more appropriate to interpret the paired electrostatic shock structures with the help of EIC waves.

Auroral kilometric radiation (AKR) is a high density radiation observed in the frequency range  $50 - 750$  kHz. Observations from ISIS 1 reveal that AKR is generated in the extraordinary electromagnetic mode which propagates almost perpendicular to the background magnetic field. It was found to be generated within the density depleted regions with peak density such that  $\omega_{pe} < 0.2 \Omega_e$ , with  $\Omega_e \sim 520$  kHz ( $\omega_{pe}$  and  $\Omega_e$  being the plasma and the cyclotron frequencies for the electrons). Most intense kilometric radiation is found to be emitted from the auroral zone at a distance of  $1.5 - 2.5 R_E$  (earth radii) from the earth (Gurnett, 1974; Benson and Calvert, 1979). Coherent

EIC waves have been observed in this region, travelling with velocities  $\sim 50$  km/sec (Kintner et al., 1978). Density fluctuations associated with these waves are less than 0.5 (Kelley et al., 1975).

Quite a few models have been proposed to explain the AKR. One such model, which is in good agreement with observations, is proposed by Grabbe et al. (1980). According to this model, the low amplitude electromagnetic wave interacts with the coherent EIC waves to give rise to a beat wave. In presence of a high energy electron beam, the beat wave absorbs energy from the beam. This beat wave then interacts with the EIC wave giving rise to the electromagnetic wave, which in turn gets amplified. An important assumption of this model is that low frequency density fluctuations (assumed to be produced by coherent EIC waves like those seen by Temerin et al. (1980)) play an important role in AKR. Our present calculations confirm the presence of coherent EIC waves in the auroral plasma. Further, according to our model, the amplitude of the coherent EIC waves is larger due to the presence of the second electron component. For example, in the presence of about 0.1% of the hotter electron component (at  $\sim 5$  keV) in the bulk electron population (at  $\sim 50$  eV) the calculated density fluctuation of the EIC wave is  $\sim 0.25$ , whereas, it would

have been 0.2 if the hotter electron component was not present. Now, the growth rate ( $K$ ) of the electromagnetic wave is proportional to the square of the density fluctuations associated with the coherent EIC waves (Grabbe et al., 1980). So the increase, in density fluctuations, increases the growth rate.

If the source region for the AKR is modelled to be a cylinder of radius 100 km and length 2000 km, the radiated power per unit area ( $S$ ) is  $\sim 10^{-3} \text{ W/m}^2$ , whereas, the power per unit area ( $S_n$ ) associated with the electromagnetic wave is  $10^{-15} \text{ W/m}^2$  (Gurnett, 1974). So the path length ( $\ell$ ) required to amplify the electromagnetic wave to the observed AKR level is given by the relation  $S/S_n = \exp(2K\ell) \approx 10^{12}$ . We have calculated  $\ell$  according to this formula and found that an increase in the density fluctuation from 0.2 to 0.25 reduces the path length from 140 km to 110 km. Hence the presence of the second electron species is more favourable for observation of AKR.

Density fluctuations associated with EIC waves travelling with velocity  $\sim 50 \text{ km/sec}$  are calculated to be 0.4 and 0.45 in an one electron component and a two electron component plasma respectively. These are in good agreement with the observations which demand that they should be less than 0.5.

### 3.7 Conclusions

In summary, we conclude that in a plasma with two electron components, rarefactory as well as compressive EIC solitary waves can exist. The compressive EIC solitary waves are forbidden in an one electron component plasma. The amplitude of the rarefactory solitary EIC wave increases due to the presence of the second electron species. For certain composition of the two electron components, these rarefactory and compressive EIC solitary waves coexist. Solitary EIC waves, in a two-electron species plasma, can be a source for the observed perpendicular shocks in the auroral plasma.

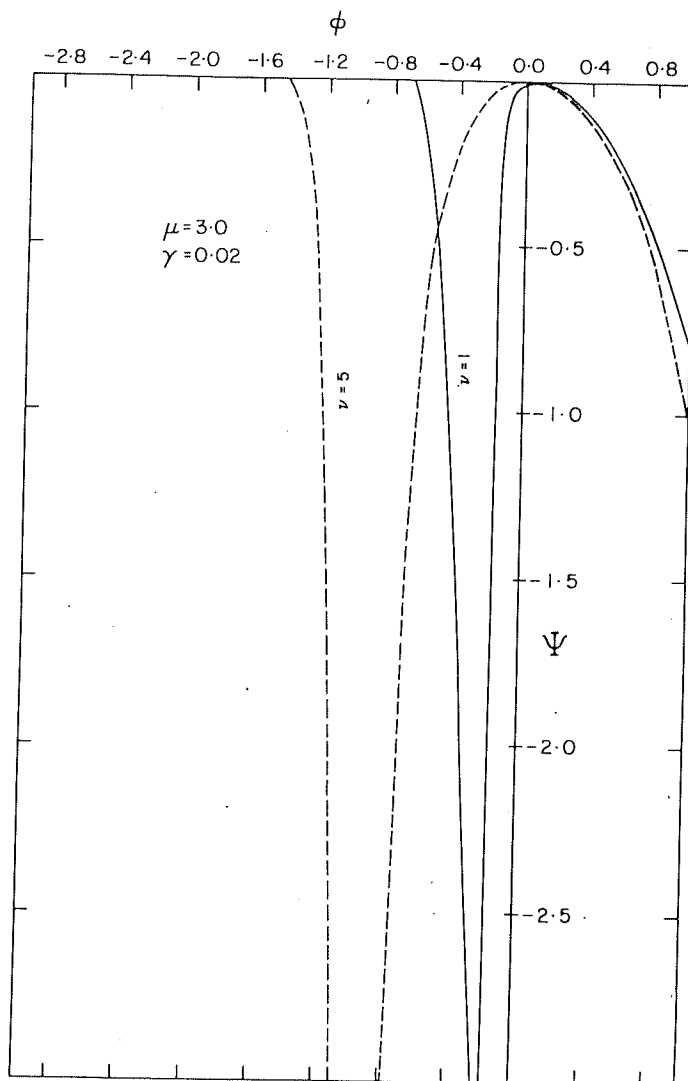


Fig. 1: Potential  $\Psi(\phi)$  vs.  $\phi$ . The solid and broken curves correspond to single electron species and two electron species plasma respectively.

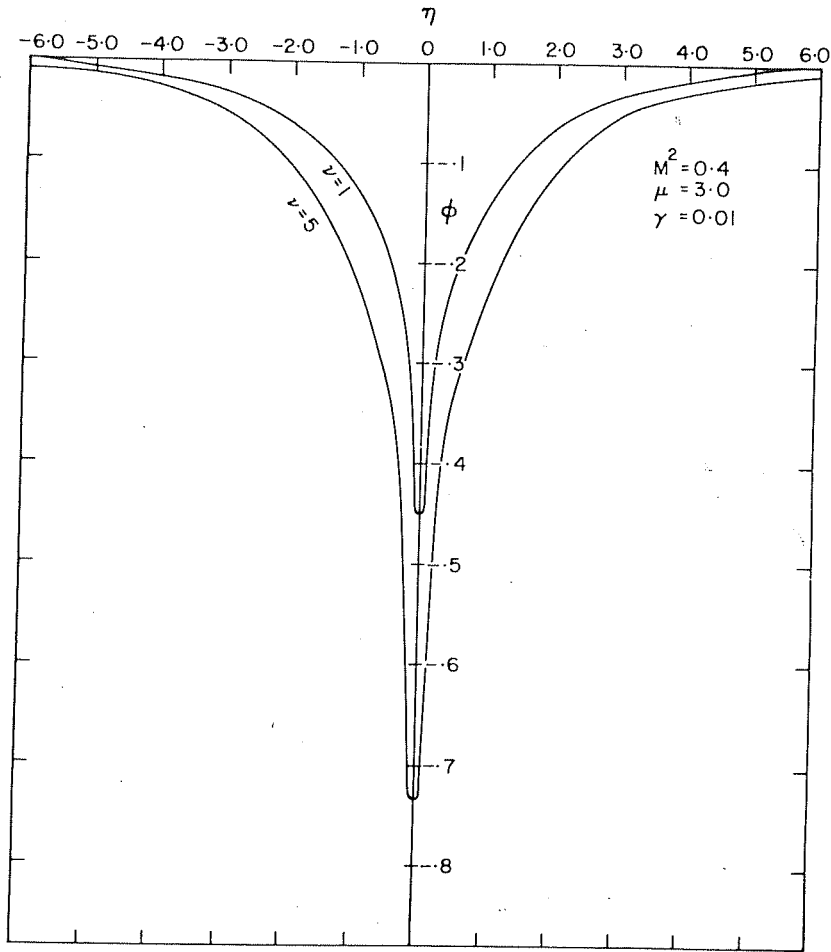


Fig. 2: Profile of the rarefactive EIC solitary wave  
 for  $\nu = 1$  and 5 corresponding to single electron  
 species and two electron species plasma respectively.

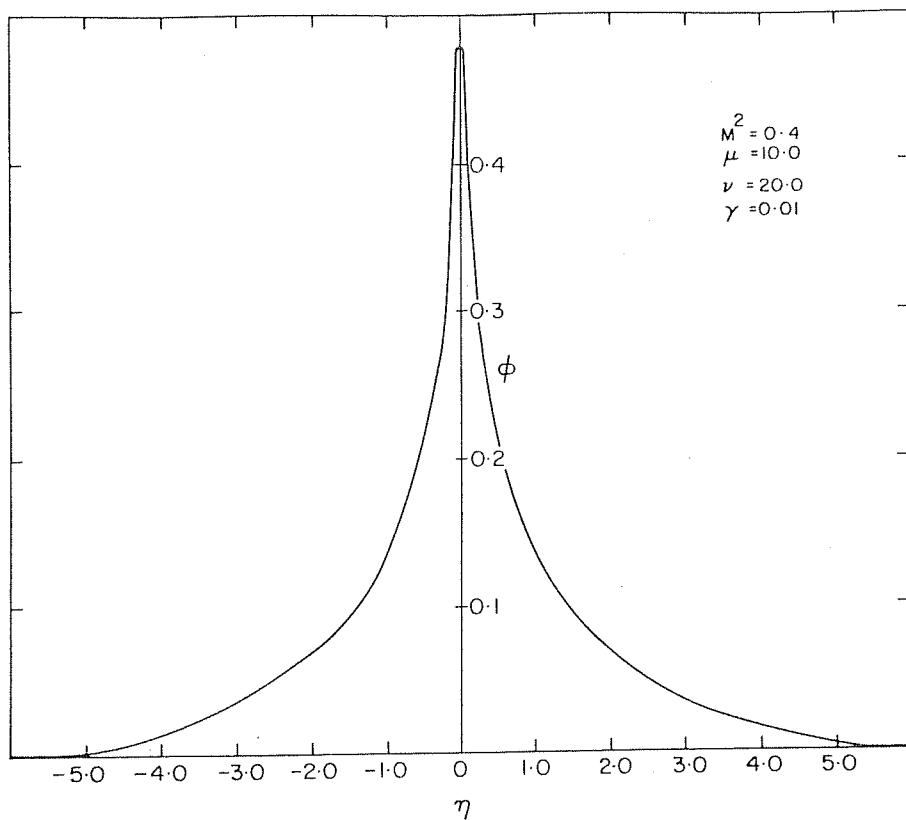
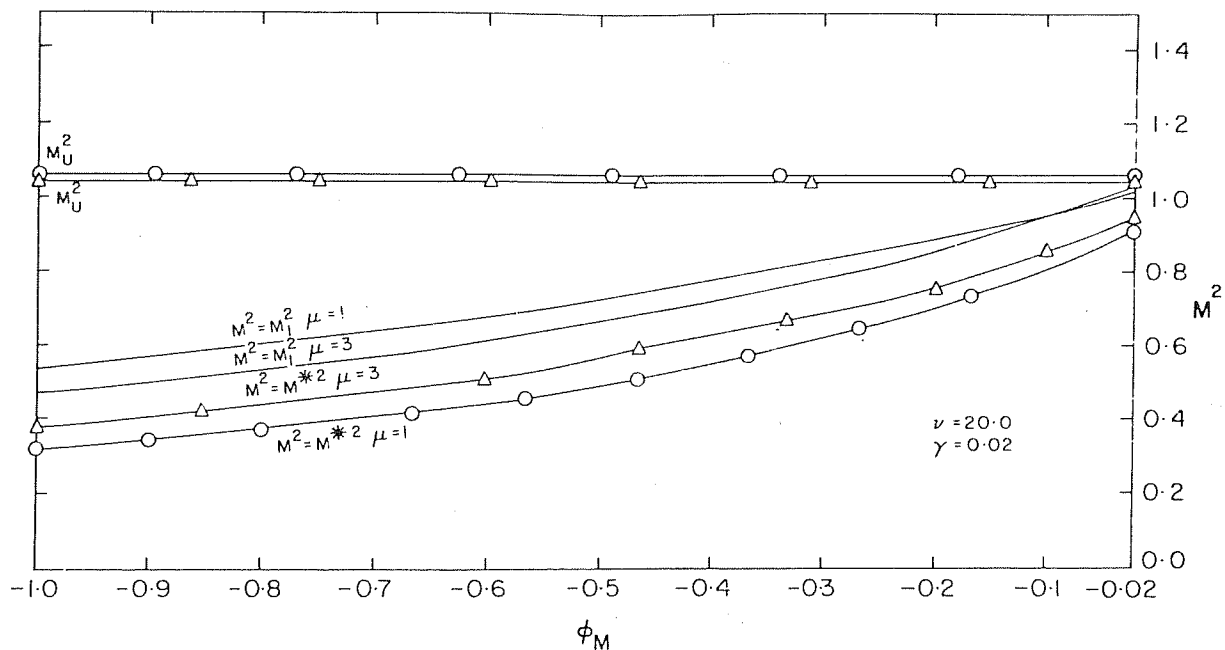


Fig.3: Profile of the compressive EIC solitary wave in a two electron component plasma. Compressive EIC solitary wave does not exist in a single electron species plasma.



**Fig.4:**  $M^2 v_s \phi_M$  for rarefactive EIC solitary waves ( $\phi_M < 0$ ) for  $\nu = 20$ ,  $\gamma = 0.02$  and  $\mu = 1$  and  $3$ . The upper allowed value is given by  $M_U^2$ . The regions bounded by lines  $\circ\circ\circ$  ( $\mu = 1$ ),  $\triangle\triangle\triangle$  ( $\mu = 3$ ) are the allowed regions.



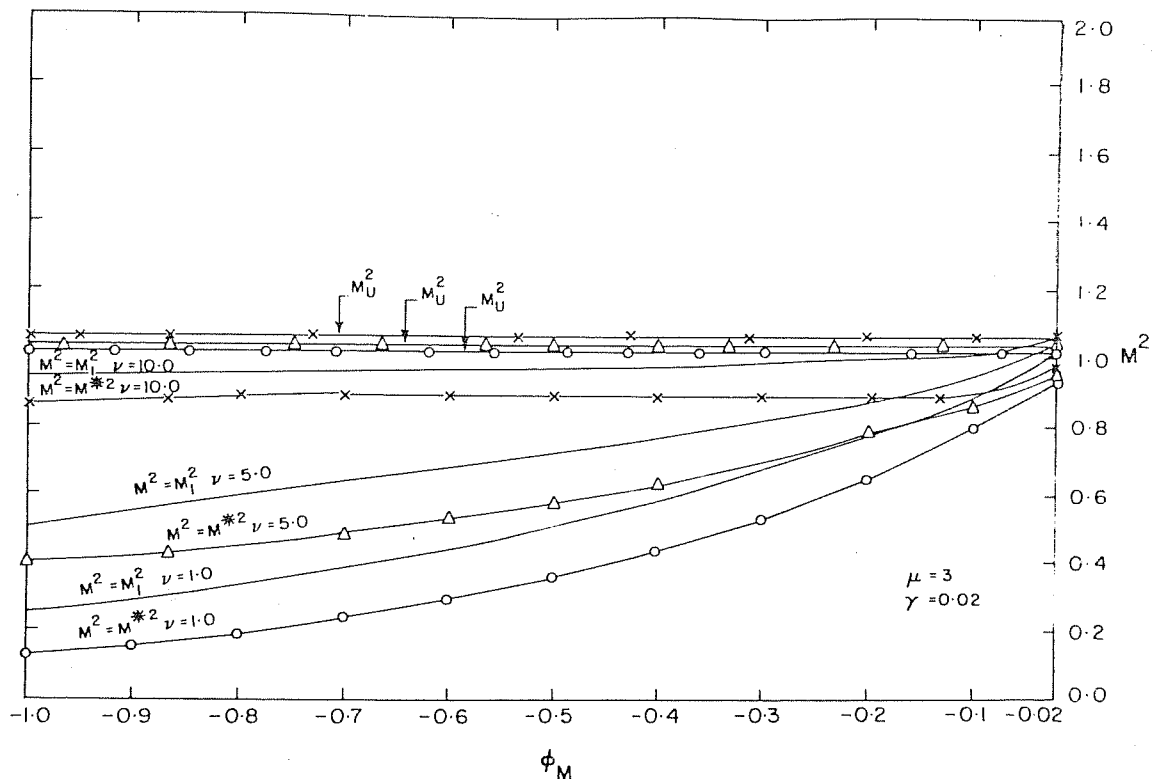


Fig. 5:  $M^2 v_s \phi_M$  ( $\phi_M < 0$ ) for  $\mu = 3$ ,  $\gamma = 0.02$  and  $\nu = 1, 5$  and 10. The upper allowed value is given by  $M_U^2$ . The regions bounded by lines  $-o-o-$  ( $\nu = 1$ ),  $-\triangle-\triangle-$  ( $\nu = 5$ ),  $-x-x-$  ( $\nu = 10$ ) are the allowed regions.

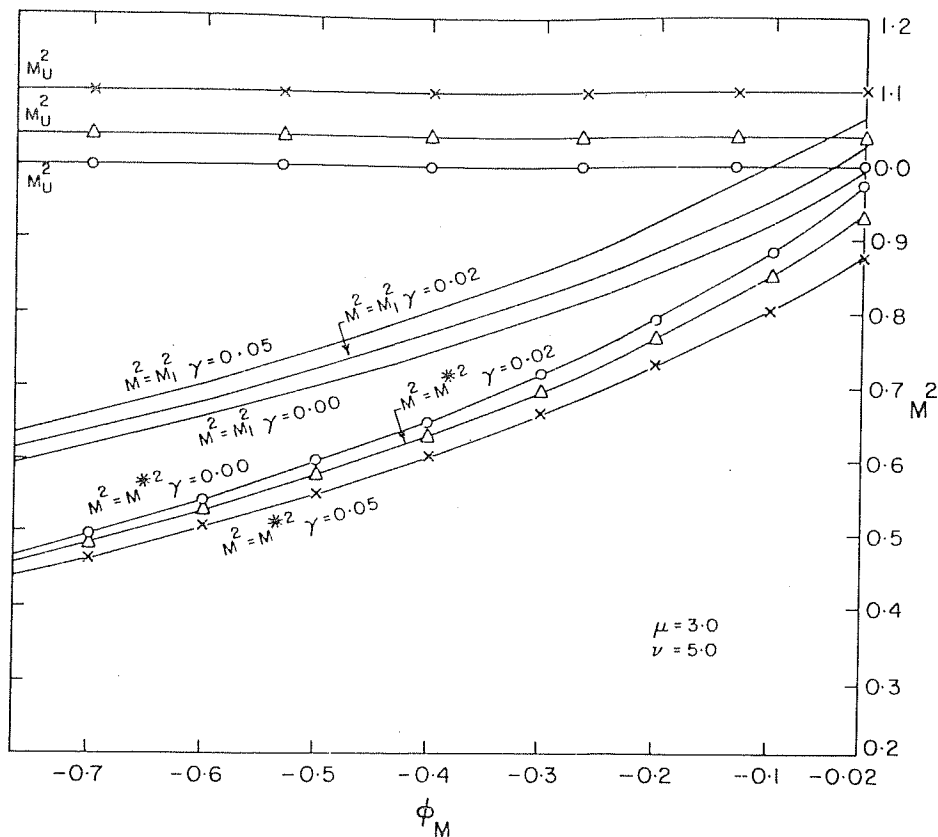
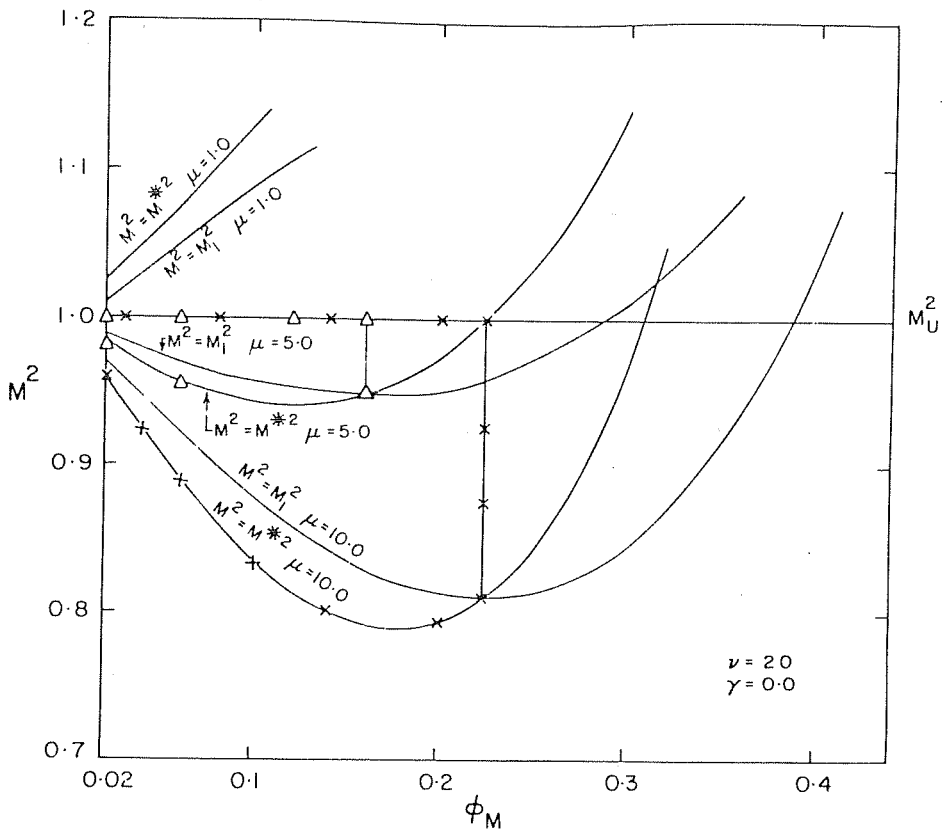


Fig. 6:  $M^2 v_s \phi_M (\phi_M < 0)$  for  $\mu = 3$ ,  $\nu = 5$  and  $\gamma = 0.0, 0.02$  and  $0.05$ . The upper allowed value is given by  $M_u^2$ . The regions bounded by lines  $\text{---}\circ\text{---}$  ( $\gamma = 0.0$ ),  $\text{---}\triangle\text{---}$  ( $\gamma = 0.02$ ),  $\text{---}\times\text{---}$  ( $\gamma = 0.05$ ) are the allowed regions.



**Fig.7:**  $M^2$  vs  $\phi_M$  for compressive EIC solitary waves ( $\phi_M > 0$ ) for  $\nu = 20$ ,  $\gamma = 0.0$  and  $\mu = 1, 5$  and  $10$ . The upper allowed value is given by  $M_u^2$ . Solitary waves do not exist for  $\mu = 1$ . The regions bounded by lines  $\triangle-\triangle$  ( $\mu = 5$ ),  $\times-\times$  ( $\mu = 10$ ) are the allowed regions.

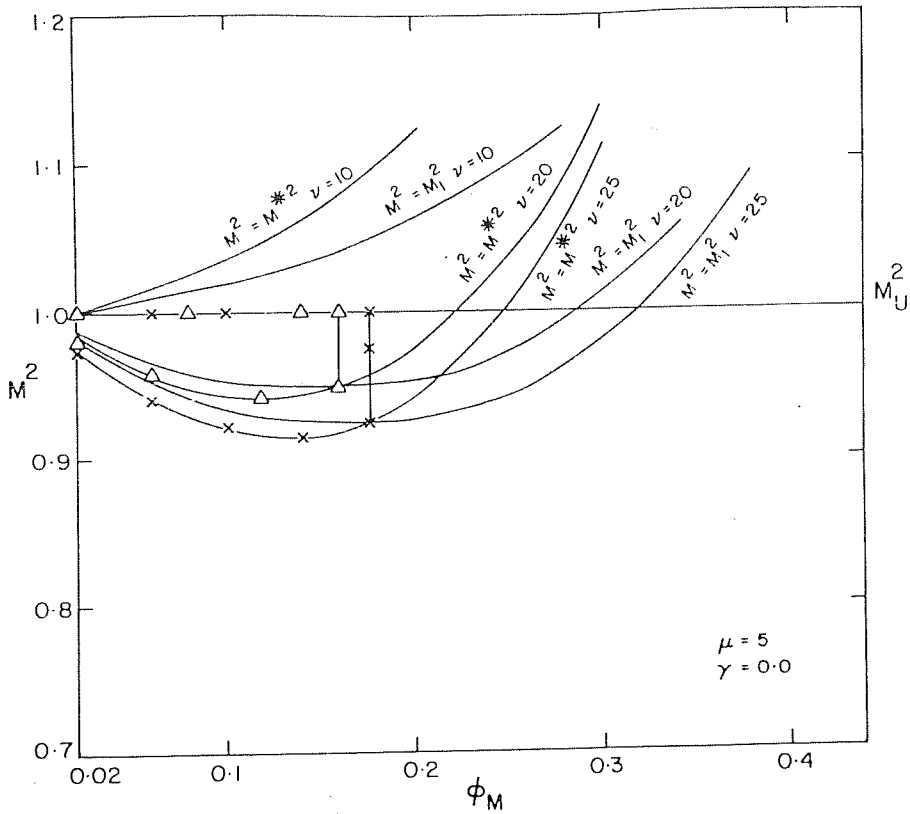


Fig.8:  $M^2 v_s \phi_M$  ( $\phi_M > 0$ ) for  $\mu = 5$ ,  $\gamma = 0.0$  and  $\nu = 10, 20$  and  $25$ . The upper allowed value is given by  $M_u^2$ . Solitary waves do not exist for  $\nu = 10$ . The regions bounded by lines  $\triangle-\triangle$  ( $\nu = 20$ ),  $\times-\times$  ( $\nu = 25$ ) are the allowed regions.

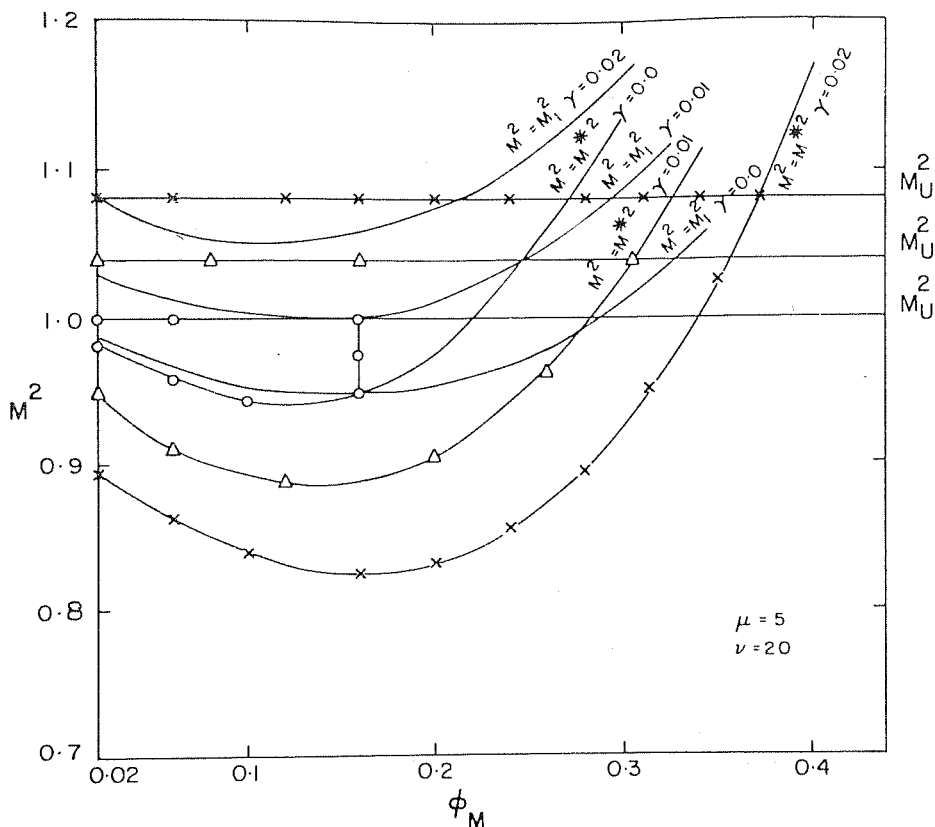


Fig.9:  $M^2 v_s \phi_M$  ( $\phi_M > 0$ ) for  $\mu = 5$ ,  $\nu = 20$  and  $\gamma = 0.0, 0.01$  and  $0.02$ . The upper allowed value is given by  $M_U^2$ . The regions bounded by lines  $\circ-\circ-$  ( $\gamma = 0.0$ ),  $\triangle-\triangle-$  ( $\gamma = 0.01$ ),  $\times-\times-$  ( $\gamma = 0.02$ ) are the allowed regions.

## CHAPTER 4

### EVOLUTION OF NONLINEAR ION ACOUSTIC WAVES IN AN INHOMOGENEOUS TWO-ELECTRON TEMPERATURE PLASMA

#### 4.1 Introduction

The problem of nonlinear wave propagation in dispersive medium is of general interest (Kadomtsev and Karpman, 1971). In a weakly dispersive homogeneous plasma, nonlinear ion acoustic waves (IAW) are governed by Korteweg-de Vries (KdV) equation (Washimi and Taniuti,

1966; Taniuti and Wei, 1968; Davidson, 1972). But when the plasma is strongly dispersive, the wave broadens quickly and the KdV equation cannot describe the system correctly. In such plasmas, by using reductive perturbation technique, Taniuti and Yajima (1969) had shown that the nonlinear Schrödinger equation (NSE) governs the wave envelope. In this method, stretched space time variables are used; their scaling is decided apriori. To avoid the apriori scaling of space and time variables, one can follow the Krylov-Bogoliubov-Mitropolsky (KBM) perturbation scheme (Bogoliubov and Mitropolsky, 1961) to derive the NSE (Kakutani and Sugimoto, 1974; Buti, 1976, 1977; Sharma and Buti, 1976, 1977; Mohan and Buti, 1979).

In reality, plasmas are far from being perfectly homogeneous. In such plasmas, interaction of the waves with the inhomogeneities present in the system can become important and can modify the propagation characteristics of these waves. In presence of an extremely weak inhomogeneity (inhomogeneity scalelength  $L$  very large compared to the width of the envelope solitons), Karpman (1979) had shown that a perturbed NSE governs the IAW envelope. Solving the perturbed NSE by inverse scattering method, Karpman (1979) had shown that the perturbation acting on the

envelope soliton does not lead to the formation of a tail, which is a small amplitude wave packet with growing length. The perturbation results in some deformation of the soliton shape. when the inhomogeneity is weak but not so weak that it can be considered as a perturbation as in the case of Karpman (1979), Chen and Liu (1978) had shown that in presence of a linear density gradient, the envelope solitons are accelerated uniformly, whereas, the acceleration is nonuniform for arbitrary density gradients. However, if the inhomogeneity scalelength is comparable to the width of the envelope solitons, a modified nonlinear Schrödinger equation (MNSE) governs the IAW envelope and an analytical solution is not possible (Mohan and Buti, 1979). Their numerical computations showed that an envelope soliton, while propagating towards increasing density, splits into two solitary waves.

In this chapter, we have investigated the non-linear IAW in a highly dispersive inhomogeneous two-electron-temperature plasma with nonuniform temperatures. The density inhomogeneity scalelengths are assumed to be comparable to the wavelengths of the envelope solitons whereas temperature inhomogeneity scalelengths are much larger. This is because the heat conductivity ( $\sim T_{1,2}^{5/2}$ ,



where  $T_{1,2}$  are the electron temperatures) is too large at high electron temperatures to maintain large gradients. We have derived the MNSE by using the KBM method. MNSE is solved numerically to study the time evolution of envelope solitons and envelope holes. It is seen that an envelope soliton propagating in the direction of increasing density splits into two solitary waves. Time required for splitting of the envelope soliton is found to depend on the wave number and initial amplitude as well as the ratios of the density and temperature of both the electron components. For an envelope hole, the effect of the second electron species is more prominent and unlike the one electron component plasma, splitting of the envelope hole does not take place within a reasonable length of time (Dash and Buti, 1983).

#### 4.2 Modified Nonlinear Schrödinger Equation

Let us consider a collisionless, highly dispersive plasma with cold ions and hot electrons with two distinct velocity distributions. The medium has inhomogeneities both in densities and temperatures. The forces due to these gradients are balanced by the presence of a zero

order electric field  $E_0$  and an external force  $F$  due to gravitational field. The basic fluid equations governing the system are the ion continuity equation, momentum equation for the ions and both the electron components and the poisson's equation; namely

$$\frac{\partial n}{\partial t} + \frac{\partial}{\partial x}(nv) = 0, \quad (4.1)$$

$$\frac{\partial v}{\partial t} + v \frac{\partial v}{\partial x} = \frac{eE}{m_i} + \frac{F}{m_i}, \quad (4.2)$$

$$eN_1E + \frac{\partial}{\partial x}(N_1T_1) = 0, \quad (4.3)$$

$$eN_2E + \frac{\partial}{\partial x}(N_2T_2) = 0, \quad (4.4)$$

and

$$\frac{\partial E}{\partial x} + 4\pi e(N - N_1 - N_2) = 0, \quad (4.5)$$

where  $N$  and  $N_{1,2}$  are the ion and electron densities,  $v$  is the ion fluid velocity and  $E$  is the electric field. In writing equations (4.3) and (4.4), we have assumed that both the electron components are separately in equilibrium

with the electric field  $E$ . This is justified provided the phase velocity of the wave is much smaller than the thermal velocities of both the electron components separately, i.e.  $T_{\text{eff}}/m_i \ll T_{1,2}/m_e$  where  $T_{\text{eff}} = T_1 T_2 / (N_{10} T_2 + N_{20} T_1)$  (Bütli, 1980). For the sake of convenience, let us normalise the densities, fluid velocity, electric field and the space and time variables to the local equilibrium values of ion density  $N_0 = N_{10} + N_{20}$ , ion acoustic speed  $(T_{\text{eff}}/m_i)^{1/2}$ , characteristic electric field  $T_{\text{eff}}/e \lambda_{D_{\text{eff}}}$ , effective Debye length  $\lambda_{D_{\text{eff}}}$  and ion plasma period  $\omega_{p_i}^{-1}$  respectively, ( $\lambda_{D_{\text{eff}}} = (T_{\text{eff}}/4 \pi N_0 e^2)^{1/2}$ ). Then Eq.(4.1) to (4.5) can be written as

$$\frac{\partial N}{\partial t} + \frac{\partial}{\partial x} (vN) + (\alpha + \frac{1}{2} \beta_{\text{eff}}) vN = 0, \quad (4.6)$$

$$\frac{\partial v}{\partial t} + \frac{1}{2} \beta_{\text{eff}} v^2 + v \frac{\partial v}{\partial x} - E - F = 0, \quad (4.7)$$

$$N_1 T_{\text{eff}} E + (\alpha + \beta_1) N_1 T_1 + T_1 \frac{\partial N_1}{\partial x} = 0, \quad (4.8)$$

$$N_2 T_{\text{eff}} E + (\alpha + \beta_2) N_2 T_2 + T_2 \frac{\partial N_2}{\partial x} = 0, \quad (4.9)$$

and

$$\frac{\partial E}{\partial x} + \frac{1}{2}(\alpha + \beta_{\text{eff}})E - N + N_1 + N_2 = 0, \quad (4.10)$$

where  $\alpha = n_0^{-1} dN_0/dx$ ,  $\alpha_{1,2} = n_{1,2,0}^{-1} dN_{1,2,0}/dx$ ,

$\beta_{1,2} = T_{1,2,0}^{-1} dT_{1,2}/dx$  and  $\beta_{\text{eff}} = \beta_1 + \beta_2 + \alpha_1 n_{1,0} +$

$\alpha_2 n_{2,0} - \{n_{1,0} T_{2,0}(\alpha_1 + \beta_2) + n_{2,0} T_{1,0}(\alpha_2 + \beta_1)\} (n_{1,0} T_{2,0} + n_{2,0} T_{1,0})^{-1}$

are the inhomogeneity scalelengths. In Eqs.(4.6) to (4.10), the terms containing  $\alpha$ 's and  $\beta$ 's are due to the normalisation with respect to the local equilibrium parameters whose space dependence has been assumed to be of the form:

$$N_0 = n_0(1 + \alpha x), \quad (4.11)$$

$$N_{1,2,0} = n_{1,2,0}(1 + \alpha_{1,2} x), \quad (4.12)$$

$$T_{1,2} = T_{1,2,0}(1 + \beta_{1,2} x), \quad (4.13)$$

and

$$T_{\text{eff}} = T_{\text{eff},0}(1 + \beta_{\text{eff}} x). \quad (4.14)$$

For weak nonlinearities, we can expand  $E, N, N_{1,2}$  and  $v$  about their unperturbed uniform states as follows:

$$\begin{bmatrix} E \\ N \\ N_1 \\ N_2 \\ v \end{bmatrix} = \begin{bmatrix} \lambda E_0 \\ 1 \\ N_{10} \\ N_{20} \\ 0 \end{bmatrix} + \epsilon \begin{bmatrix} E_1 \\ N_1 \\ N_{11} \\ N_{21} \\ v_1 \end{bmatrix} + \epsilon^2 \begin{bmatrix} E_2 \\ N_2 \\ N_{12} \\ N_{22} \\ v_2 \end{bmatrix} + \dots, \quad (4.15)$$

where  $\lambda$  is a small parameter defining the strength of the zero order electric field arising due to inhomogeneities in densities and temperatures. As outlined in chapter 1, we choose a monochromatic plane wave solution of the form

$$E_1 = a \exp(i\psi) + \bar{a} \exp(-i\psi), \quad (4.16)$$

where  $\psi = kx - \omega t$  is the phase factor and 'a' is the complex amplitude which varies slowly with space and time according to Eq.(1.14). Substituting Eqs.(4.15) and (4.16)

in Eqs.(4.6) - (4.10), writing  $\alpha_{1,2} = \epsilon \rho_{1,2}$ ,

$\beta_{1,2} = \epsilon^2 \nu_{1,2}$  and  $\beta_{\text{eff}} = (\epsilon \rho_{\text{eff}} + \epsilon^2 \nu_{\text{eff}})$ ,

where  $\rho_{1,2}, \rho_{\text{eff}}, \nu_{1,2}, \nu_{\text{eff}}$  are of order unity,

the  $\epsilon$  - order equations give the following solutions:

$$N_1 = \frac{i k}{\omega^2} (a e^{i\psi} - \bar{a} e^{-i\psi}),$$

$$N_{11} = \frac{i}{k} \frac{N_{10}}{T_1} T_{\text{eff}} (a e^{i\psi} - \bar{a} e^{-i\psi}),$$

$$N_{21} = \frac{i}{k} \frac{N_{20}}{T_2} T_{\text{eff}} (a e^{i\psi} - \bar{a} e^{-i\psi}),$$

and

$$v_1 = \frac{i}{\omega} (a e^{i\psi} - \bar{a} e^{-i\psi}).$$

Moreover the linear dispersion relation is given by.

$$\mathcal{D}(k, \omega) \equiv \omega^2 - k^2 + \omega^2 k^2 = 0. \quad (4.17)$$

The zero order electric field required to balance the gradients is simply given by

$$E_0 = -(\rho + \epsilon q), \quad (4.18)$$

where  $\rho = (\beta_1 N_{10} T_1 + \beta_2 N_{20} T_2)/T_{\text{eff}}$ ,  $q = (v_1 N_{10} T_1 + v_2 N_{20} T_2)/T_{\text{eff}}$  and  $\lambda$  turns out to be of order  $\epsilon$ .

To order  $\epsilon^2$ , the set of equations (4.6) to (4.10) give the following equation for  $E_2$ :

$$\begin{aligned}
& (\omega^2 - k^2) E_2 - \omega^2 k^2 \frac{\partial^2 E_2}{\partial y^2} + i \left[ A_1 \frac{\partial \partial}{\partial \omega} - B_1 \frac{\partial \partial}{\partial k} \right. \\
& \left. + \frac{a \omega^2}{2k} \left\{ f(4+k^2) - \frac{2py}{T_{\text{eff}}} + f_{\text{eff}} \right\} \right] + i a^2 \cdot x \\
& \left( -\frac{3k^3}{\omega^2} + \frac{\omega^2}{k} y \right) e^{2iy} + \text{C.C} = 0, \quad (4.19)
\end{aligned}$$

where

$$y = \left( \frac{N_{10}}{T_1^2} + \frac{N_{20}}{T_2^2} \right) T_{\text{eff}}^2,$$

and

$$f_{\text{eff}} = f_1 N_{10} + f_2 N_{20} - (f_1 N_{10} T_2 + f_2 N_{20} T_1) (N_{10} T_2 + N_{20} T_1)^{-1}.$$

The resonant secularity in the solution for  $E_2$  can be removed by putting

$$A_1 + v_g B_1 + h a = 0, \quad (4.20)$$

where  $v_g = \omega^3/k^3$  is the group velocity of IAW and

$h = (\omega^3/4k^3) \left\{ f(4+k^2) - 2py/T_{\text{eff}} + f_{\text{eff}} \right\}$ . The last term on the left hand side of Eq.(4.20) arises due to inhomogeneities in the system. For single electron species i.e., for  $T_1 = T_2$ , the expression for  $h$  agrees with that obtained by Mohan and Buti (1979). On replacing  $A_1$  and  $B_1$  by  $\partial a / \partial t_1$  and  $\partial a / \partial x_1$  respectively, where

$t_1 = \epsilon t$  and  $x_1 = \epsilon x$ , and substituting  $a = Ae^{-ht}$ , Eq. (4.20) can be written as,

$$\frac{\partial A}{\partial t_1} + V_g \frac{\partial A}{\partial x_1} = 0.$$

Hence  $A$  is constant in a frame of reference moving with the velocity  $V_g$  and so the wave amplitude ' $a$ ', as a whole damps with a damping rate  $h$ . On using the relation (4.20), the second order quantities are given by

$$E_2 = i \frac{(3k^4 - \omega_y^4)}{3k^3\omega^4} a^2 e^{2i\psi} + b e^{i\psi} + c.c.,$$

$$N_2 = - \left\{ \frac{3k^2(3\omega^2 + 1) - \omega_y^4}{6k^2\omega^6} \right\} a^2 e^{2i\psi} +$$

$$\left( \frac{k^2 - 1}{k^2} B_1 + \frac{ik}{\omega^2} b - \frac{2k}{\omega^3} h a \right) e^{i\psi} + c.c. + \delta_N,$$

$$N_{12} = \frac{N_{10}}{T_1} T_{eff} \left\{ - \frac{(3k^4 - \omega_y^4 + 3k^2\omega^4 T_{eff}/T_1)}{6k^4\omega^4} a^2 e^{2i\psi} \right. \\ \left. + \left( \frac{a}{k^2} \frac{p T_{eff} p T_1}{T_1} + \frac{ik}{k} b - \frac{B_1}{k^2} \right) e^{i\psi} \right\} + c.c. + \delta_{N_1}$$



$$N_{22} = \frac{N_{20}}{T_2} T_{\text{eff}} \left\{ - \left( \frac{3k^4 - \omega^4 y + 3k^2 \omega^4 T_{\text{eff}}/T_2}{6k^4 \omega^4} \right) a^2 e^{2i\psi} \right.$$

$$\left. + \left( \frac{a}{k^2} \frac{T_1 - T_2}{T_2} + \frac{i}{k} b - \frac{B_1}{k^2} \right) e^{i\psi} + \text{c.c.} + \delta_{N_2} \right\},$$

and

$$v_2 = - \left\{ \frac{3k^4(\omega^2 + 1) - \omega^4 y}{6k^3 \omega^5} \right\} a^2 e^{2i\psi} - \left( \frac{\omega}{k^3} B_1 + \frac{2}{\omega^3} h a \right. \\ \left. - \frac{i}{\omega} b \right) e^{i\psi} + \text{c.c.} + \delta_v.$$

The complex quantity  $b$  and real quantities  $\delta_N, \delta_{N_1}, \delta_{N_2}$  and  $\delta_v$  depend on 'a' and  $\bar{a}$  only.  $\delta_N, \delta_{N_1}, \delta_{N_2}$  and  $\delta_v$  are determined from the conditions for removal of secularities arising from constants of integration, from the third order solutions. They are found to be

$$\delta_v = -d^{-1} \left[ (F_+ \phi_v + \frac{1}{2} \psi_v) e^{F_+ \xi} \int_{\xi}^{\xi - F_+ \xi'} e^{-|a|^2} d\xi' \right. \\ \left. - (F_- \phi_v + \frac{1}{2} \psi_v) e^{F_- \xi} \int_{-\infty}^{\xi - F_- \xi'} e^{-|a|^2} d\xi' \right] \\ + \left( \frac{2k}{\omega^3} + V_g \right) (1 - V_g^2)^{-1} |a|^2, \quad (4.21)$$

$$\delta_N = -(1+k^2)^{3/2} d^{-1} \left[ (F_+ \Phi_N + \frac{1}{2} \Psi_N) \times \right. \\ \left. e^{F_+ \xi} \int_{-\infty}^{\xi} e^{-F_+ \xi'} |a|^2 d\xi' - (F_- \Phi_N + \frac{1}{2} \Psi_N) \times \right. \\ \left. e^{F_- \xi} \int_{-\infty}^{\xi} e^{-F_- \xi'} |a|^2 d\xi' \right] + \left( \frac{2k}{\omega^3} v_g + 1 \right) (1-v_g^2)^{-1} |a|^2, \quad (4.22)$$

$$\delta_{N_1} = \frac{N_{10}}{T_1} T_{\text{eff}} \delta_N + \gamma_1, \quad (4.23)$$

and

$$\delta_{N_2} = \frac{N_{20}}{T_2} T_{\text{eff}} \delta_N - \gamma_1, \quad (4.24)$$

with  $\xi = \epsilon(x - v_g t)$  and  $\gamma_i$  as an arbitrary absolute constant which is chosen to be zero to make  $\delta_N$  finite. The other quantities appearing in Eqs. (4.21) and (4.22) are defined as follows:

$$\Phi_v = \int (k^2 + 2)^2 \left( \frac{k^6}{\omega^6} + 1 \right) - \frac{2k}{T_{\text{eff}}} (k^2 + 2) \left\{ y \left( \frac{k^6}{\omega^6} + 1 \right) - (1 + k^2)^3 \right\} + \rho_{\text{eff}} \left\{ k^2 + 2(1 + k^2)^3 \right\},$$

$$\psi_v = \rho^2 (k^2 + 2)^2 (2k^6 + 6k^4 + 7k^2 + 6) + \frac{4p^2 y^2}{T_{\text{eff}}^2} x$$

$$(k^2 + 2) + \rho_{\text{eff}}^2 \{ k^2 + 2(1 + k^2)^3 \} - \frac{4p\rho}{T_{\text{eff}}} (k^2 + 2) \{ y x$$

$$(k^2 + 2)(k^4 + k^2 + 2) - (1 + k^2)^3 \} + 2\rho\rho_{\text{eff}} (k^8 +$$

$$7k^6 + 16k^4 + 17k^2 + 6) - \frac{2p\rho_{\text{eff}}}{T_{\text{eff}}} \{ 2y (k^6 + 3k^4 +$$

$$4k^2 + 2) - (1 + k^2)^3 (k^2 + 2) \} ,$$

$$\phi_N = 2\rho (k^2 + 2)^2 - \frac{2p}{T_{\text{eff}}} (k^2 + 2) \{ 2y - (1 + k^2)^3 \} +$$

$$\rho_{\text{eff}} \{ k^2 + 2(1 + k^2)^3 \} ,$$

$$\psi_N = \rho^2 (k^2 + 2)^2 (k^2 + 6) + 2\rho\rho_{\text{eff}} (2k^6 + 7k^4 + 11k^2$$

$$+ 6) - \frac{4p\rho}{T_{\text{eff}}} (k^2 + 2) \{ y (k^2 + 4) - (1 + k^2)^3 \} +$$

$$\rho_{\text{eff}}^2 \{ k^2 + 2(1 + k^2)^3 \} + \frac{4p^2 y^2}{T_{\text{eff}}^2} (k^2 + 2) - \frac{2p\rho_{\text{eff}}}{T_{\text{eff}}} (k^2 +$$

$$2) \{ 2y - (1 + k^2)^3 \} ,$$

$$d = 2k^4(k^4 + 3k^2 + 3) \left[ p^2(k^2 + 2)^2 + \frac{p^2}{T_{eff}} \{ (1+k^2)^3 + 4y(y-1) \} + \frac{1}{4} p_{eff}^2 (1+k^2)^3 + \frac{2pp}{T_{eff}} (k^2 + 2)(1-2y) + p p_{eff} (k^2 + 2) + \frac{p p_{eff}}{T_{eff}} \{ (1+k^2)^3 - 2y \} \right]^{1/2},$$

and

$$F_{\pm} = \{ 2k^2(k^4 + 3k^2 + 3) \}^{-1} \left[ - \left[ p(2k^6 + 6k^4 + 5k^2 - 2) - \frac{p}{T_{eff}} \{ (1+k^2)^3 - 2y \} + \frac{1}{2} p_{eff} \{ (1+k^2)^3 - 2 \} \right] \pm (1+k^2)^{3/2} \{ 2k^4(k^4 + 3k^2 + 3) \}^{-1} d \right].$$

While determining  $\delta_N$  and  $\delta_V$ , it is assumed that  $|a|^2$  is bounded and all its derivatives tend to zero as

$$\xi \rightarrow \pm \infty.$$

Removal of resonant secularities from the third order solutions then yields the relation,

$$\ddot{z}(A_2 + V_g B_2) + \dot{z} h'_1 a + h_2 \frac{\partial a}{\partial \xi} + p \frac{\partial^2 a}{\partial \xi^2} + a [Q |a|^2 + Q_+ e^{F_+ \xi} \int_{-\infty}^{\xi} e^{-F_+ \xi'} |a|^2 d\xi' - Q_- e^{F_- \xi} \int_{-\infty}^{\xi} e^{-F_- \xi'} |a|^2 d\xi'] - R a = 0, \quad (4.25)$$

where

$$h_1' = (\omega^3/4k^3) \{ \nu_{\text{eff}} + 2(\nu_1 N_{10}/T_1 + \nu_2 N_{20}/T_2) T_{\text{eff}} - qy/T_{\text{eff}} \},$$

$$h_2 = -(\omega^3/4k^3) \{ p(k^2+10) + p_{\text{eff}}(2k^2-1)/k^2 + (py/T_{\text{eff}})(4k^2+6)/k^2 \},$$

$$P = -3\omega^5/2k^4,$$

$$Q = -\omega^3 \{ 12k^6(k^4+3k^2+3) \}^{-1} [ 3k^{10} + 6k^8 - (q-3y')k^6 - (33+6y-9y'-y^2)k^4 - (30+12y-9y'-3y^2)k^2 - (9+9y-3y'-3y^2) ],$$

$$R = (\omega^5/16k^4) [ p^2(5k^2+32) + p p_{\text{eff}}(2k^4+12k^2-8)/k^2 - 4(p p_{\text{eff}}/T_{\text{eff}})(q+y(k^2-2)/k^2) + (p^2/T_{\text{eff}}^2) \{ 16y' - 12y^2 - (1+k^2)/k^2 \} ],$$

$$y' = (N_{10}/T_1^3 + N_{20}/T_2^3) T_{\text{eff}}^3,$$

and

$$Q_{\pm} = \{ 4k(k^4 + 3k^2 + 3)d \}^{-1} \left[ \{ p^2 D_1 + (p^2/T_{\text{eff}}) D_2 \right. \\ \left. + p p_{\text{eff}} D_3 + (p p_{\text{eff}}/T_{\text{eff}}) D_4 + p_{\text{eff}}^2 D_5 + (p^2/T_{\text{eff}}^2) D_6 \right. \\ \left. \pm (1+k^2)^3 H \{ 2k^4(k^4 + 3k^2 + 3) \}^{-1} d \right],$$

with

$$D_1 = (k^2 + 2)^2 \{ k^{10} + (10 - y)k^8 + (34 - 5y)k^6 + (56 - 9y)k^4 + (40 - 8y)k^2 + (12 - 4y) \},$$

$$D_2 = (k^2 + 2) \{ 2k^{14} + (22 - 8y)k^{12} + (32 - 50y)k^{10} - (22 + 154y + 4y^2)k^8 - (26 + 283y + 28y^2)k^6 + (17 - 307y - 60y^2)k^4 + (40 - 168y - 44y^2)k^2 + (12 - 28y + 8y^2) \},$$

$$D_3 = - \{ k^{16} + 5k^{14} - (3 - 3y)k^{12} - (76 - 19y)k^{10} - (134 - 54y)k^8 - (335 - 80y)k^6 - (192 - 58y)k^4 - (16 - 16y)k^2 - (81 - 2y) \},$$

$$D_4 = k^2(k^2+2) \{ 4k^{12} + (30-6y)k^{10} + (96-35y)k^8 + (168-98y)k^6 + (168-152y)k^4 + (92-130y)k^2 + (20-43y) \} ,$$

$$D_5 = \frac{1}{2} \{ k^{14} + (9-y)k^{12} + (34-6y)k^{10} + (70-16y)k^8 + (81-22y)k^6 + (48-15y)k^4 + (9-3y) \} ,$$

$$D_6 = k^2(k^2+2) \{ (4-2y)k^8 + (10-8y)k^6 + (24-12y+24y^2-4y^3)k^4 + (16-16y+50y^2+12y^3)k^2 + (4-10y+38y^2-12y^3) \} ,$$

and

$$H = 2P(k^2+2)^2 \{ k^6 + 3k^4 + 4k^2 + 3 - y \} + \frac{2P(k^2+2)}{T_{eff}} \{ k^8 + (6-3y)k^6 + (12-9y)k^4 + (10-11y)k^2 + (3-7y+2y^2) \} + P_{eff} \{ 2k^8 + (12-2y)k^6 + (25-6y)k^4 + (23-7y)k^2 + (6-y) \} .$$

with the help of Eqs. (1.14) and (1.18), Eq.(4.42) can be

written as

$$\begin{aligned}
 & i \frac{\partial a}{\partial \tau} + i h_1 a + h_2 \frac{\partial a}{\partial \xi} + P \frac{\partial^2 a}{\partial \xi^2} + \\
 & a \left[ Q |a|^2 + Q_+ e^{F_+ \xi} \int_{-\infty}^{\xi} e^{-F_+ \xi'} |a|^2 d\xi' - \right. \\
 & \left. Q_- e^{F_- \xi} \int_{-\infty}^{\xi} e^{-F_- \xi'} |a|^2 d\xi' \right] - R a = 0, \quad (4.26)
 \end{aligned}$$

where  $\tau = \epsilon^2 t$  and  $h_1 = (1/\epsilon)h + h'_1$ . This is the MNSE governing the IAW. The additional nonlinear nonlocal term arises due to the constant terms in the second order solutions and is governed by the effective inhomogeneity scalelengths of the system. In a single electron temperature plasma, i.e. when  $T_1 = T_2$ , Eq. (4.26) reduces to the MNSE obtained by Mohan and Buti (1979). The last term in Eq. (4.26) can be removed by a simple transformation  $a \rightarrow a \exp(-iR\tau)$ .



### 4.3 Linear Stability

To study the linear stability, let us consider a small amplitude plane wave solution for Eq.(4.26), namely,

$$a = a_0 \exp [\tilde{\epsilon} (K \xi - \Omega \tau)],$$

where  $a_0$  is a constant amplitude and  $K$  and  $\Omega$  are the wave-number and frequency of the IAW envelope respectively. So the linear dispersion relation becomes

$$\Omega = PK^2 - \left( Q - \frac{Q_+}{F_+} + \frac{Q_-}{F_-} \right) |a|^2 - \tilde{\epsilon} (h_1 + Kh_2). \quad (4.27)$$

Thus one immediately gets the growth rate as

$$\gamma = - \left( \frac{\omega^3}{4k^3} \right) \left( S_1 + S_2 - \frac{K'}{k} S_3 \right), \quad (4.28)$$

where

$$S_1 = \alpha(4 + k^2) - 2\epsilon p y / T_{\text{eff}} + \epsilon p_{\text{eff}},$$

$$S_2 = 2(\beta_1 N_{10}/T_1 + \beta_2 N_{20}/T_2) T_{\text{eff}} - \epsilon^2 q y / T_{\text{eff}} + \epsilon^2 z_{\text{eff}},$$

$$S_3 = \alpha(k^2 + 10) + \epsilon(p y / T_{\text{eff}}) \frac{4k^2 + 6}{k^2} + \epsilon p_{\text{eff}} \frac{2k^2 - 1}{k^2},$$

and  $K' = \epsilon K$  ( $\ll k$ ) is the envelope wave number as seen

in the  $(x,t)$  coordinate frame.

In Eq.(4.28) the last two terms are smaller than the first term. Hence temperature gradients and envelope wavenumber  $K'$  donot affect the growth rate very much. Since growth rate is negative for propagation antiparallel to density gradients, in the small amplitude limit IAW damps as it propagates towards increasing density.

#### 4.4 Nonlinear Analysis

The linear theory helps us to study only the initial stages of the evolution of the waves. But to study the long time behaviour of the finite amplitude waves, Eq.(4.26) has to be solved. In Eq.(4.26) also, terms containing density gradients are much larger than the terms containing temperature gradients. So the behaviour of finite amplitude IAW, like the small amplitude case, is mostly affected by density gradients. Unlike the perturbed NSE, whose analytical solutions can be obtained by inverse scattering method, (Karpman, 1979), our Eq.(4.26) cannot be solved analytically. Hence we have solved it numerically. For this we follow the Dufort-Frankel scheme (Richtmyer and Morton, 1967; Smith, 1969) with asymptotic boundary conditions for

the solutions. The accuracy of the results is checked by varying the time and space step sizes.

We start with an initial waveform which corresponds to the stationary soliton solution of the NSE in a homogeneous plasma given by  $a = a_0 \operatorname{sech}(|Q/2P|^{1/2} a_0 \xi)$ . To demonstrate the effect of the second electron component explicitly, we have first determined the time evolution of this envelope soliton in an one electron component plasma for constant initial amplitude  $a_0$  but for different values of wave number  $k$ . From figure 1, we find that the threshold time for splitting ( $\tau^*$ ) for envelope solitons with  $k = 1.6$  and  $1.8$  are  $0.5$  and  $0.55$  respectively. We have chosen the sequence of time  $\tau$  in all the figures in such a manner that the onset of splitting for different envelope solitons can be shown clearly. However, for plasmas with two electron components, with temperature ratio  $D(= T_1/T_2) = 5$  and density ratio  $\mu(= N_1/N_2) = 3$ , fig.2 shows that the threshold time for splitting of envelope solitons increases from  $0.65$  to  $0.8$  as  $k$  increases from  $1.6$  to  $2.0$ . Maximum amplitude of the envelope soliton just before it starts splitting ( $A_0$ ), corresponding width ( $W$ ) and  $\tau^*$  for different values of  $k$  in an one electron species as well as in a two electron species plasma are shown in table 1.

From this table, it is apparent that  $\tau^*$  in a two electron species plasma is larger compared to that in an one electron species plasma for a given wavenumber  $k$ . However, in both the cases,  $\tau^*$  increases with an increase in  $k$ . This can be explained as follows: When the wavenumber increases, energy of the envelope soliton increases. The effect of a given inhomogeneity on the envelope soliton of lower energy is stronger than that of higher energy. Hence splitting occurs earlier for solitons with lower wavenumbers. In other words, as  $k$  increases, magnitude of the nonlinear nonlocal term decreases. Since this term is responsible for splitting, when its magnitude decreases, it becomes less effective and splitting occurs after a longer duration.

We have also determined the effect of a given inhomogeneity on the envelope solitons with different  $a_0$ . Fig.3 shows that as  $a_0$  increases from 1.6 to 2.0,  $\tau^*$  decreases from 0.6 to 0.55 in an one electron component plasma. Similarly, fig.4 shows that in a two electron component plasma with  $D = 5$  and  $\mu = 3$ ,  $\tau^*$  decreases from 0.7 to 0.65 as  $a_0$  increases from 1.6 to 2.0. In table 2, we have compared the values of  $A_0$ ,  $W$  and  $\tau^*$  for different values of  $a_0$  in an one electron species and a two electron species plasma for a given  $k$ . As in the previous case,

here also splitting of an envelope soliton is delayed when the second electron species is introduced. From table 2, we find that  $\tau^*$  in both types of plasmas decreases as  $a_0$  increases. The reason for this is: the nonlinear nonlocal term depends on  $|a|^2$  which in turn depends on  $|a_0|^2$ . So as  $a_0$  increases, magnitude of the nonlinear nonlocal term increases and hence the threshold time for splitting decreases.

From tables 1 and 2 we find that the width and the maximum amplitude of envelope solitons in a two electron species plasma are smaller than the corresponding values in an one electron species plasma. This shows that as the second electron component is introduced, the width and the maximum amplitude of the envelope solitons decrease. The reason for this decrease in the width and the maximum amplitude of the envelope solitons is as follows: As the second electron component is introduced, effective temperature of the system decreases and consequently the strength of the dispersion also decreases. To balance this smaller dispersion, strength of nonlinearity and hence the amplitude must decrease (Goswami and Buti, 1976).

In laboratory plasma,  $D$  can be varied from less than 2 to about 5 while  $\mu$  can be varied from about  $1/6$

to 3 (Jones et al., 1975). Time evolution of the envelope solitons with different  $D$  are plotted in fig.5. Here we find that as  $D$  increases, width of the envelope soliton decreases and it takes a longer time for the envelope soliton to split into two solitary waves. Fig.6 also shows similar behaviour i.e. as  $\mu$  increases width of the envelope soliton decreases and  $\tau^*$  increases. This increase in the magnitude of  $\tau^*$  can be explained by the fact that when width of the envelope soliton decreases, effective inhomogeneity becomes weaker. Hence splitting occurs comparatively at a later time. Figs.7 and 8 show the variation of  $\tau^*$  with  $D$  and  $\mu$  respectively, keeping the other fixed. These two figures show that  $\tau^*$  increases with increase of  $D$  or  $\mu$ .

For investigating the time evolution of the envelope hole, which is the stationary solution of the NSE when  $PQ < 0$ , we consider the initial waveform,  $a = a_0 \times \{1 - \tilde{a}^2 \text{sech}^2(\frac{1}{2} \sqrt{PQ} |a_0 \tilde{a}|)\}^{1/2}$ . The density and temperature ratio of both the electron components are varied between 1/6 to 3 and 2 to 5 respectively, as in the case of envelope solitons. But contrary to the case of envelope solitons, envelope holes do not split into two envelope holes for quite a long time as they

propagate towards increasing density. However, for  $D = 1$ , which corresponds to one electron species plasma, the envelope hole splits into two envelope holes as found earlier (Mohan and Buti, 1979). Time evolution of envelope holes is plotted in fig.9 which shows that  $\tau^*$  for a single electron species plasma is 0.25, whereas, for a two electron species plasma with  $\mu = 1$  and  $D = 5$ , splitting does not occur till  $\tau = 1.2$ . Since real time  $t = \epsilon^{-2} \tau$  and in our calculation  $\epsilon = 0.1$ , we find that even though an envelope hole splits into two envelope holes in an one electron component plasma at  $t = 25 \omega_{p_i}^{-1}$ , when the second electron species is introduced, the envelope hole does not split till  $t = 120 \omega_{p_i}^{-1}$ . Nonoccurrence of splitting of envelope holes in a two electron component plasma within practical length of time can be explained as follows: when the second electron species is introduced, magnitude of the nonlinear nonlocal term is significantly reduced and is not strong enough to cause splitting within a reasonable length of time. As a typical example, magnitude of nonlinear nonlocal term for  $k = 1.0$ ,  $a_0 = 1.5$  and  $\tilde{a} = 0.8$  for an one electron component plasma is 2.85, whereas the same is reduced to 1.25 in a two electron component plasma

with  $D = 5$  and  $\mu = 1$ . Hence the second electron component is responsible for the quenching of splitting of the envelope holes for the range of parameters we have chosen.

#### 4.5 Conclusions

From the above studies, it can be concluded that the width and maximum amplitude of the envelope soliton become smaller when it propagates in a two electron species plasma. Besides, it takes longer time for the envelope soliton to split into two solitary waves in a two electron component plasma. The effect of the second electron species on the envelope holes is found to be much more drastic, so much so that it can even annul the splitting of the envelope holes propagating towards increasing density.



Table 1

$A_0$ ,  $W$  and  $\tau^*$  for various values of  $k$  for  $a_0 = 2.0$

$k$	One Electron Component Plasma			Two Electron Component Plasma		
	$A_0$	$W$	$\tau^*$	$A_0$	$W$	$\tau^*$
1.6	2.09	0.7	0.50	1.005	1.20	0.65
1.8	1.018	0.725	0.55	0.697	0.69	0.65
2.0	0.561	0.9	0.775	0.605	0.7	0.80

Table 2

$A_0$ ,  $W$  and  $\tau^*$  for various values of  $a_0$  for  $k = 1.8$

$a_0$	One Electron Component Plasma			Two Electron Component Plasma		
	$A_0$	$W$	$\tau^*$	$A_0$	$W$	$\tau^*$
1.6	0.663	0.875	0.6	0.4657	0.76	0.7
1.8	0.832	0.75	0.575	0.577	0.71	0.675
2.0	1.018	0.725	0.55	0.697	0.689	0.65

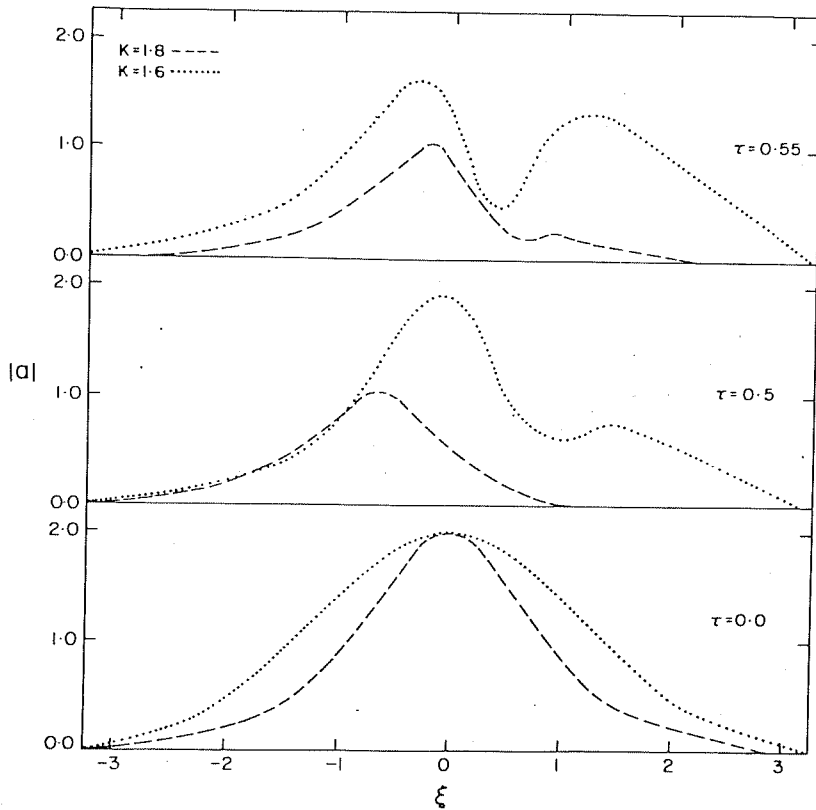


Fig. 1:  $|a|$  Vs.  $\xi$  . Evolution of an envelope soliton in an one electron component plasma with  $\alpha^{-1} = L/\lambda_D = 10$ ,  $\beta = 1$ ,  $\mathcal{U} = 1$ ,  $a_0 = 2$  and  $k = 1.6$  and  $1.8$ .

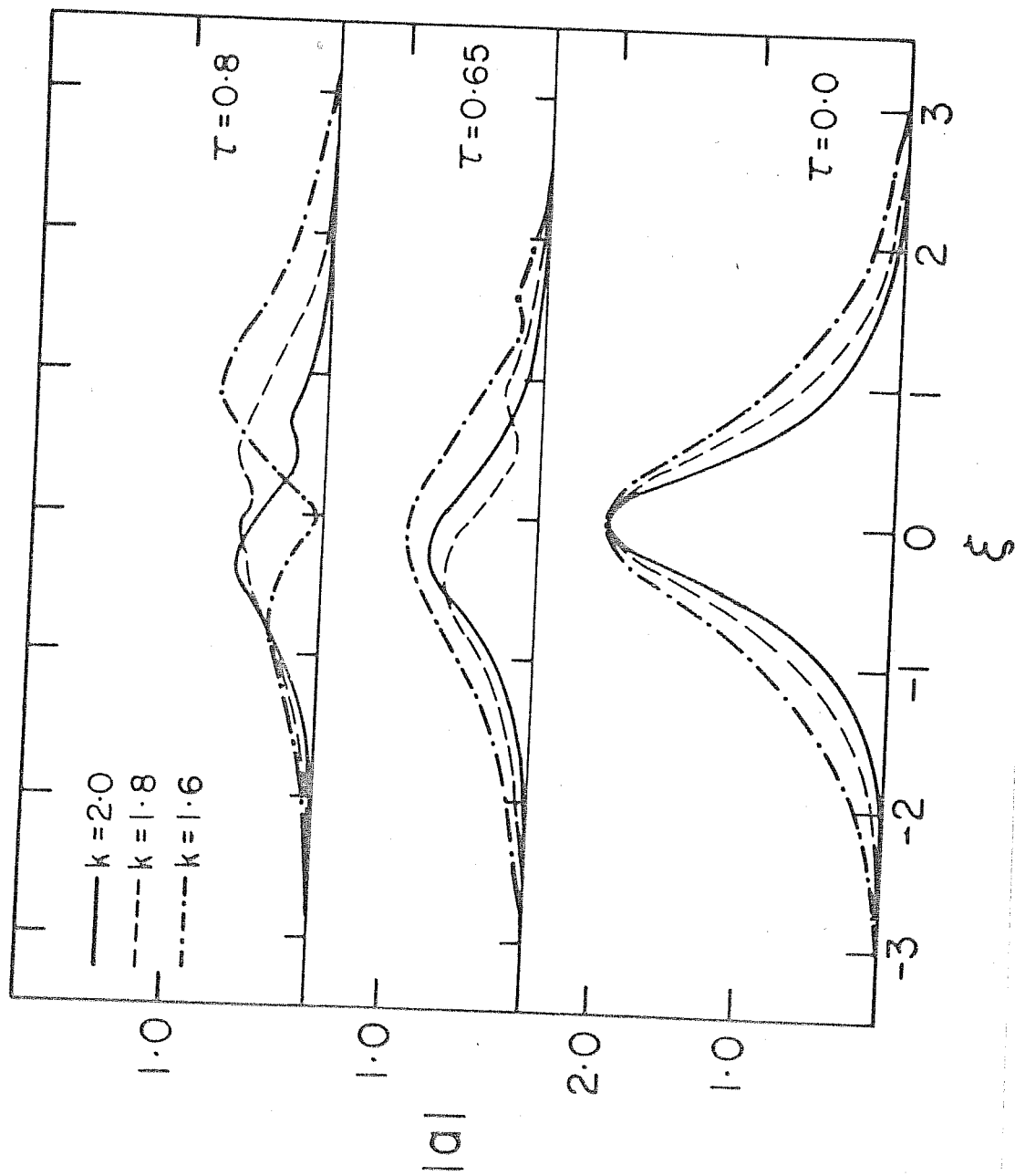


Fig.2:  $|a| v_s \xi$ . Evolution of an envelope soliton in an one electron component plasma with  $\alpha^1 = L/\lambda_D = 10$ ,  $\beta = 1$ ,  $\omega = 1$ ,  $a_0 = 2$  and  $k = 1.6$  and  $1.8$

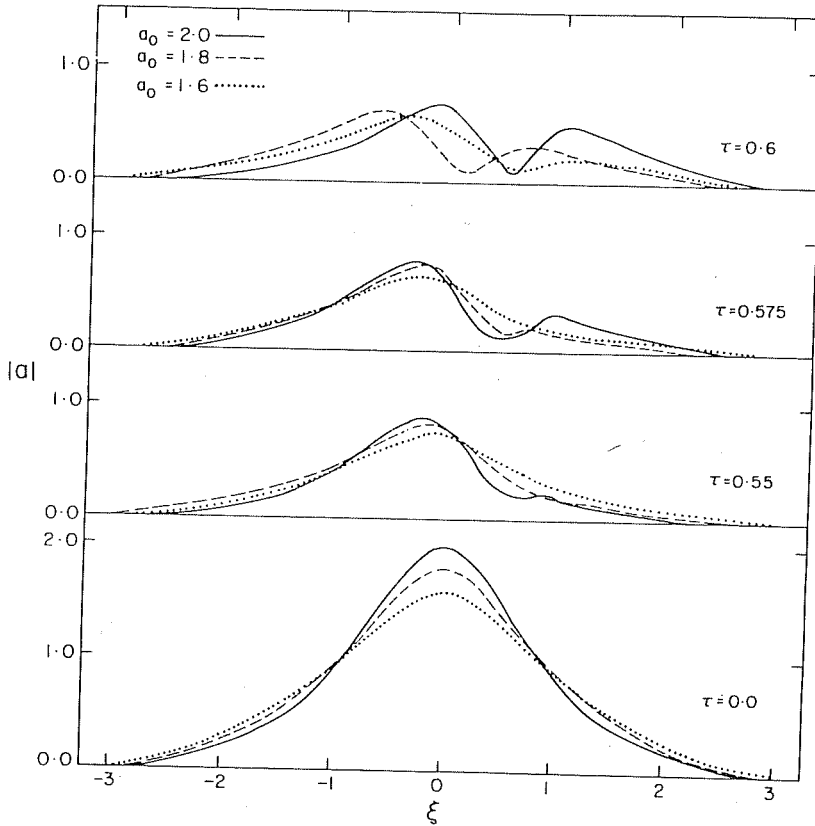


Fig. 3:  $|a|$  Vs.  $\xi$ . Evolution of an envelope soliton in an one electron component plasma with  $\alpha^{-1} = 10$ ,  $f = 1$ ,  $\nu = 1$ ,  $k = 1.8$  and  $a_0 = 1.6, 1.8$  and  $2.0$ .

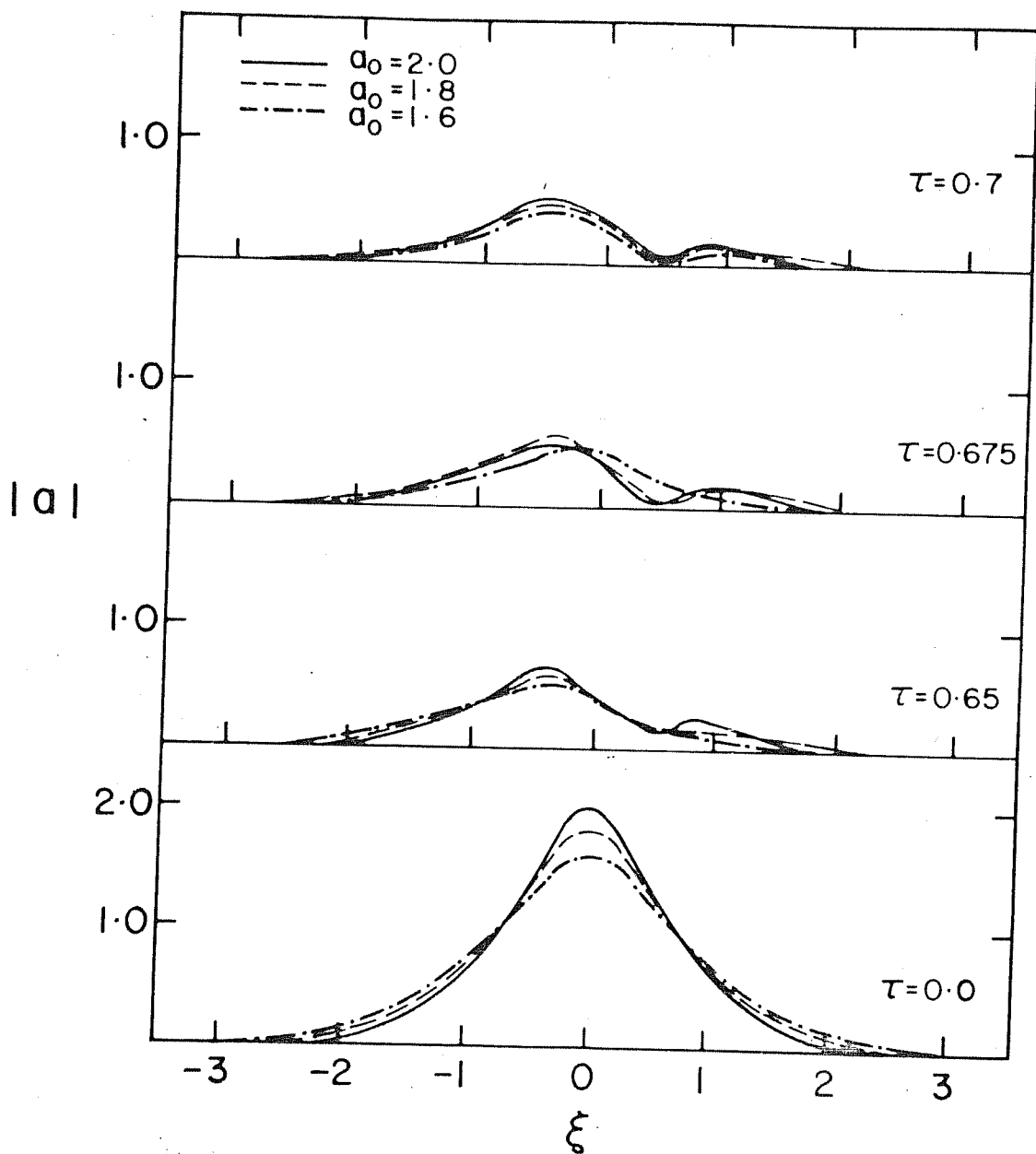


Fig.4:  $|a|/v_s \xi$ . Evolution of an envelope soliton in a two electron component plasma with  $\alpha^{-1} = 10$ ,  $\beta_1 = \beta_2 = 1$ ,  $\nu_1 = \nu_2 = 1$ ,  $\mu = 3$ ,  $D = 5$ ,  $k = 1.8$  and  $a_0 = 1.6, 1.8$  and  $2.0$ .

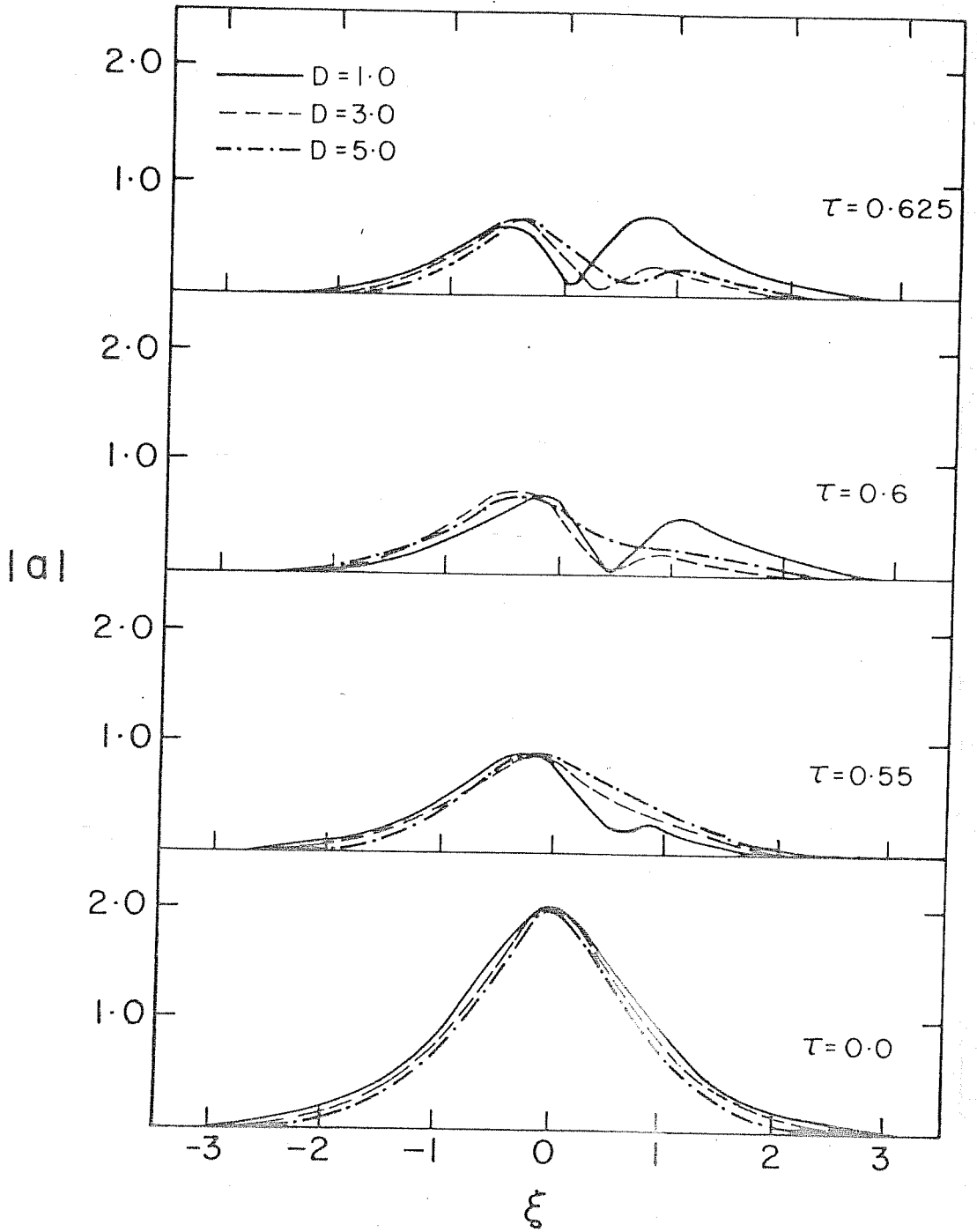


Fig.5:  $|a| v_s \xi$ . Evolution of an envelope soliton in a two electron component plasma with  $\alpha^{-1} = 10$ ,  $\beta_1 = \beta_2 = 1$ ,  $\nu_1 = \nu_2 = 1$ ,  $k = 1.8$ ,  $a_0 = 2.0$ ,  $\mu = 1$  and  $D = 1, 3$  and  $5$ .

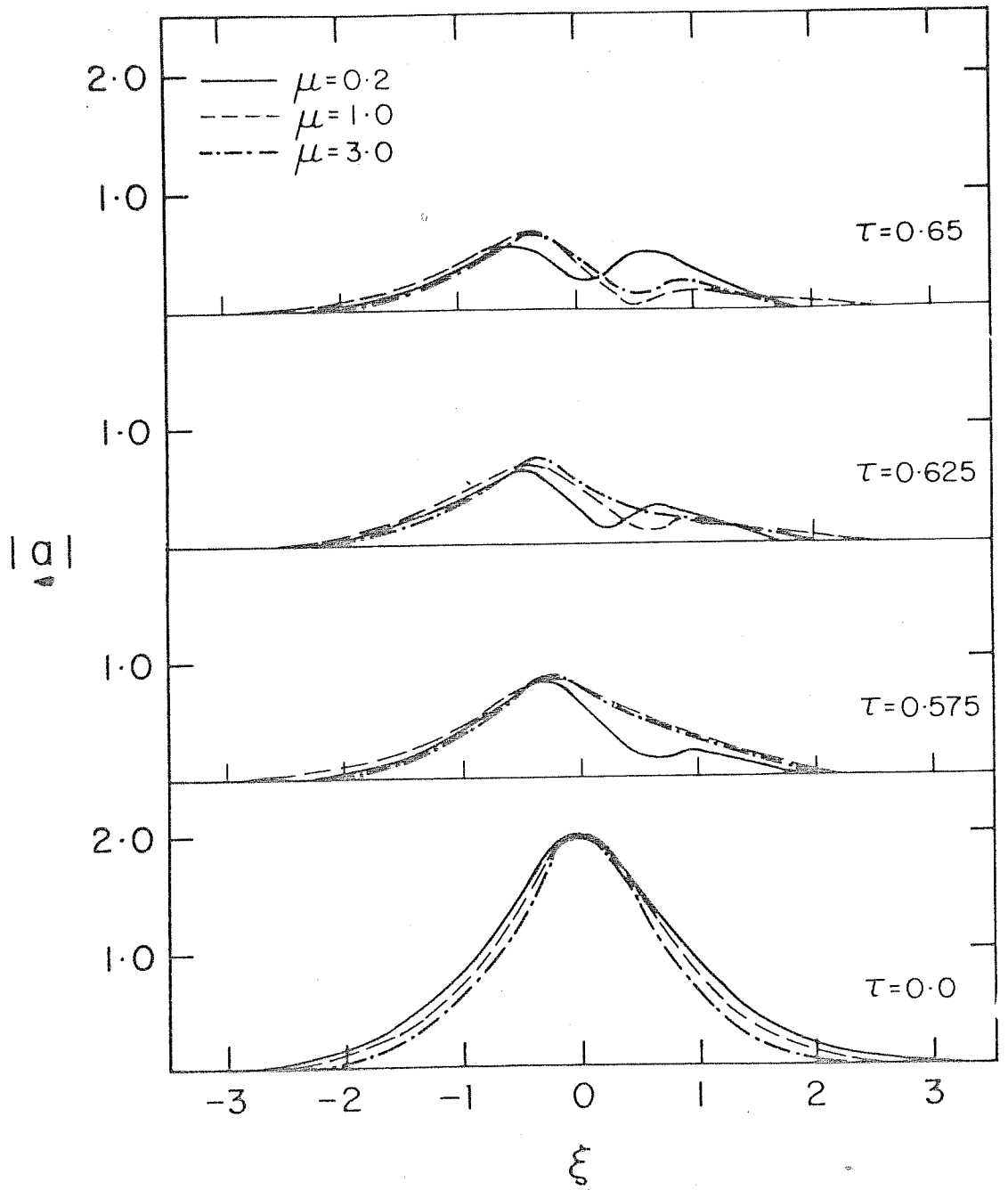


Fig. 6 :  $|a| v_s \xi$ . Evolution of an envelope soliton in a two electron component plasma with  $\alpha^{-1} = 10$ ,  $\beta_1 = \beta_2 = 1$ ,  $\nu_1 = \nu_2 = 1$ ,  $k = 1.8$ ,  $a_0 = 2.0$ ,  $D = 5$  and  $\mu = 0.2, 1$  and  $3$ .



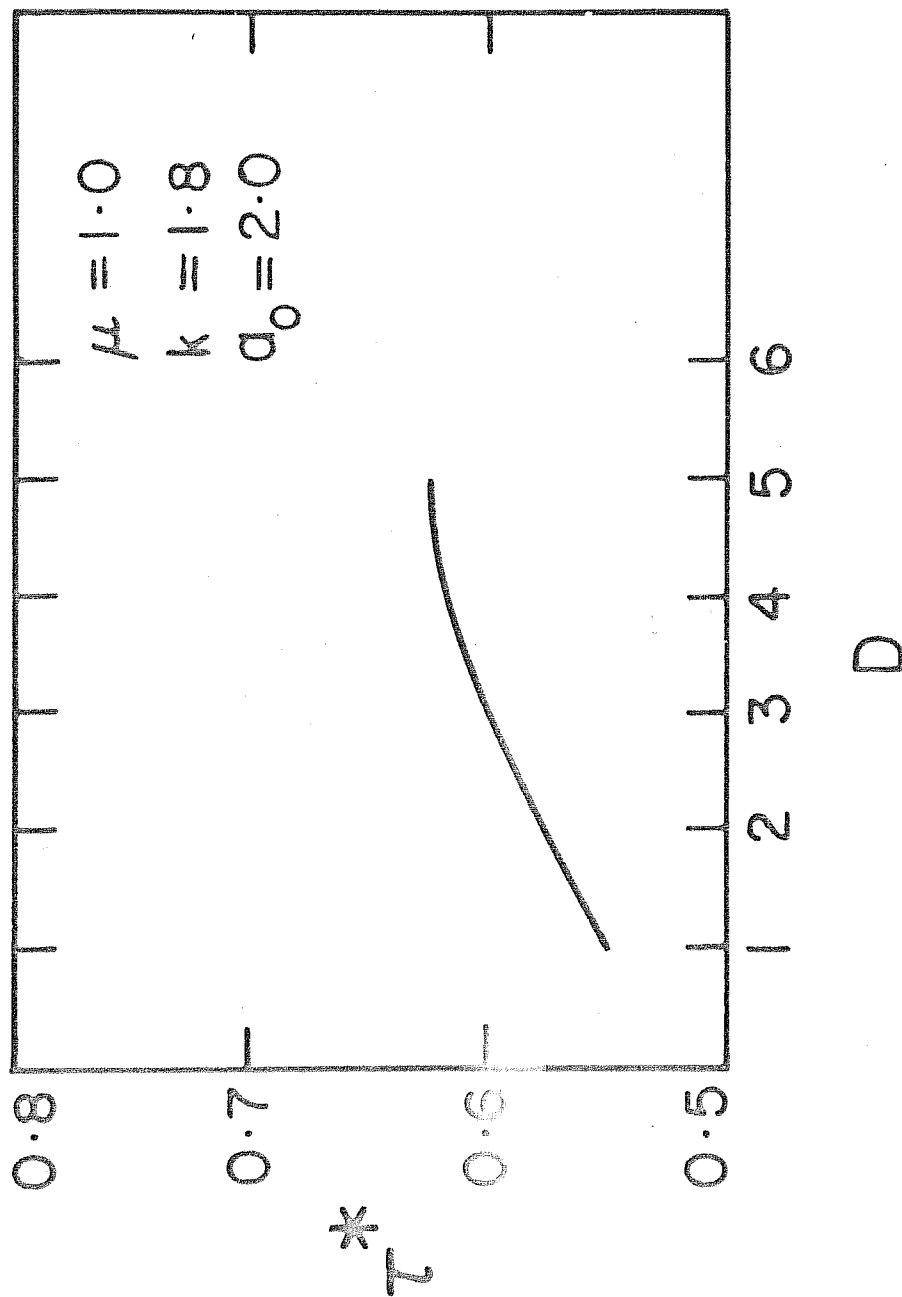


Fig. 7 :  $\tau^* V_s D$  for  $\alpha^{-1} = 10$ ,  $\beta_1 = \beta_2 = 1$ ,  
 $\mathcal{V}_1 = \mathcal{V}_2 = 1$ ,  $k = 1.8$ ,  $a_0 = 2.0$  and  $\mu = 1$ .

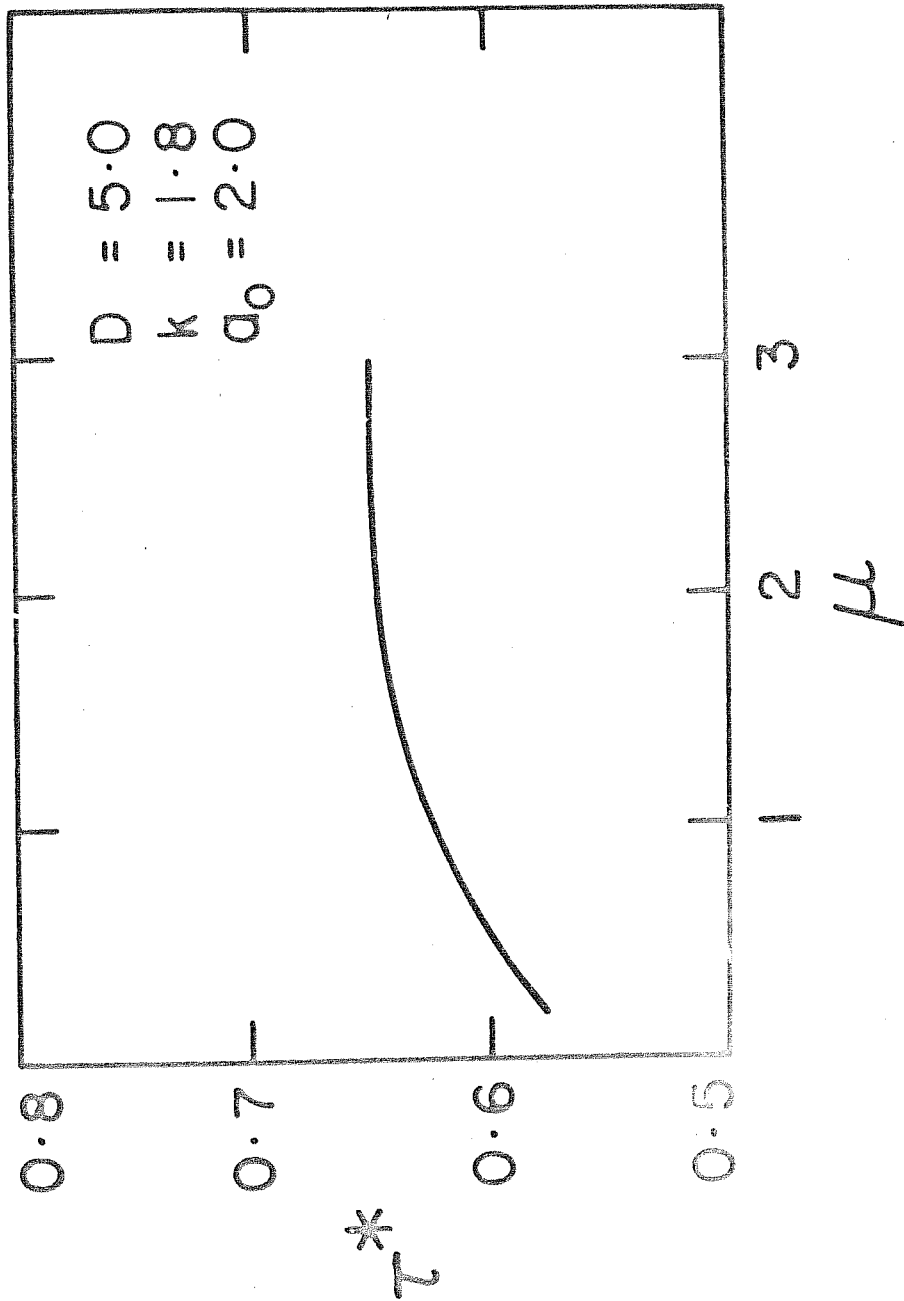


Fig. 8 :  $\tau^* v_s \mu$  for  $\alpha^{-1} = 10$ ,  $\beta_1 = \beta_2 = 1$ ,  
 $\omega_1 = \omega_2 = 1$ ,  $k = 1.8$ ,  $a_0 = 2.0$  and  $D = 5$ .

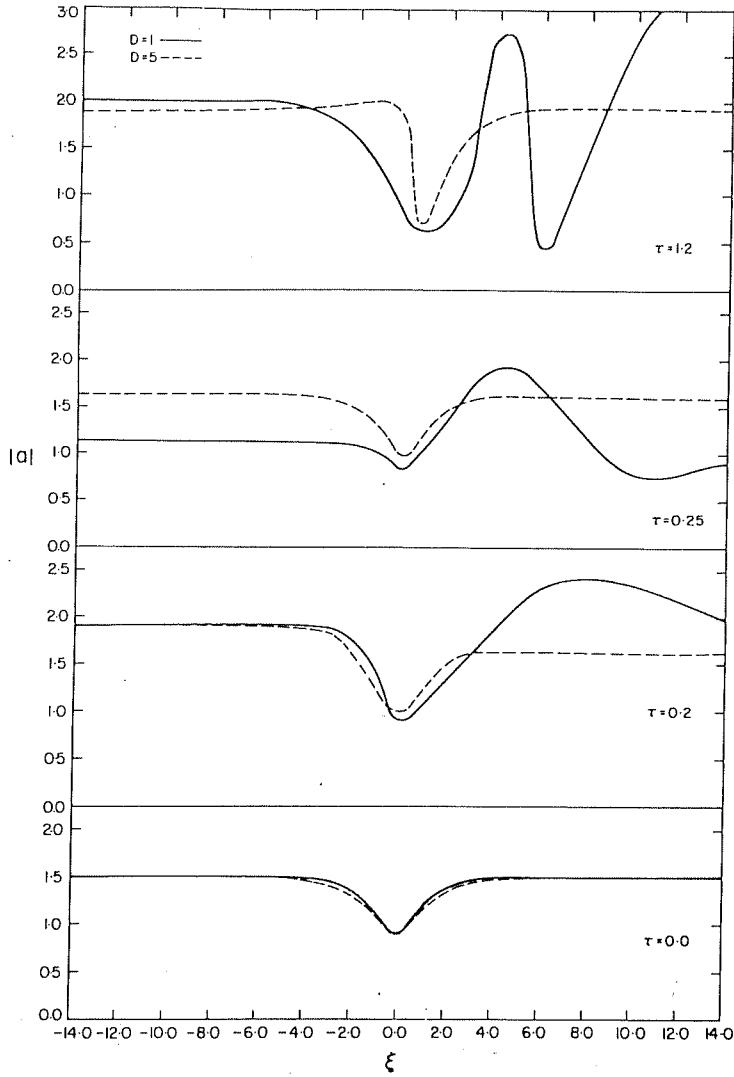


Fig. 9:  $|a|$  vs.  $\xi$ . Evolution of an envelope hole in a plasma with  $\alpha^{-1} = 10$ ,  $f_1 = f_2 = 1$ ,  $\nu_1 = \nu_2 = 1$ ,  $k = 1.0$ ,  $\tilde{a} = 0.8$ ,  $a_0 = 1.5$ ,  $\mu = 1$  and  $D = 1$  and  $5$ .

## CHAPTER 5

### ELECTRON ACOUSTIC AND ION-ION-HYBRID RESONANCE WAVES IN MULTI-ION-SPECIES MAGNETOPLASMAS

#### 5.1 Introduction

The presence of more than one species of ions is not uncommon in space as well as in laboratory plasmas. The polar orbiting satellite ISIS 2 had measured ion composition in the plasmasphere (Hoffman et al., 1974). Even though hydrogen is the major constituent, small fractions of  $O^+$ ,  $He^+$ ,  $O^{++}$  and  $N^+$  are also present. On the basis of the results from the GEOS 1 and 2, Balsiger et al. (1980) had concluded that the ring current has ions like

$H^+$ ,  $He^+$ ,  $He^{++}$ ,  $O^+$  and  $O^{++}$ . Johnson et al. (1977) had also reported the presence of  $He^+$  and  $O^+$  ions in the ring current, besides  $H^+$ . The direct identification of ions in the magnetotail had been accomplished with the mass spectrometer aboard the ISEE 1 satellite which confirms the presence of  $O^+$  streams (Hardy et al., 1977; Frank et al., 1977). ISEE 1,2 measurements also indicate the presence of  $He^+$ ,  $He^{++}$  ions in the magnetotail (Williams et al., 1979; Peterson et al., 1981).

In the fusion plasma devices, impurity ions are frequently present. Besides deuterons, which constitute the bulk of ions in the 2xIIB mirror machine, 2-5% of protons are also present (Bardet et al., 1975). A few percent of impurity ions like  $H^+$ ,  $O^{7+}$ ,  $C^{5+}$ ,  $C^{4+}$  etc. are present in the deuteron plasma in ATC experiment (Takahashi et al., 1977). Small quantities of  $T^+$ ,  $H^+$ ,  $^3He^+$  can be present even in the PLT tokamak (Hosea et al., 1979).

Several authors have shown that the presence of more than one species of ions can have a profound effect on the dispersion properties of the plasma. In case of two species of ions, Buchsbaum (1960) had shown that a new mode, known as the Ion-Ion-Hybrid Resonance (IIHR) mode, can exist in a cold magnetoplasma. The IIHR is a low frequency mode, arising due to the resonance between the

motion of two species of magnetised ions. This mode plays an important role in the rf heating of the fusion plasmas (Swanson, 1976; Janzen, 1980). The ions and the electrons in these systems have finite temperature. So to have a better understanding of rf heating of plasmas, it is necessary to investigate the characteristics of the IIHR wave in a warm plasma.

In the previous chapters we have confined our studies to plasmas where electrons are more energetic than the ions. But this may not necessarily be true everywhere. There are many situations where ions are hotter than the electrons. For example, ions in the terrestrial ring current around  $7R_E$  (Russel and Thorne, 1970), at distances of  $23-40 R_E$  in the magnetotail (Johnson et al., 1974; Frank et al., 1976), etc. are of keV range, whereas, the electrons have energies of the order of few eV. The ions in the fusion devices like the 2XIIB mirror machine, PLT tokamak are also hotter than the electrons (Coensgen et al., 1976; Eubank et al., 1979).

When the ions are hotter than the electrons, the plasma can support electron acoustic (EA) waves which propagate almost perpendicular to the magnetic field, with frequencies lying between the ion and electron gyrofrequencies (Arefev, 1970). These waves have the phase velocity,

$\omega/k = (T_i \cos^2 \theta / m_e)^{1/2}$ . In a weakly nonlinear system, with single ion species, the EA waves are governed by the KdV equation (Pokroev and Stepanov, 1973; Mohan and Buti, 1980), whereas, the dynamics of these waves can be represented in terms of an energy integral of a classical particle if complete ion and electron nonlinearities are taken into account (Buti, et al., 1980). Furthermore, Buti (1980a) had investigated the exact nonlinear EA waves in a multi-ion-component plasma and had shown that the presence of the second ion species gives rise to supersonic holes (density depressions) for sufficiently large perturbations. In all these studies, ions were assumed to be unmagnetised. However, for low frequency wave propagation ( $\omega \sim \Omega_i$ ,  $\Omega_i$  being the ion cyclotron frequency), ions must be considered as magnetised.

The EA waves arise due to balance between ion thermal pressure and the electron inertia. Hence their properties strongly depend on the ion temperature. If more than one species of ions with different temperatures are present, the system is governed by the effective temperature, which is a function of the temperature and relative concentration of the individual ion components (Buti, 1980a). So the dispersion characteristics of the EA waves will be modified when the temperature and relative concentration of the two species of ions are varied.

Since magnetised plasmas with multi-ion-species, with ion temperature larger than the electron temperature, can sustain both EA and IIHR waves, some regions in the earth's magnetosphere (ring current, magnetotail, etc.) and the 2XIIB mirror machine can support EA and IIHR waves. In this chapter, we study the propagation characteristics of the IIHR and EA waves in a warm plasma with two species of ions which are considered to be magnetised.

## 5.2 Dispersion Relation

Let us consider a plasma containing two species of ions which are magnetised and are more energetic than the electrons i.e.  $T_{1,2} > T_e \neq 0$  ( $T_{1,2,e}$  being the temperatures of the two species of ions and electrons respectively). The magnetic field  $\underline{B}_0$  is along the z-direction and we consider wave propagation almost perpendicular to the magnetic field so that  $0 \ll k_z / k \ll (m_e/m_i)^{1/2}$ . The basic equations governing such a system are the continuity equation and momentum equation for the electrons and both species of ions and the poisson's equation, namely,



$$\frac{\partial n_e}{\partial t} + \nabla \cdot (n_e \underline{v}_e) = 0, \quad (5.1)$$

$$\frac{\partial n_\alpha}{\partial t} + \nabla \cdot (n_\alpha \underline{v}_\alpha) = 0, \quad (5.2)$$

$$m_e n_e \left( \frac{\partial \underline{v}_e}{\partial t} + \underline{v}_e \cdot \nabla \underline{v}_e \right) = -e n_e \left( \underline{E} + \frac{1}{c} \underline{v}_e \times \underline{B}_0 \right) - T_e \nabla n_e, \quad (5.3)$$

$$m_\alpha n_\alpha \left( \frac{\partial \underline{v}_\alpha}{\partial t} + \underline{v}_\alpha \cdot \nabla \underline{v}_\alpha \right) = z_\alpha e n_\alpha \left( \underline{E} + \frac{1}{c} \underline{v}_\alpha \times \underline{B}_0 \right) - T_\alpha \nabla n_\alpha, \quad (5.4)$$

and

$$\nabla^2 \phi = 4\pi e (n_e - z_1 n_1 - z_2 n_2). \quad (5.5)$$

In equations (5.1) to (5.5),  $m, n$  and  $\underline{v}$  are the mass, density and velocity; the subscripts  $e$  and  $\alpha = 1, 2$  refer to the electrons and two species of ions. The ions have charges  $z_1 e$  and  $z_2 e$ . We have neglected the effect of the finite larmour radius and used the scalar pressure

in writing Eq.(5.4); neglect of finite larmour radius effect is justified later. We are interested in investigating the nature of the EA and IIHR waves. So we focus our attention to the frequency regime  $k_z v_j \ll \omega \ll k_x v_j$  ( $v_j = (T_j/m_j)^{1/2}$  is the thermal velocity of the  $j^{\text{th}}$  species, where  $j = e, 1$  and  $2$ ) in which these two modes propagate.

Let us consider electrostatic perturbations of the form

$\phi \sim \exp \{ i (k_x x + k_z z - \omega t) \}$ . Linearising Eqs. (5.1) to (5.5), we obtain

$$n_{e_1} = - \frac{e \phi n_0}{m_e \omega^2} \left[ \frac{k^2 \omega^2 - k_z^2 \Omega_e^2}{\omega^2 - \Omega_e^2 - k^2 v_e^2} \right], \quad (5.6)$$

and

$$n_{\alpha_1} = \frac{Z_\alpha e \phi n_{\alpha_0}}{m_\alpha \omega^2} \left[ \frac{k^2 \omega^2 - k_z^2 \Omega_\alpha^2}{\omega^2 - \Omega_\alpha^2 - k^2 v_\alpha^2} \right], \quad (5.7)$$

where  $n_0, n_{\alpha_0}$  are the electron and ion equilibrium densities and  $\Omega_e (= eB_0/m_e C)$  and  $\Omega_\alpha (= Z_\alpha eB_0/m_\alpha C)$  are the electron and ion gyrofrequencies respectively. In obtaining Eqs.(5.6) and (5.7) we have neglected  $k_z^2 v_\alpha^2$  with respect to  $\omega^2$ . Substituting Eqs.(5.6) and (5.7) in Eq.(5.5), we get the dispersion relation,

$$\omega^8 - P\omega^6 + Q\omega^4 - R\omega^2 + S = 0, \quad (5.8)$$

where

$$P = \sum_j (\Omega_j^2 + k^2 V_j^2 + \omega_{Pj}^2),$$

$$Q = \frac{1}{2} \sum_{\substack{j, j', j'' \\ j \neq j' \neq j''}} \left[ (\Omega_j^2 + k^2 V_j^2)(\Omega_{j'}^2 + k^2 V_{j'}^2) \right. \\ \left. + (\omega_{Pj}^2 + \omega_{Pj'}^2)(\Omega_{j''}^2 + k^2 V_{j''}^2) \right] + \\ \frac{k_z^2}{k^2} \sum_j \Omega_j^2 \omega_{Pj}^2,$$

$$R = \prod_j (\Omega_j^2 + k^2 V_j^2) + \frac{1}{2} \sum_{\substack{j, j', j'' \\ j \neq j' \neq j''}} \left[ \omega_{Pj}^2 (\Omega_{j'}^2 \right. \\ \left. + k^2 V_{j'}^2)(\Omega_{j''}^2 + k^2 V_{j''}^2) + \frac{k_z^2}{k^2} (\Omega_j^2 + \right. \\ \left. k^2 V_j^2)(\Omega_{j'}^2 \omega_{Pj'}^2 + \Omega_{j''}^2 \omega_{Pj''}^2) \right],$$

and

$$S = \frac{1}{2} \frac{k_z^2}{k^2} \sum_{\substack{j, j', j'' \\ j \neq j' \neq j''}} \omega_{Pj}^2 \Omega_j^2 (\Omega_{j'}^2 + k^2 V_{j'}^2)(\Omega_{j''}^2 + k^2 V_{j''}^2).$$

In the above equations  $\omega_{pj}$  is the plasma frequency of the  $j^{\text{th}}$  species and the summations and multiplication are carried over all the species  $j$ , i.e., the electrons and the two species of ions.

In the limit of low frequency waves with  $\omega^2 \sim \Omega_1 \Omega_2$  and neglecting terms of the order of  $m_e/m_\alpha$ , Eq.(5.8) reduces to

$$Q\omega^4 - R\omega^2 + S = 0, \quad (5.9)$$

which has two roots namely,

$$\omega^2 = [R \pm (R^2 - 4QS)^{1/2}] / 2Q. \quad (5.10)$$

If  $R^2$  is assumed to be much larger than  $4QS$  (this assumption holds good in the magnetospheric plasmas and also the 2XIIB mirror machine), the two roots of Eq. (5.9) can be simplified to,

$$\omega_I^2 \approx R/Q, \quad (5.11)$$

and

$$\omega_{II}^2 \approx S/R. \quad (5.12)$$

In the limit of cold plasmas and  $k_z = 0$ , Eq. (5.11) reduces to

$$\omega^2 = \frac{\Omega_1 \Omega_2 \left( \frac{Z_1 n_{10}}{n_0} \Omega_2 + \frac{Z_2 n_{20}}{n_0} \Omega_1 \right)}{\left( \frac{Z_1 n_{10}}{n_0} \Omega_1 + \frac{Z_2 n_{20}}{n_0} \Omega_2 \right)} \quad (5.13)$$

This is the IIHR (Buchsbaum, 1960) and hence the mode given by Eq.(5.11) can be identified with the IIHR wave. The IIHR wave given by Eq.(5.11) is modified due to the finite temperature of the plasma and finite  $k_z$ .

When the ions are unmagnetised and electrons are taken to be cold, Eq.(5.12) simply gives  $\omega^2 = k_z^2 T_{eff} / m_e$  where  $T_{eff} = n_0 T_i T_2 (n_{10} Z_1^2 T_2 + n_{20} Z_2^2 T_1)^{-1}$  is the effective ion temperature. This is similar to the dispersion relation of the usual EA wave in a single ion species plasma, with the ion temperature  $T_i$  replaced by the effective ion temperature  $T_{eff}$ . Hence from Eq. (5.12) we find that the characteristic frequency of the EA wave is modified by the presence of the second ion species and also due to the fact that the ions are magnetised.

### 5.3 Discussion

The analytic expressions for the EA and IIHR waves given by Eqs.(5.11) and (5.12) are not exact solutions of the dispersion relation (5.9). To obtain exact solutions

of Eq.(5.9) for some physical systems like the magnetosphere and the 2XIIB mirror machine, we have solved it numerically.

ISIS2 satellite data show that at an altitude of 1400 km in the plasmasphere,  $H^+$  is the dominant ion species with  $O^+$  and  $He^+$  constituting 2-5% of the ion population (Hoffman, 1974). These ions are in the 1-12 keV energy range, whereas, the electrons have 100 eV energy. In the ring current around  $7 R_E$ ,  $O^+$  and  $He^+$  form less than 10% and  $He^{++}$  forms less than 3% of the total ion population (Johnson, 1979).  $H^+$  is the bulk ion species in this region also. These ions have energies of the order of 40 keV and the electrons have energies around 1-4 keV only.

In the 2XIIB mirror machine, impurity ions like carbon, proton etc. are present in the deuteron plasma. These ions have energies around 14 keV, while the electron energy is  $\sim 100$  eV (Coensgen et al., 1976).

We have studied the nature of the EA and IIHR waves and investigated the effect of the variation of concentration, temperature and mass of the second ion species on these modes in the magnetospheric plasmas and the 2XIIB mirror machine (Dash, Sharma and Buti, 1983). For computations we have taken the major ion species to be protons and the minority species could be  $He^+$  or  $O^+$  in the

magnetosphere, whereas, in the 2XIIB mirror machine deuteron is the major ion species with carbon or oxygen ions forming the other component.

We have computed the contribution due to the finite larmour radius for the magnetospheric plasmas and the 2XIIB mirror machine and found that it forms only 1-3% of the scalar pressure. So the error introduced in our calculations by neglecting the effect of finite larmour radius is not significant.

We have plotted the  $\omega$ -k diagram for different values of the ratios of the temperature and mass of the two species of ions.  $\omega$  and k are normalised with respect to  $(\Omega_e \Omega_i)^{1/2}$  and  $\rho_i^{-1} (= \Omega_i / v_{ti})$  respectively. The following observations are made from these diagrams.

Figs.1 and 2 show the  $\omega$ -k diagram for the EA and IHR waves in the magnetospheric plasmas ( $B = 0.31$  gauss) for different  $\mathcal{V} (= T_1/T_2)$  and  $D (= m_2/m_1)$ ; the subscripts 1 and 2 refer to the majority and minority ion species respectively. From Fig.1, we can see that the EA and IHR wave frequencies increase when  $\mathcal{V}$  decreases from 4 to 0.4, i.e. temperature of the minority ion species ( $O^+$ ) increases. This happens because when oxygen ions become hotter,

effective temperature of the ions increase, consequently their contribution to the characteristic frequencies increases, which results in the increase in EA and IIHR frequencies. Fig.2 shows that as  $D$  increases from 4 to 16, the EA and IIHR wave frequencies decrease. When  $D$  increases i.e. the minority ion species becomes heavier, corresponding thermal velocity and cyclotron frequency decrease and so the EA and IIHR wave frequencies also decrease. We have also computed the EA and IIHR wave frequencies for different concentrations of the minority ion species. Our calculations indicate that the EA frequency decreases and IIHR frequency increases when the concentration of the oxygen ion increases. Since the second ion species forms a very small percentage ( $\sim 2 - 5\%$ ) of the total ion population, change in the frequencies corresponding to the variation in their concentration is very small. For this reason we have not plotted the  $\omega$ - $k$  diagram for this case. Figs. 3 and 4 show the  $\omega$ - $k$  diagram for the EA and IIHR waves in the 2XIIB mirror machine ( $B = 5600$  gauss). From Fig.3, it can be seen that the EA and IIHR frequencies increase as  $\mathcal{V}$  decreases from 4 to 1. Fig.4 shows that as  $D$  increases from 1 to 8, the EA and IIHR wave frequencies decrease. Calculations of the EA and IIHR wave frequencies for different compositions of the two ion species in the 2XIIB mirror machine shows that the former decreases while the later increases when the



concentration of the impurity ions increases. The change in the characteristic frequencies are very small for the variation in the concentration of the impurity ion species and so the corresponding  $\omega$ - $k$  diagram is not shown.

#### 5.4 Summary

The dispersion relation for the EA and IIHR waves in a two-ion-species magnetoplasma in the low frequency regime ( $\omega \sim \Omega_{\alpha}$ ) is derived. This equation is solved numerically to obtain the characteristic frequencies of the EA and IIHR waves for different values of the ratios of the temperature, mass and density of the two ion species. In the magnetosphere and the 2XIIB mirror machine, it has been found that the frequencies of the EA and IIHR waves increase when temperature of the minority ion species increases, but decrease when the minority ion species becomes heavier. However, increase in the minority ion density decreases the EA frequency but increases the IIHR frequency.

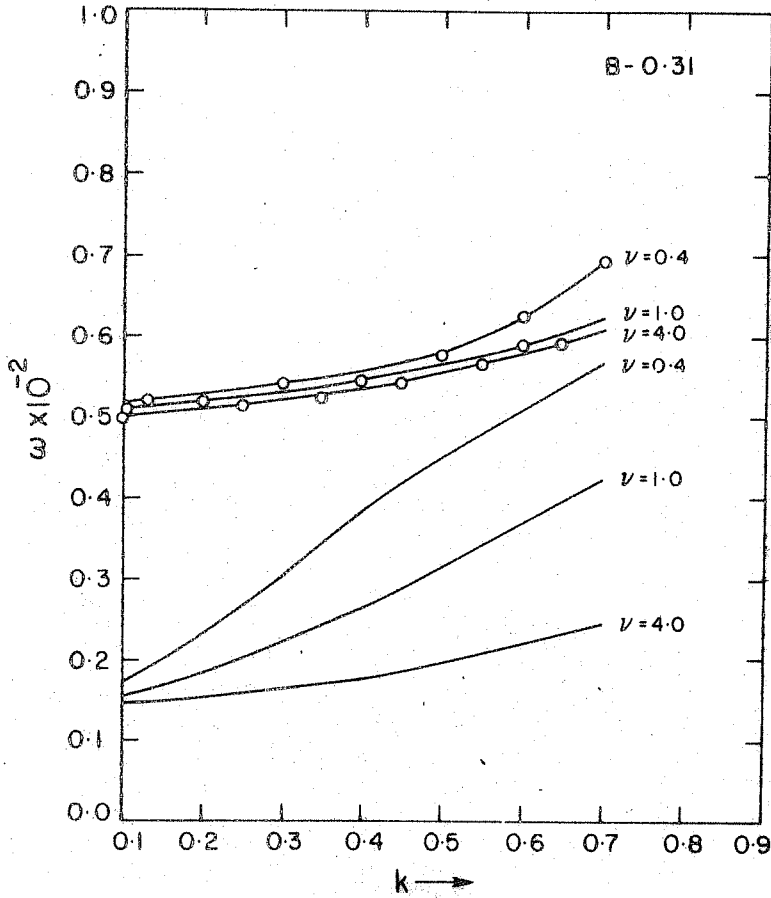


Fig. 1:  $\omega$  Vs  $k$  in the magnetospheric plasma for  $\nu = 0.4, 1.0$  and  $4.0$ .  $k_z/k = 5 \times 10^{-3}$ . The basic modes are the EA (—) and IIHR (-o-o-) waves.

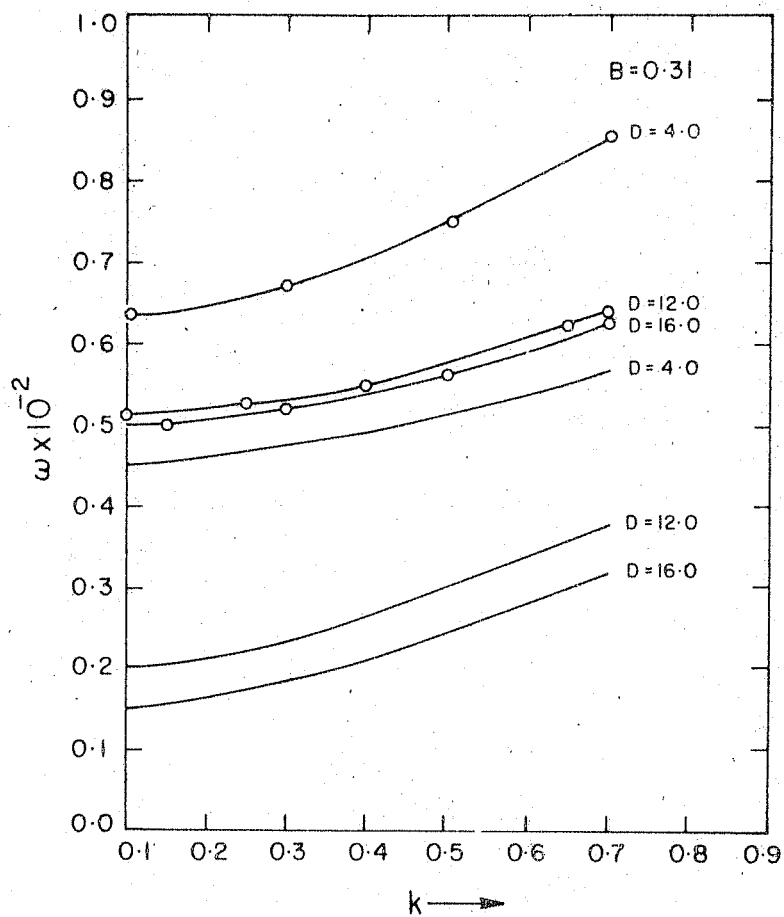


Fig. 2:  $\omega$  Vs  $k$  in the magnetospheric plasma for  $D = 4, 12$  and  $16$ .  $k_z/k = 5 \times 10^{-3}$ . The basic modes are the EA (—) and IIHR (-o-o-) waves.

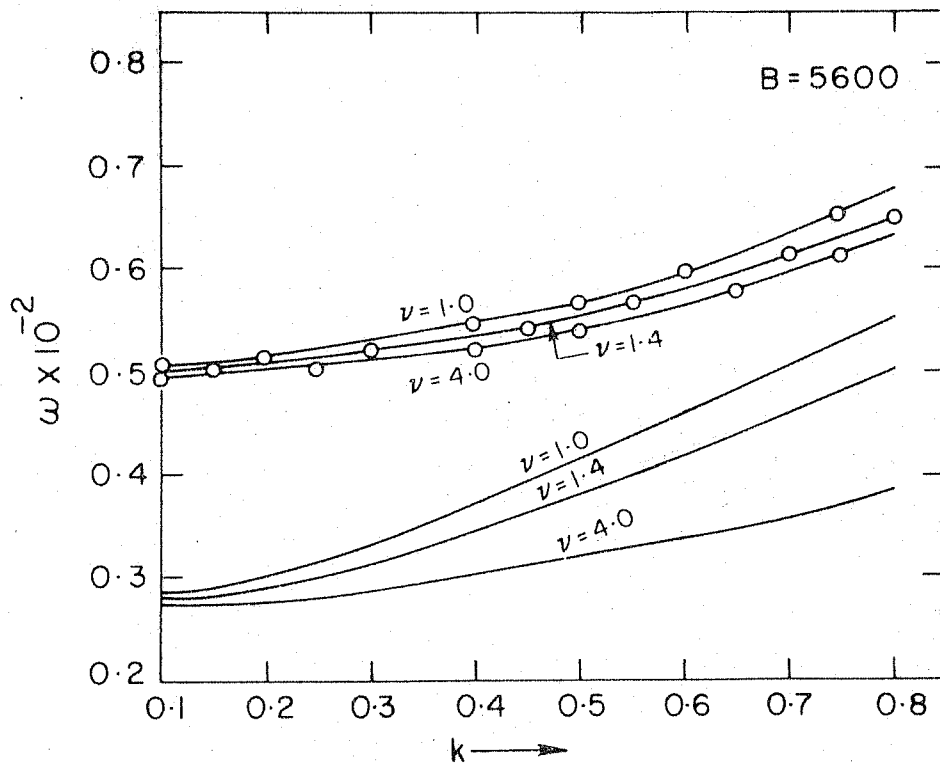


Fig. 3:  $\omega$  Vs  $k$  in the 2 x IIB mirror machine for  $\nu = 1, 0, 1.4$  and 4.0.  $k_z/k = 5 \times 10^{-3}$ . The basic modes are the EA (—) and IIHR (—o—o—) waves.

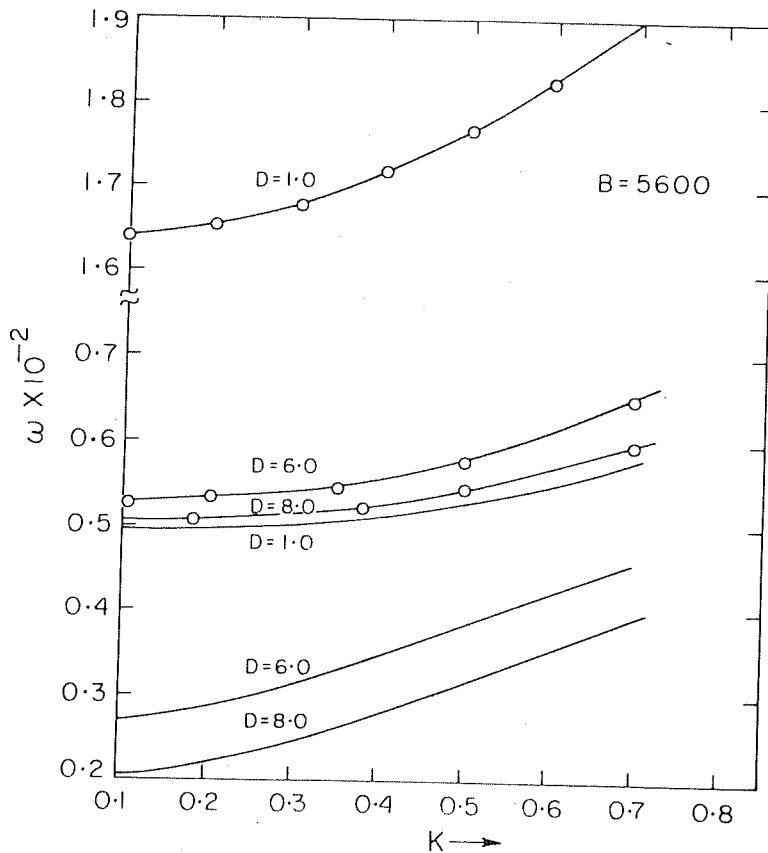


Fig. 4:  $\omega$  Vs.  $k$  in the 2 x IIB mirror machine for  $D = 1, 6$  and  $8$ .  $k_z / k = 5 \times 10^{-3}$ . The basic modes are the EA (—) and IIHR (—o—o—) waves.

## CHAPTER 6

### ELECTRON ACOUSTIC AND ION-ION-HYBRID RESONANCE

### - DRIFT INSTABILITY IN INHOMOGENEOUS MULTI-ION-

### SPECIES MAGNETOPLASMAS

#### 6.1 Introduction

One of the most interesting characteristics of plasmas is their ability to sustain a large variety of waves. The presence of an external magnetic field further increases the number of waves which can be supported by the plasma. Some of these waves can propagate at nearly equal frequencies. In general, these waves can have different wavenumbers, but

for some critical set of plasma parameters, the wavenumbers can coalesce. Considering the case of a wave propagating through an inhomogeneous plasma and approaching a region where local plasma parameters correspond to such a coalescence, the incident wave may be reflected or refracted in the same mode or absorbed or converted into the complementary mode, or even may undergo some combination of all these. The theory of mode conversion attempts to find out as to what happens to the incident wave when it passes through the coalescence region.

While propagating across a weakly inhomogeneous plasma, a fast electromagnetic plasma wave can be mode converted into a slow ion plasma mode at the lower hybrid critical layer and is reflected back (Stix, 1965). Travelling outwards, this new mode slows down further and its velocity and wavelength become comparable to the ion thermal velocity and the electron Larmor radius. If the wave frequency is close to the harmonics of the ion cyclotron frequency, this slow wave can undergo ion cyclotron damping and the ions can get heated. In this way the process of mode conversion can lead to particle heating in plasma.

Since the earlier experiments of TFR (TFR Group, 1977), ATC (Takahashi et.al. 1977) etc. it has been realised that

the presence of a small concentration of minority ions can have a profound effect on the dispersion properties of the plasma. Due to the presence of two or more distinct ion species, a new resonance, that is, the ion-ion-hybrid resonance (IIHR) is excited. Within this IIHR layer, mode conversion between different waves may take place. Theoretical analysis of mode conversion of the launched fast Alfvén wave into the ion-Bernstein wave near this IIHR layer had been carried out by several authors (Swanson, 1976; Jacquinet et al, 1977; Perkins, 1977; Stix and Swanson, 1982).

When magnetised plasmas have gradients in density or temperature in a direction perpendicular to the magnetic field and the direction of wave propagation, drift waves are excited (Kadomtsev, 1965; Krall and Trivelpiece, 1973). The phase velocity of these waves, across the magnetic field, is of the order of the drift velocity of the particles. These drift waves can couple with the lower hybrid and the electron acoustic (EA) modes resulting in the corresponding drift instabilities (Mohan and Yu, 1983; Sharma et al, 1983).

Mode conversion between two modes with frequencies  $\omega_1$  and  $\omega_2$  occurs when for a given value of wavenumber  $k$ ,  $\omega_1$  becomes equal to  $\omega_2$ . In a homogeneous medium, this condition can not be satisfied unless the two waves have



equal frequencies initially. However, if the medium has inhomogeneities along the direction of propagation, say the  $y$ -axis,  $k$  is a function of  $y$ . In that case, there may exist some  $k = k(y_0)$  for which  $\omega_1$  and  $\omega_2$  are equal and mode conversion can occur between them. For this reason, mode conversion is usually studied in inhomogeneous plasmas where gradients are along the direction of propagation (Stix, 1965; Swanson, 1976; Perkins, 1977; Colestock and Kashuba, 1982). However, if the gradients are perpendicular to the magnetic field and the direction of wave propagation,  $k \neq k(y_0)$ . But the drifts, which arise due to the density gradients, are along the  $y$ -direction and can couple with the waves propagating along that direction. This can modify the frequencies so that  $\omega_1 = \omega_2$  may occur at some  $y = y^*$  leading to mode conversion between them. Hence the gradients in the perpendicular direction can act as effective inhomogeneity along the propagation direction so far as the process of mode conversion is concerned. Keeping this in mind, in this chapter, we investigate the possibility of mode conversion between the EA and IIHR waves when the density gradients are perpendicular to the magnetic field and the direction of wave propagation. We also study the drift instability of the EA and IIHR waves.

We consider a two-ion-species magnetoplasma where the ions are hotter than the electrons. Numerical analysis of the dispersion relation shows that the coupling between the drift wave and the EA and IIHR waves can give rise to instabilities when the inhomogeneity scalelength  $L (= n_{e_0} (dn_e/dx)^{-1}$ , where  $n_{e_0}$  is the equilibrium electron density) is smaller than a certain threshold value. It is noted that the region of instability, for both the modes, increases with a decrease in the inhomogeneity scalelength. We have also found that for weakly inhomogeneous plasmas, drift waves are not strong enough to modify the frequencies and in the framework of fluid theory, mode conversion does not occur between the EA and IIHR waves in the terrestrial magnetosphere and the 2xIIB Mirror machine (Dash et al., 1983).

## 6.2 Dispersion Relation

Let us consider a two-ion-species inhomogeneous magnetoplasma where the ions are more energetic than the electrons. We assume a slab model of the plasma with the constant magnetic field  $B$  along the  $Z$ -direction ( $\underline{B} = B_0 \hat{Z}$ ) and the density gradients along the  $x$ -direction. The waves are assumed to propagate almost perpendicular to the magnetic field so that  $0 < k_z/k \ll (m_e/m_i)^{1/2}$ . The electrons and ions

are governed by the continuity and momentum equations given by

$$\frac{\partial n_j}{\partial t} + \nabla \cdot (n_j \underline{v}_j) = 0, \quad (6.1)$$

and

$$m_j \left( \frac{\partial \underline{v}_j}{\partial t} + \underline{v}_j \cdot \nabla \underline{v}_j \right) = z_j e n_j (\underline{E} + \frac{1}{c} \underline{v} \times \underline{B}) - T_j \nabla n_j. \quad (6.2)$$

In equations (6.1) and (6.2),  $z_j$ ,  $n_j$ ,  $T_j$ ,  $n_j$  and  $\underline{v}_j$  are the charge, mass, temperature, density and velocity of the  $j^{\text{th}}$  component, where  $j=e$ , 1 and 2 corresponds to the electrons and the two species of ions. The space dependence of densities are assumed to be of the form  $n_j = n_{j0} (1 + \alpha_j x)$ , where the strength of inhomogeneities are defined as

$\alpha_j = -n_{j0}^{-1} dn_j / dx$ . In writing Eq.(6.2), we have neglected the effect of finite Larmor radius in the pressure term, as was done in chapter 5. The Poisson's equation closes the system of equations (6.1) and (6.2) and is given by

$$-\nabla^2 \phi = 4\pi e \sum_j z_j n_j, \quad (6.3)$$

where the summation is carried over all the species present in the system. Let us consider electrostatic perturbations of the form

$$\phi \sim \exp \{ i (k_y y + k_z z - \omega t) \}. \quad (6.4)$$

The perturbations are such that the parallel phase velocities are much larger than the electron and ion thermal velocities, i.e.,  $\omega/k_z \gg v_{tj} = (T_j/m_j)^{1/2}$ . Due to the inhomogeneities in the system, the electrons and ions have a diamagnetic drift  $v_{dj} = -c T_j \kappa_j / Z_j e B$ . Linearising equations (6.1) and (6.2) and eliminating perturbed velocities, we obtain the perturbed densities as

$$n_{e1} = \frac{Z_e e \phi n_0}{m_e \omega^2} \frac{k^2 \omega^2 - A_e \omega - k_z^2 \Omega_e^2}{\omega^2 - 2\omega_{e*} \omega - B_e} \quad (6.5)$$

and

$$n_{1,2,1} = \frac{Z_{1,2} e \phi n_{1,2,0}}{m_{1,2} \omega^2} \frac{k^2 \omega^2 - A_{1,2} \omega - k_z^2 \Omega_{1,2}^2}{\omega^2 - 2\omega_{1,2*} \omega - B_{1,2}}, \quad (6.6)$$

where

$$A_e = k_z^2 \omega_{e*} + k_y \alpha_e \Omega_e , \quad (6.7)$$

$$A_{1,2} = k_z^2 \omega_{1,2*} - k_y \alpha_{1,2} \Omega_{1,2} , \quad (6.8)$$

$$B_e = \Omega_e^2 + k^2 v_{te}^2 - \omega_{e*}^2 - \alpha_e \Omega_e v_{de} , \quad (6.9)$$

and

$$B_{1,2} = \Omega_{1,2}^2 + k^2 v_{t1,2}^2 - \omega_{1,2*}^2 + \alpha_{1,2} \Omega_{1,2} v_{d1,2} , \quad (6.10)$$

with  $\omega_{j*} = k_y V_{dj}$  as the drift frequency of the  $j^{\text{th}}$  species and  $k^2 = k_y^2 + k_z^2$ . Substituting Eqs. (6.5) and (6.6) in (6.3) and simplifying, we get the dispersion relation

$$\omega^8 - C_1 \omega^7 + C_2 \omega^6 + C_3 \omega^5 + C_4 \omega^4 - C_5 \omega^3 - C_6 \omega^2 + C_7 \omega + C_8 = 0 , \quad (6.11)$$

where

$$c_1 = 2 \sum_j \omega_{j*} ,$$

$$c_2 = \sum_{\substack{j, j', j'' \\ j \neq j' \neq j''}} (B_j - 2\omega_{j*} \omega_{j'*} + \omega_{p_j}^2) ,$$

$$c_3 = 2 \sum_{\substack{j, j' \\ j \neq j'}} \left[ \omega_{j*} B_{j'} + \omega_{p_j}^2 \left( \omega_{j'*} + \frac{1}{2} \frac{A_j}{k^2} \right) \right] ,$$

$$c_4 = \sum_{\substack{j, j', j'' \\ j \neq j' \neq j''}} \left[ \frac{1}{2} B_j B_{j'} - 2\omega_{j*} \omega_{j'*} B_{j''} + \omega_{p_j}^2 (B_{j''} - 2 \frac{A_j}{k^2} \omega_{j'*} - 2\omega_{j*} \omega_{j''*} + \frac{k_z^2}{k^2} \Omega_j^2) \right] ,$$

$$c_5 = \sum_{\substack{j, j', j'' \\ j \neq j' \neq j''}} \left[ \frac{1}{2} \omega_{j*} B_{j'} B_{j''} + \omega_{p_j}^2 (2\omega_{j'*} B_{j''} + \right.$$

$$\left. \frac{A_j}{k^2} B_{j'} + 2 \frac{k_z^2}{k^2} \Omega_j^2 \omega_{j'*} \right) \right] ,$$

$$c_6 = \prod_j B_j + \sum_{\substack{j, j', j'' \\ j \neq j' \neq j''}} \left[ \omega_{p_j}^2 \left( \frac{1}{2} B_{j'} B_{j''} - 2 \frac{A_j}{k^2} \omega_{j*} B_{j''} \right) + \frac{k_z^2}{k^2} \Omega_j^2 \left( B_{j'} - 2 \omega_{j*} \omega_{j''*} \right) \right],$$

$$c_7 = \sum_{\substack{j, j', j'' \\ j \neq j' \neq j''}} \omega_{p_j}^2 \left( \frac{1}{2} \frac{A_j}{k^2} B_{j'} B_{j''} + 2 \frac{k_z^2}{k^2} \Omega_j^2 \omega_{j*} B_{j''} \right),$$

and

$$c_8 = \frac{1}{2} \frac{k_z^2}{k^2} \sum_{\substack{j, j', j'' \\ j \neq j' \neq j''}} \omega_{p_j}^2 \Omega_j^2 B_{j'} B_{j''}.$$

In the low frequency ( $\omega^2 \sim \Omega_1 \Omega_2$ ) limit, on neglecting terms of the order of  $m_e/m_{1,2}$ , Eq.(6.11) can be written as

$$P\omega^4 - Q\omega^3 + R\omega^2 + C_7\omega + C_8 = 0, \quad (6.12)$$

where

$$P = C_4 - \sum_{\substack{j, j', j'' \\ j \neq j' \neq j''}} \left( \frac{1}{2} B_j B_{j'} - 2 \omega_{j*} \omega_{j'*} B_{j''} \right),$$

$$Q = C_5 - \frac{1}{2} \sum_{\substack{j, j', j'' \\ j \neq j' \neq j''}} \omega_{j*} B_{j'} B_{j''},$$

and

$$R = C_6 - \prod_j B_j.$$

When the plasma is homogeneous, Eq.(6.12) reduces to Eq.(5.22) which has two roots corresponding to the EA and IIHR modes. When inhomogeneities are present in the system, Eq.(6.12) shows that these two modes get coupled. This means that the drift waves, arising due to the inhomogeneities in the system, couple with the EA and IIHR modes, and modify their frequencies.

### 6.3 EA and IIHR Drift Instabilities

In chapter 5, we showed that both EA and IIHR modes can exist in some regions of the terrestrial magnetosphere and the 2XIIB mirror machine. While studying the dispersion



relation for the EA and IIHR modes, in chapter 5, we had assumed the plasma to be homogeneous. But in reality, these plasmas are not homogeneous. They are, as a matter of fact, weakly inhomogeneous so that the inhomogeneity scalelength  $L$  is larger than the larmour radius  $\rho_{1,2}$  of the ions, where  $\rho_{1,2} = (T_{1,2} m_{1,2})^{1/2} / Z_{1,2} eB$ . In such weakly inhomogeneous plasmas, the EA and IIHR waves are governed by Eq. (6.12). Since it is not possible to solve Eq.(6.12) analytically, we have computed its roots numerically for parameters relevant to the magnetosphere and the 2XIIB mirror machine.

We have plotted the  $\omega$ - $k$  diagram for the EA and IIHR waves for different values of  $L$ . The frequency, wave-number and the inhomogeneity scalelength are normalised with respect to  $(\Omega_e \Omega_i)^{1/2}$ ,  $\rho_i^{-1}$  and  $\rho_i^{-1}$  respectively. Fig.1 shows the  $\omega$ - $k$  diagram corresponding to the magnetospheric plasma ( $B = 0.31$  gauss). In fig.1(a),  $L = \infty$ , i.e. the plasma is homogeneous and the two branches of EA and IIHR modes are found to be symmetric. When  $L$  decreases, the two branches of each of the modes are no longer symmetric, as shown in figs.1(b). As  $L$  decreases further and becomes equal to a certain critical value, say  $L_{CE}(= 1.85 \rho_i)$ ,

fig.1(c) shows that the two branches of the EA mode couple to each other giving rise to complex frequencies, which results in the drift instability. The growth rate for the EA-drift instability ( $\gamma_E$ ) is found to be  $0.8 \times 10^{-3} (\Omega_e \Omega_1)^{1/2}$  for  $k = 0.8 \beta_1^{-1}$ . It is also noted that, for EA-drift instability,  $\gamma_E$  is of the same order as that of the real part of the frequency ( $\omega_{RE}$ ). The two branches of the IIHR wave are also modified by the inhomogeneities in the system, but they are still independent of each other. Further decrease in  $L$  maintains the EA-drift instability and for  $L=L_{CI}(=1.25\beta_1)$ , two branches of the IIHR mode couple with each other giving rise to the IIHR-drift instability for wavenumbers lying between  $0.6 \beta_1^{-1}$  and  $0.8 \beta_1^{-1}$ ; growth rate  $\gamma_I$  is found to be  $1.7 \times 10^{-3} (\Omega_e \Omega_1)^{1/2}$  for  $k = 0.7 \beta_1^{-1}$ . However, unlike the case of EA-drift instability, growth rate of IIHR-drift instability is much smaller compared to the real part of its frequency ( $\omega_{RI}$ ), i.e.  $\gamma_I \ll |\omega_{RI}|$ . Fig.2 shows the  $\omega$ - $k$  diagram corresponding to the 2XIIB mirror machine for which typically  $B$  is 5600 gauss. Fig.2(a) which corresponds to the homogeneous case shows that the two branches of EA and IIHR modes are symmetric, whereas fig.2(b) shows that their symmetry is broken when  $L$  decreases to  $2\beta_1$ . For  $L = 1.56 \beta_1$ , EA mode becomes drift

unstable with a growth rate  $\gamma_E = 0.6 \times 10^{-3} (\Omega_e \Omega_1)^{1/2}$  for  $k = 0.8 \vartheta_1^{-1}$  (fig.2(c)). When  $L$  decreases further, fig. 2(d) shows that for  $L = 1.4 \vartheta_1$ , IIHR mode becomes drift unstable within the wavenumber range  $0.4 \vartheta_1^{-1}$  and  $0.6 \vartheta_1^{-1}$ . The growth rate of this instability ( $\gamma_I$ ) is found to be  $1.6 \times 10^{-3} (\Omega_e \Omega_1)^{1/2}$  for  $k = 0.5 \vartheta_1^{-1}$ . In this case also  $\gamma_E \approx |\omega_{RE}|$ , whereas  $\gamma_I \ll |\omega_{RI}|$ .

#### 6.4 Discussion and Conclusions

From figs.1 and 2, we see that the inhomogeneities in the system modify the EA and IIHR modes and for the inhomogeneity scalelength  $L$  smaller than the critical scalelength  $L_E$ , the EA wave becomes drift unstable, whereas, the IIHR wave becomes drift unstable only when  $L$  is smaller than  $L_{CI}$ . The magnitude of  $L_{CE}$  and  $L_{CI}$  are obtained numerically for plasmas in the magnetosphere and also the 2XIIB mirror machine and it is found that  $L_{CI}$  is smaller than  $L_{CE}$  in both the cases. The reason for this is the following: As we can see in figs.1(a) and 2(a), the separation between the two branches of IIHR mode is larger than the separation between the two branches of the EA mode. So a larger density gradient is required for the two branches of the IIHR mode to couple with each other and become drift unstable

than for the EA mode.

From figs.(1) and (2), it is noted that the region of instability and also the growth rates for both the modes increase with an increase in the strength of inhomogeneity. As the strength of inhomogeneity increases, the drift frequency increases and hence the coupling between the drift mode and the EA and IIHR modes becomes more effective. This is the reason for the increase in the region of EA and IIHR drift instabilities and the growth rates when the inhomogeneities are stronger.

When we increase the strength of inhomogeneities further (but still within the limit of our approximation, i.e.  $L > \rho_{1,2}$ ), we find that both EA and IIHR modes are drift unstable, but contrary to our expectations, mode conversion between the EA and IIHR does not occur. The absence of mode conversion between these waves can be due to the fact that we have considered weak inhomogeneities for which the drift frequencies are not large enough to modify the EA and IIHR frequencies to such an extent that mode conversion may be possible. For this, we are planning to look into the case of stronger inhomogeneities appropriately including the kinetic effects.

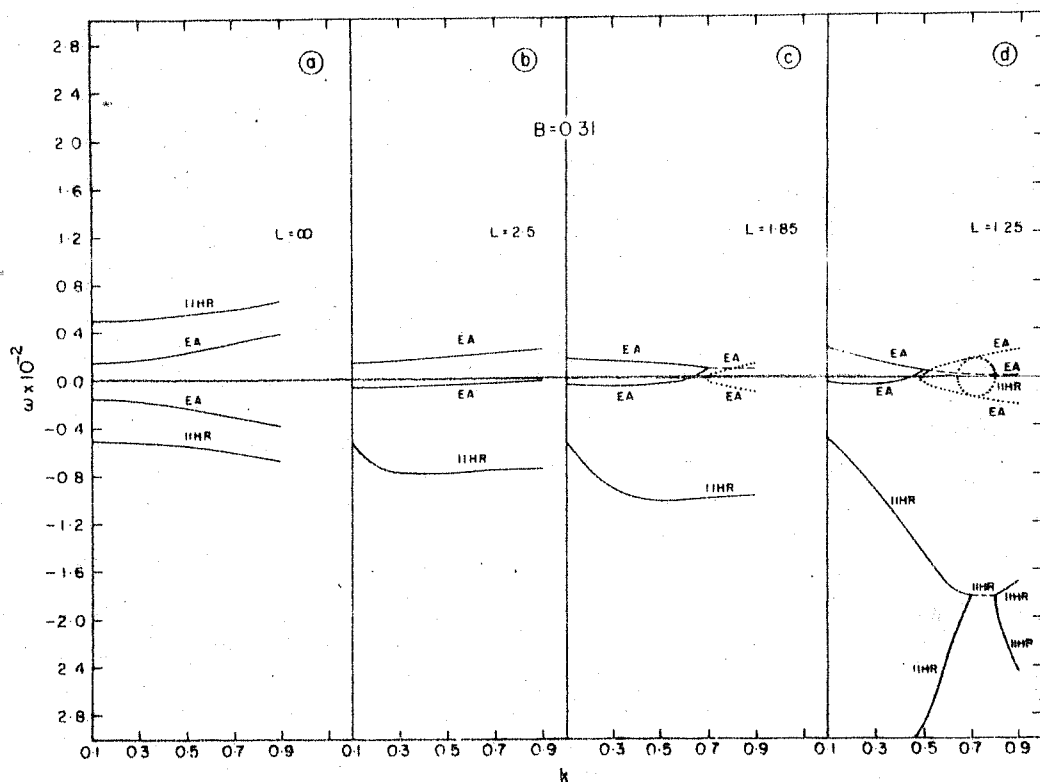


Fig.1.  $w$  vs  $k$  in the magnetospheric plasmas with  $k_z/k = 5 \times 10^{-3}$ ,  $T_1/T_2 = 2$ ,  $T_1/T_E = 20$  and 2% of  $O^+$  impurity for  $L = \infty$ , 2.5, 1.85 and 1.25. The solid lines represent  $w$  when it is real. When  $w$  is complex the real part of  $w$  is denoted by the dashed lines and the dotted lines correspond to the imaginary part of  $w$ . Frequency of the second branch of IIHR in figs.1(b) and 1(c) is very high and is not shown.

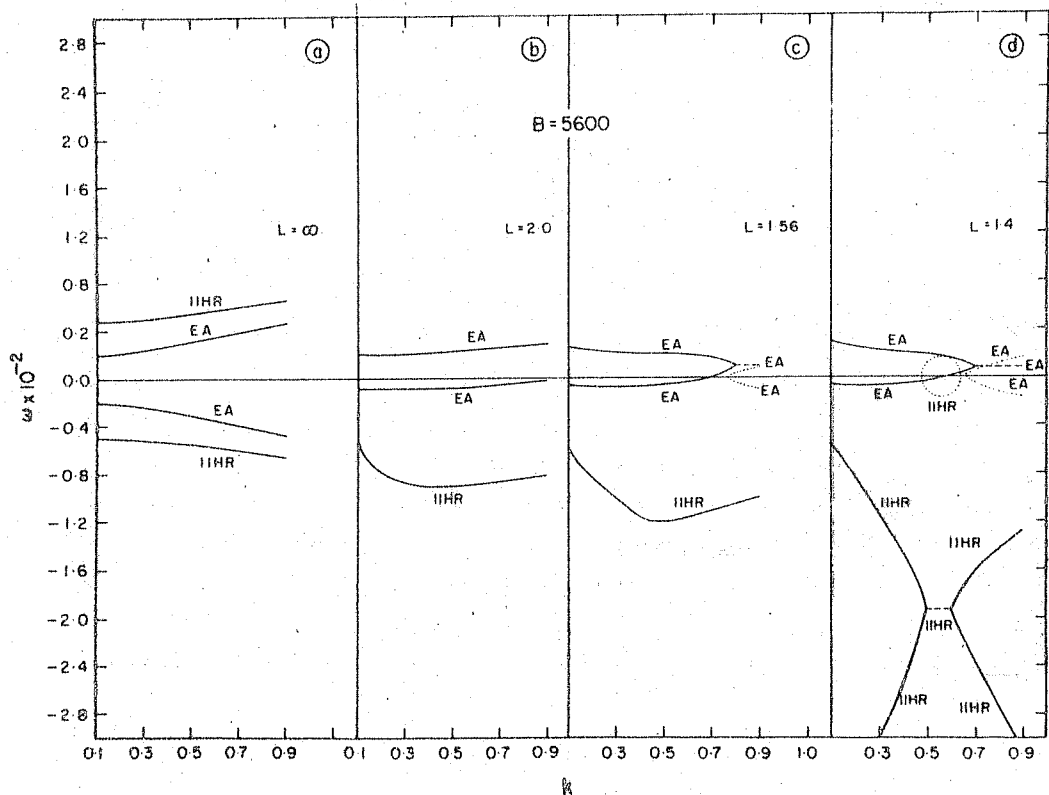


Fig.2.  $w$  vs  $k$  in the 2XIIB mirror machine with  $k_z/k = 5 \times 10^{-3}$ ,  $T_1/T_2 = 1.4$ ,  $T_1/T_E = 140$  and 2% of  $O^+$  impurity for  $L = \infty$ , 2, 1.56 and 1.4. The solid lines represent  $w$  when it is real. When  $w$  is complex, its real part is denoted by the dashed lines and the dotted lines correspond to the imaginary part of  $w$ . Frequency of the second branch of IIHR in figs.2(b) and 2(c) is very high and is not shown.

# REFERENCES

- Arefev V.I.(1970) Sov. Phys. Tech. Phys. 14 1487
- Balsiger H., Eberhardt P., Geiss J. and Young D.J.(1980)  
J. Geophys. Res. 85 1645
- Banks P.M. and Kockarts G. (1973) Aeronomy, Part B  
(New York: Academic Press)
- Bardet R., Briand P., Dupas L., Gormezano C. and Melin G.  
(1975) Nucl. Fusion 15 865
- Benson R.F. and Calvert W. (1979) Geophys.Res. Lett.6 479
- Bogoliubov N.N. and Mitropolsky Y.A.(1961) Asymptotic Methods  
in the Theory of Nonlinear Oscillations  
(Delhi: Hindustan)
- Böhmer H., Hauck J.P., Rynn N.(1976) Phys.Fluids 19 450
- Buchsbaum S.J.(1960) Phys. Fluids 3 418
- Buti B. (1976) IEEE Trans.Plasma Sci. PS4 292
- Buti B. (1977) Phys. Rev. Lett. 38 498
- Buti B. (1980) Phys. Lett. 76A 251
- Buti B. (1980a) J. Plasma Phys.24 169
- Buti B., Mohan M.and Shukla P.K.(1980) J.Plasma Physics  
23 341
- Buti B. and Yu M.Y.(1981) J.Plasma Phys.26 309
- Chen H.H.and Liu C.S.(1978) Phys.Fluids 21 377
- Coensegen F.H., Cummins W.F., Gormezano C., Logan B.G.,  
Molvik A.W., Nexsen W.E., Simonen T.C.,  
Stallard B.W. and Turner W.C.(1976) Phys.  
Rev. Lett. 37 143

- Colestock P.L. and Kashuba R.J.(1982) Plasma Physics  
Laboratory, Princeton, New Jersey, United States,  
Report No. PPPL-1980
- Dash S.S. and Buti B. (1981) Phys.Lett.81A 347
- Dash S.S. and Buti B. (1983) Plasma Phys.25 341
- Dash S.S. and Buti B. (1983a) (To be published)
- Dash S.S., Sharma A.S.and Buti B.(1983) (To be published)
- Davidson R.C.(1972) Methods in Nonlinear Plasma Theory  
(New York: Academic Press)
- Edgley P.D., Franklin R.N., Hamberger S.M.and Motley R.W.  
(1975) Phys. Rev. Lett. 34 1269
- Eubank et.al.(1979) Phys. Rev. Lett. 43 270
- Feldman W.C., Asbridge J.R., Bame S.J., Montgomery M.D.and  
Gary S.P. (1975) J.Geophys.Res.80 4181
- Frank L.A.(1971) J.Geophys.Res.76 2265
- Frank L.A., Ackerson K.L.and Lepping R.P.(1976) J.Geophys.  
Res.81 5859
- Frank L.A., Ackerson K.L.and Yeager D.M.(1977) J.Geophys.  
Res. 82 129
- Garret H.B. (1979) Rev.Geophys.Space Phys. 17 397
- Goswami B.N.and Buti B.(1976) Phys.Lett.57A 149
- Grabbe C.L., Papadopoulos K.and Palmadesso P.J.(1980)  
J.Geophys.Res.85 3337
- Gurnett D.A.(1974) J. Geophys. Res. 79 4227
- Gurnett D.A.and Frank L.A.(1978) J.Geophys.Res.83 58



- Hardy D.A., Freeman J.W. and Hills H.K. (1978) J. Geophys. Res. 82 5529
- Hoffman J.H., Dodson W.H., Lippincott C.R. and Hammack H.D. (1974) J. Geophys. Res. 79 4246
- Hosea et. al. (1979) Phys. Rev. Lett. 43 1802
- Horwitz J.L. (1982) Rev. Geophys. Space Phys. 20 929
- Hudson M.K., Lysak R.L. and Mozer F.S. (1978) Geophys. Res. Lett. 5 143
- Ikezi H., Taylor R.J. and Baker D.R. (1970) Phys. Rev. Lett. 27 718
- Jacquinet J., McVey B.D. and Scharer J.E. (1977) Phys. Rev. Lett. 39 88
- Janzen G. (1980) J. Plasma Phys. 23 321
- Johnson R.G., Sharp R.D. and Shelley E.G. (1974) J. Geophys. Res. 79 3135
- Johnson R.G., Sharp R.D. and Shelley E.G. (1977) Geophys. Res. Lett. 4 403
- Johnson R.G. (1979) Rev. Geophys. Space Phys. 17 696
- Jones W.D., Lee A., Gleeman S.M. and Doucet H.J. (1975) Phys. Rev. Lett. 35 1349
- Kadomtsev B.B. (1965) Plasma Turbulence (New York: Academic Press)
- Kadomtsev B.B. and Karpman V.I. (1971) Sov. Phys. - Usp. 14 40
- Kakutani T. and Sugimoto N. (1974) Phys. Fluids 17 1617
- Karpman V.I. (1979) Physica Scripta 20 462

- Kelley M.C., Bering E.A. and Mozer F.S. (1975) Phys. Fluids 18 1590
- Kintner P.M., Kelley M.C. and Mozer F.S. (1978) Geophys. Res. Lett. 5 139
- Krall N.A. and Trivelpiece A.W. (1973) Principles of Plasma Physics (Kogakusha: Mc Graw-Hill)
- Krokhin O.N. and Sibenko S.P. (1981) Kratkiye Soobsheniya po fizika, No. 5, 31
- Lashmore-Davies C.N. and Martin T.J. (1973) Nucl. Fusion 13 193
- Lisak M. (1980) J. Plasma Phys. 24 445
- Mizera P.F. and Fennel J.F. (1977) Geophys. Res. Lett. 4 311
- Mohan M. and Buti B. (1979) Plasma Phys. 21 713
- Mohan M. and Buti B. (1980) Plasma Phys. 22 873
- Mohan M. and Yu M.Y. (1983) J. Plasma Phys. 29 127
- Morales G.J. and Lee Y.C. (1974) Phys. Rev. Lett. 33 1016
- Motley R.W. and D'Angelo N. (1963) Phys. Fluids 6 296
- Mozer F.S., Carlson C.W., Hudson M.K., Torbert R.B., Paraday B., Yatteau J. and Kelley M.C. (1977) Phys. Rev. Lett. 38 292
- Oleson N.L. and Found C.G. (1949) J. Appl. Phys. 20 416
- Perkins F.W. (1977) Nucl. Fusion 17 1197
- Peterson W.K., Sharp R.D., Shelley E.G., Johnson R.G. and Balsiger H. (1981) J. Geophys. Res. 86 761
- Pokroev A.G. and Stepanov K.N. (1973) Sov. Phys. Tech. Phys. 18 461

- Richtmyer R.D. and Morton K.W.(1967) Difference Methods  
for Initial Value Problems (Tracts in Mathematics  
No.4, New York: Interscience)
- Russel C.T. and Thorne R.M.(1970) Cosmic Electrodyn.1 67
- Sagdeev R.Z. (1966) Review of Plasma Physics, Vol.4, ed.  
M.A. Lenotovich (Consultant Bureau:New York)
- Sakanaka P.H. (1972) Phys. Fluids 15 304
- Sharma A.S. and Buti B.(1976) J.Phys.A:Math.Gen.9 1823
- Sharma A.S. and Buti B.(1977) IEEE Trans.Plasma Sci.PS5 293
- Sharma A.S., Mohan M.and Yu M.Y.(1983) Phys.Lett.97A 387
- Smith G.D.(1969) Numerical Solution of Pratial Differential  
Equations (London:Oxford University Press)
- Stix T.H.(1965) Phys.Rev.Lett.15 878
- Stix T.H.and Swanson D.G. (1982) Plasma Physics Laboratory,  
Princeton,New Jersey,United States, Report No.  
PPPL-1903
- Swanson D.G.and Ngan Y.C.(1975) Phys.Rev.Lett.35 517
- Swanson D.G. (1976) Phys.Rev.Lett.36 316
- Takahashi H., Daughney C.C., Ellis R.A., Goldston R.J.,  
Hsuan H., Nagashima T., Paoloni F.J., Sivo A.J.  
and Suckewer S.(1977) Phys.Rev.Lett.39 31
- Taniuti T. and Wei C.C.(1968) J.Phys.Soc.Japan 24 941
- Taniuti T. and Yajima N.(1969) J.Math.Phys.10 1369
- Taniuti T.(1974) Prog.Theor.Phys.Suppl.No.55 1
- Tappert F.D.(1972) Phys. Fluids 15 2446

- Temerin M., Woldorff M. and Mozer F.S. (1979) Phys. Rev. Lett. 43 1941
- TFR Group (1977) Proceedings of 6<sup>th</sup> International Conference on Plasma Physics & Controlled Fusion, Innsbruck, Vol. 3, p. 39, IAEA
- Tobert R.B. and Mozer F.S. (1978) Geophys. Res. Lett. 5 135
- Washimi H. and Taniuti T. (1966) Phys. Rev. Lett. 17, 996
- Weynants R.R. (1974) Phys. Rev. Lett. 33 78
- Williams D.J., Fritz T.A., Wilken B. and Keppler E. (1979) J. Geophys. Res. 84 6385
- Witt E. and Lotko W. (1983) Phys. Fluids 26 2176
- Yu M.Y. (1977) J. Plasma Phys. 18 139